Impacts of Motorcycle Dedicated Lanes on Traffic Flow & Safety of Unsignalized Intersections–A Microsimulation Case Study in Kampala, Uganda

MSc Thesis

Musa Mwine
5283876

Delft University of Technology
Faculty of Civil Engineering & Geosciences
Department of Transport and Planning

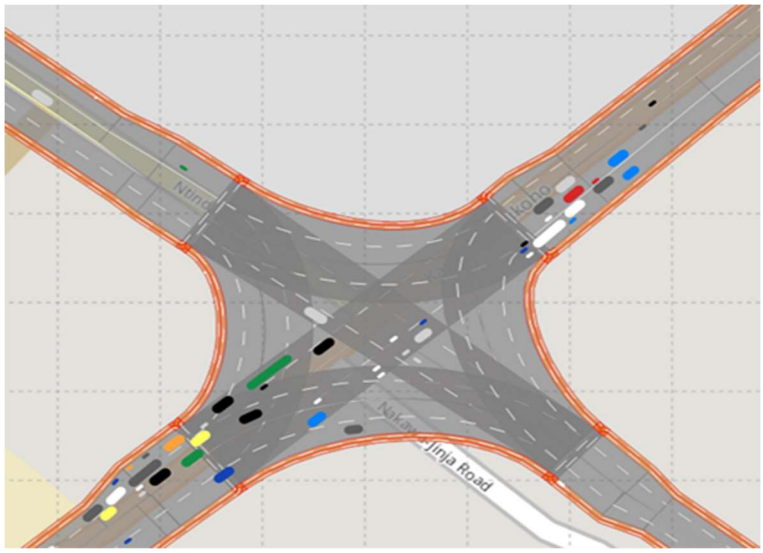

TU Delft

SWOV
INSTITUTE FOR ROAD SAFETY RESEARCH

Impacts of Motorcycle Dedicated Lanes on Traffic Flow & Safety of Unsignalized Intersections–A Microsimulation Case Study in Kampala, Uganda

Master of Science in Civil Engineering

Track: Transport and Planning

by

Musa Mwine

July 2022

Assessment Committee:

TU Delft

Dr. Haneen Farah

Dr. Maria Salomons

Dr. Amir Pooyan Afghari

Dr. Narayana Raju

SWOV

Dr. Ragnhild Davidse

Mr. Govert Schermers

TU Delft

SWOV INSTITUTE FOR ROAD SAFETY RESEARCH

Abstract

Traffic congestion and undeveloped public transport define the modus operandi in Kampala, the capital city of Uganda. Most people see motorcycles as a solution to escape the growing traffic congestion and poor public transport. Motorcycles are considered a fast, cheap, and efficient alternative mode of transport. However, Kampala is characterized by poor road infrastructure for vulnerable road users such as motorcyclists and their passengers. The roads are neither structurally maintained nor marked and above all a motorcycle is not considered as a design vehicle. In addition, motorcyclists in Kampala follow a "law of the jungle" mentality as they do not follow traffic rules or respect other road users. Such conditions exacerbate the risk of all road users. This study thus aimed to determine the traffic efficiency and safety effectiveness of introducing motorcycle dedicated lanes in non–lane based and mixed traffic. These effects were studied by microsimulation of unsignalized intersections without priority markings in urban areas of developing countries.

The use of microsimulation was best suited for this study since dedicated motorcycle lanes are not yet implemented in Kampala. The study centered on an intersection commonly known as "Spear Motors" in Kampala, but the concept can be applied to other unsignalized intersections in urban areas of developing countries. In addition, off-peak traffic was simulated since traffic police controls the intersection during peak time and microsimulation model cannot simulate traffic while a policeman (or two) is on duty.

Video images of the intersection were officially obtained from Uganda Police and processed to traffic data such as traffic volume, trajectories, composition, and conflicts. Video data could be analyzed with high precision and its collection is less risky and time consuming compared to manual observations. In addition, geometric data (lane width, slope, intersection dimensions, coordinates, and aerial pictures) about the intersection was physically collected during a daytime site visit.

A representation of the current traffic conditions at the intersection, referred to as the base model, was developed in VISSIM 21 which has been used in previous studies especially in India to simulate non-lane based and mixed traffic. The base model was calibrated using both maximum occupation time and maximum queue length of vehicles on the minor roads using Particle Swarm Optimization (PSO). Thus, the model was calibrated using traffic flow parameters but not safety indicators. PSO capitalizes on swarm intelligence by allowing information flow between the particles. Optimum values for eleven parameters were obtained and subsequently used in both validation and scenario development. Notably, calibration based on gap acceptance was not relevant in this use case, as vehicles usually negotiate, and hierarchy of roads is mostly not respected.

The base model was validated microscopically using occupation time and queue length of minor road vehicles and motorcycles. In addition, independent samples t-tests were carried out to further confirm that the base model could replicate observed traffic conditions. Regarding macroscopic validation, fundamental diagrams of observed and simulated data overlapped and most of the points were on the uncongested part. This was expected since off-peak traffic was simulated.

Three scenarios (see figure below) were considered in this study, which are: scenario 1 with straight crossings of motorcycles in the intersection, scenario 2 with deflected crossings and scenario 3 with a roundabout separated for the main road traffic and motorcycles. These scenarios were developed using the same data as for the validation, and Ugandan guidelines on design of roundabouts were applied.

Scenario 1: Straight crossings

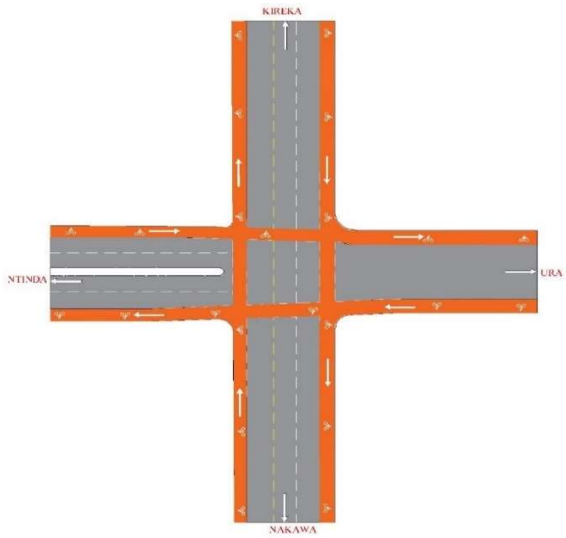

Scenario 2: Deflected crossings

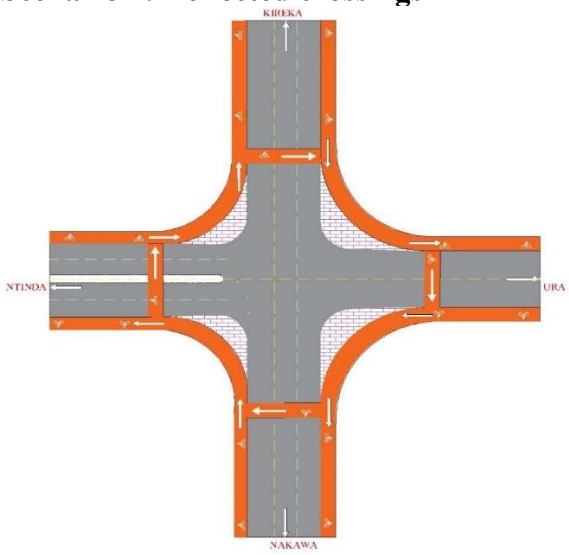

Scenario 3: roundabout

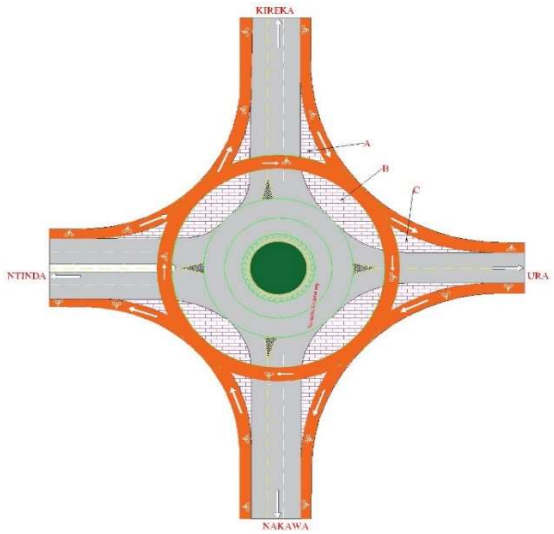

Simulations with driver behavior parameters set to optimum values were performed to replicate the actual behavior. Consequently, traffic conflicts were generated from vehicle trajectories per scenario. Post Encroachment Time (PET) and Time to Collision (TTC) were calculated for the conflicts. The use of conflicts is proactive compared to reactive approaches that use crashes.

The use of deflected crossings for motorcycles and then a roundabout separated for main traffic and motorcycles increased the flow of the intersection by 31% and 20%, respectively. Additionally, the implementation of deflected motorcycle crossings and roundabout reduced critical density by 38.6% and 63.7%, respectively. In all scenarios, the average speed was within the range of 8-25km/h both on the main road and motorcycle dedicated lanes. Regarding

delays at the intersection, most motorists were delayed by less than 25s compared to more than 50s without motorcycle dedicated lanes (base simulated scenario).

Regarding safety, more benefits are expected by using either deflected crossings or roundabout than straight crossings. The number of severe critical conflicts reduced by 87.9% with the application of a roundabout separated for main road traffic and motorcycles. This is higher than the decrease of 48.5% after the application of dedicated motorcycle lanes with deflected crossings. To determine the conflict rates per scenario, the number of severe critical conflicts was divided by total traffic simulated. Deflected crossings for motorcycles reduced severe critical conflict rate by 40% whilst it decreased by 75% with intersection improvement to a roundabout separated for main traffic and motorcycles. Severe critical conflicts categorized based on interaction and conflict types decreased more with use of a roundabout separated for main road traffic and motorcycles than motorcycle lanes with deflected crossings. Interaction types of Vehicle-to-Vehicle (V2V), Vehicle-to-Motorcycle (V2M) and Motorcycle-to-Motorcycle (M2M) were considered. On the other hand, the conflict types included crossing, rear-end and lane change. Furthermore, percentage increments of key findings are summarized in the table below for traffic flow of the major approaches and safety of the entire study intersection. Scenario 2 with deflected crossings led to an increase in traffic flow in comparison to the base scenario whilst scenario 3 with a roundabout reduced both the distributions and rates of severe critical conflicts by high margins.

Effect	**Major approaches/safety metric**	**Parameter**	**Scenario 2: Deflected crossings**	**Scenario 3: roundabout**
Traffic flow	Main Road (MR)	Critical density	-41.7	-50.0
		Average speed	15.9	24.5
		Level of Service	40.1	80.2
	Motorcycle Lane (ML)	Critical density	-36.7	-66.5
		Average speed	10.4	104.8
		Level of Service	40.3	50.2
	Both (MR & ML)	Flow	25.0	12.8
Safety (severe critical conflicts)	Distributions	Number of conflicts	-48.5	-87.9
		V2M	-39.6	-86.5
		Crossing conflicts	-55.6	-97.8
	Conflict rate	Total conflict rate	-40.0	-75.0
		V2M	-62.5	-75.0
		Crossing conflicts	-50.0	-91.7

With the high motorcycle demand of over 50% of traffic, implementation of dedicated motorcycle lanes at unsignalized intersections as well as urban roads in general will result into better flow of traffic. In addition, the motorcycle lanes will contribute to the general road safety in Kampala. Dedicated motorcycle lanes with deflected crossings can be implemented at existing 4-leg and 3-leg unsignalized intersections due to less space requirements while the option with roundabouts can work best for new projects. The study recommends that a pilot project is started in Kampala to further understand not only the driver behavior (usability) but also acceptability. Policies to advocate for the implementation of dedicated motorcycle lanes are also needed as well as education and awareness campaigns.

Preface

In my academic and professional journey, I have been persuaded to contribute to safer roads in not only my dear country Uganda but also other developing countries. The impact of road crashes in Uganda is not well quantified to date and is exceedingly higher than imagined. My long-held desire to substantially promote road safety initiated the conceptualization of this study even before coming to the Netherlands. I was awarded a Sub-Saharan Africa (SSA) Scholarship by the TU Delft Global Initiative to realize my set goal. This formed the basis to undertake a microsimulation study of motorcycle dedicated lanes and their road safety impact in Kampala, the capital city of Uganda.

The study was undertaken at the Institute for Road safety Research (SWOV) in the Hague, Netherlands. I interned at SWOV for about nine months and the team was always supportive. I was allowed to be at office every day and I tried my best to utilize the resources available to me. Even amidst the COVID-19 restrictions, the doors at SWOV were open for me to undertake my study. The team at SWOV was exceptional and I always discussed all my challenges with them.

During this study, I was assisted by many people, and I would like to appreciate some of them. First, I thank my supervisors both at TU Delft and SWOV for their enormous support during the journey. They attended all my meetings and provided feedback on time so that I could complete on time. Above all, they motivated me to always challenge myself and to do my best.

I am thankful to the Permanent Secretary of the Ministry of Works and Transport (MOWT), Mr. Bageya Waiswa who introduced me to Uganda Police Force (UPF) for the data. On the other hand, he approved my study leave for 2 years to concentrate on my master's studies in the Netherlands. I also appreciate my other superiors and workmates at MOWT that were very supportive in this academic journey.

My study was made possible by the UPF that availed video data. The Officers in the Cameras' Unit especially Allan Sekyanzi and Etuket Vincent worked tirelessly to download all the required data and ensure that all agreements are signed. The received video recordings were later processed by Transoft Solutions to what I could use in the study.

I am highly indebted to my family especially my dear wife, Daphine and my brothers who persistently made sure that I was on track to complete my studies. Daphine proofread my report and helped me improve its quality. I am also grateful for my friends and classmates that were supportive in this venture.

I am immensely proud of this report which exhibits my effort. I hope it is a pleasant read.

Musa Mwine

Delft, July 2022

Table of Contents

List of tables

List of figures

List of acronyms

Acronym	Meaning
AASHTO	American Association of State Highway and Transportation Officials
ADB	African Development Bank
cf	cumulative frequency
CID	Central Island Diameter
COM	Component Object Model
EAT	East African Time
f	frequency
FDs	Fundamental Diagrams
FHWA	Federal Highway Administration
GA	Genetic Algorithm
GDP	Gross Domestic Product
GDPR	General Data Protection Regulation
GEH Statistic	Geoffrey E. Havers Statistic
GPS	Global Positioning System
HCM	Highway Capacity Manual
HGVs	Heavy Good Vehicles
ICD	Inscribed Circle Diameter
iRAP	International Roads Assessment Programme
KCCA	Kampala Capital City Authority
LGVs	Light Good Vehicles
LoS	Level of Service
M2M	Motorcycle-to-Motorcycle
MOWT	Ministry of Works and Transport
PAHO	Pan American Health Organization
PCUs	Passenger Car Units
PET	Post Encroachment Time
PSO	Particle Swarm Optimization
SSAM	Surrogate Safety Assessment Model
SUVs	Sport Utility Vehicles
SWOV	Stichting Wetenschappelijk Onderzoek Verkeersveiligheid
TTC	Time to Collision
UGX	Ugandan Shillings
UN	United Nations
URA	Uganda Revenue Authority
USD	United Stated Dollar
V2M	Vehicle-to-Motorcycle
V2V	Vehicle-to-Vehicle
VRUs	Vulnerable Road Users
WHO	World Health Organization

1|Introduction

1.1 Background

Kampala, the capital city of Uganda has a land area of about 190km^2 and had a night-time population of about 1.5 million people in 2014 according to the Uganda Bureau of Statistic (UBOS) census (UBOS, 2020). The estimated day-time population is about 4.0 million people which increases the need for road mobility within the city (Vermeiren et al., 2015). Road transport is dominant in Kampala compared to rail and water and accounts for over 90% of transportation of people and goods according to the Kampala Capital City Authority (KCCA) (2019). The situation is worsened by the high population growth and rural-urban migration that increase the demand to safely travel from one place to another. The high traffic demand increases congestion which mainly results into loss of productive time and hence negatively affecting the economy. Researchers such as Kwikiriza (2016) propose that expansion of road infrastructure especially at intersections can increase throughput and hence minimise the effects of traffic congestion.

Road users are not only exposed to traffic congestion as explained in the above paragraph but also to road traffic crashes. According to the latest report from World Health Organization (WHO) (2018), road traffic crashes are the leading cause of death for children and young adults aged 5–29 years old in the world. They are the eighth leading cause of death for all age groups surpassing HIV/AIDS, tuberculosis and diarrhoeal diseases. Their burden is disproportionately borne by Vulnerable Road Users (VRUs) including motorcyclists and 90% of the world's road fatalities occur in low-and middle-income countries, even though these countries have approximately 54% of the world's vehicles (WHO, 2022).

In Africa, the mortality rate of a road crash increased from 24.1 per 100,000 population in 2010 to 26.6 per 100,000 population in 2016 according to a report by Segui-Gomez et al. (2021) for the World Bank. The report further specified that 53% of the road fatalities in Africa are VRUs including motorcyclists and if action is not taken, fatalities per capita is expected to double from 2015 to 2030.

Regarding road safety in Uganda, a review by the United Nations (UN) (2018) found that road crash fatalities have increased over 10 years from 2,597 to 3,503 in 2016 representing a growth of 25.9%. The same report indicated a crash severity index of 24 fatalities per 100 road crashes. In addition, Uganda registered the highest road fatalities in the East African region with an average of 10 people per day which results into an overall annual cost of approximately UGX 4.4 trillion ($1.2 billion) for road crashes. This cost is equivalent to 5% of Uganda's Gross Domestic Product (GDP). Furthermore, the report pointed out that the number of motorcycles in Kampala increased from 15,979 in 2007 to 405,124 in 2014, representing an annual growth rate of approximately 59%. Notably, motorcyclists were most involved in serious injury crashes in 2016 according to the report.

In Uganda, motorcycles (commonly known as boda bodas) are a major form of (public) transport especially in urban areas. In many cities this form of transport is extensively used as an alternative to taxi and more traditional public transport. This mode of transport is preferred because they are perceived to be very flexible especially in heavy traffic, are cheap, and have low maintenance needs during operation (Vaca et al., 2020).

In view of improving motorcycle safety, the recent global action plan for road safety for the decade 2021–2030 emphasizes the need for safe road infrastructure for motorcyclists in order to attain a target of at least 50% reduction of crashes (WHO & UN, 2021). The plan focuses on a safe system approach and notes that humans make errors and therefore, the infrastructure and solutions must be designed around those failures and be forgiving. In addition, SWOV (2008) proposes separation of traffic in terms of mass, speed and direction to improve road safety as part of the safe systems approach and hence provision of dedicated motorcycle lanes can serve the purpose.

Likewise, a study commissioned by the African Development Bank (ADB) on motorcycle safety in Africa recommended revising existing road design standards and guidelines, implementing interventions such as separate lanes dedicated for motorcycle use (Tripodi et al., 2020). Such measures are aimed at increasing both vehicular traffic flow and safety of mainly motorcyclists and their passengers but also other vulnerable road users such as pedestrians as further explained in section 2.2.

This study focussed on finding a solution to the high crash risk of motorcyclists at unsignalized intersections in Kampala and consequently affecting traffic flow. The fact that motorcyclists percolate through traffic congestion justifies why this study was more inclined to solving their apparent safety problem but in the constraints of traffic flow. In addition, an intervention that solves a problem for a certain group of people and creates another problem for another group of people may not be desirable. Of note is that Rumar (1999) emphasizes that the general problem is how to reduce exposure to traffic volume without compromising mobility. The impacts of dedicated motorcycle lanes on both traffic flow and safety will be investigated using microsimulation. In addition, surrogate safety measures such as Post Encroachment Time (PET) and Time to Collision (TTC) were applied in this study. An introduction of these methods is discussed in section 1.4.

1.2 Study objective

The objective of this study is:

To determine the effectiveness of introducing motorcycle dedicated lanes on traffic flow and safety, in non–lane based and mixed traffic. These effects were studied by microsimulation of unsignalized intersections without priority markings in urban areas of developing countries.

1.3 Study questions

The main research question of this study was:

What are the effects of introducing dedicated motorcycle lanes on traffic efficiency and safety in non–lane based and mixed traffic at unsignalized intersections in urban areas of developing countries?

The following sub-questions were investigated:

i. To what extent is microsimulation suitable for traffic flow and safety evaluation of unsignalized intersections in urban areas of developing countries?
ii. How do motorcycle dedicated lanes affect the traffic flow at unsignalized intersections?

iii. What is the impact of applying motorcycle dedicated lanes on traffic conflicts and interactions at unsignalized intersections in urban areas of developing countries using both PET and TTC?

1.4 Brief on the methods

As it has been pointed out in the main research question, microsimulation modelling was used to assess the impacts of the dedicated motorcycle lanes onto traffic performance in terms of flow and safety. The justification and limitations of microsimulation as well as the supplementary surrogate safety measures are presented in this section.

In the first place, traditional approaches have been used to evaluate infrastructure measures for road safety. These measures are reactive and generally crash based (e.g., before-after studies, black spot identification programs) but proactive approaches such as road safety audits and inspections and road infrastructure assessment (e.g., International Road Assessment Programme-iRAP) are also being widely applied. Reactive approaches are dependent on the accumulation of adequate volumes and quality of crash data to identify problems and to develop solutions (Mahmud et al., 2016). Proactive approaches aim at detecting problems before they are built by assessing the safety of road design throughout the design life cycle whereas inspections note changes in time and prevent deterioration. Secondly, traditional approaches are prone to discrepancies in crash registration and reporting, as pointed out by WHO (2018), which are more pronounced in developing countries like Uganda.

Conversely, simulating traffic in a virtual environment can be used to study the impact of traffic flow and safety interventions. This approach which is referred to as microsimulation has been used in the past for traffic flow and road safety interventions that have not been implemented as specific data are extracted from the model in a microsimulation tool (Hasain & Ahmed, 2021). For example, detectors can be used to count vehicles and record speed for traffic flow analysis and user trajectories on planned dedicated motorcycle lanes can be obtained in microsimulation software applications such as VISSIM, PARAMICS, AIMSUN among others and further analysed to generate traffic conflicts. These software applications allow the incorporation of driver behavior and vehicle parameters into the modelling environment. The observed speed distribution, acceleration, deceleration and vehicle characteristics are used in microsimulation modelling. To be specific, these microsimulation models have underlying behavioral and vehicle models with parameters covering aspects such as headways, stopping and lane change behavior, acceleration/deceleration which can be changed to approximate local conditions. The interactions of different road users in a simulated environment can be studied and hence understanding traffic flow and road safety.

Nevertheless, the use of microsimulation has several limitations in road safety as suggested by different researchers. Firstly, Caliendo and Guida (2012) note that heavy assumptions are made for driving behavior to avoid crashes during microsimulation. Henceforth microsimulation models must be well calibrated to reflect prevailing driver behavior and traffic flow. Secondly, Mahmud et al. (2019) pointed out that vehicle trajectories in microsimulation are not modelled in a realistic way as vehicles stick to particular lanes. In order to model non-lane based and mixed traffic, free flow lane change is used to enable vehicles, especially motorcycles, to overtake whenever possible. Cars can overtake on multi-lane carriageways since they are not limited by the lane. Thirdly, most microsimulation development and application relates to homogenous traffic conditions in developed countries (Lenorzer et al., 2015). Some vehicle

types like taxis in Kampala are not included but can be imported. Fourthly, single vehicle crashes are not considered as well as those crashes involving more than two vehicles in the analysis of conflicts (Gettman & Head, 2003). These flaws limit the accuracy of microsimulation models and thus the ability to replicate traffic conditions in developing countries. Notwithstanding these limitations, Mahmud et al. (2019) conclude that even if microsimulation development aims more at transportation efficiency than safety, traffic safety microsimulation provides a detailed and controlled environment for road safety analysis.

In an attempt to overcome the deficiencies of traditional approaches, researchers have developed surrogate safety approaches (Mahmud et al., 2019; Tarko, 2018) in which near misses and/or serious conflicts are captured instead of crash data. Conflict is defined as an observable situation in which two or more road users approach each other in time and space to such an extent that there is a risk of collision if their movements remain unchanged (Gettman & Head, 2003; Goyani et al., 2019; Vedagiri & Killi, 2015). These surrogate safety measures include Time to Collision (TTC) and Post Encroachment Time (PET) and are defined in section 2.5.2. Some researchers have found that the causes of traffic conflicts are similar to those for crashes (Bulla-Cruz et al., 2020; El-Basyouny & Sayed, 2013; Sacchi et al., 2013). Yet, the relationship between traffic conflicts and crashes is debatable and some studies recommended further testing of the correlation between conflicts and crashes (Zheng et al., 2014). Despite reservations, conflict analysis is relatively commonplace in road safety research. Conflict measuring techniques have been used for numerous years and are evolving to automatic identification through image processing technologies. Also, many state-of-the-art traffic microsimulation models have adopted surrogate safety measures as standard output.

It is important however, not to overemphasis the strengths of using surrogate safety measures such as TTC and PET in research, they also have weaknesses as identified in some studies. For instance, Mahmud et al. (2019) found that TTC ignores many potential conflicts due to acceleration or deceleration and is not suitable for lane change conflicts. TTC is premised on an assumption that consecutive vehicles maintain constant speed and thus disregards acceleration variation towards the leading vehicle or during lane changes. Consequently, use of TTC to analyze unsignalized intersections where vehicles must decelerate as they approach and accelerate at the exit results into underestimating conflicts. In addition, both TTC and PET are unable to quantify conflict severity since they do not consider the magnitude of evasive actions.

In summary, microsimulation can be used to study traffic flow and safety can be evaluated when surrogate safety measures such as PET and TTC are generated from simulated trajectories. However, these safety measure do not give information on conflict severity. These methods are further discussed in section 2.5 under literature review.

1.5 Problem statement

The methods summarized in the preceding section were employed to address the main problem of road safety especially to motorcyclists by introducing dedicated motorcycle lanes and their impact on traffic congestion at unsignalized intersections. These problems are discussed below.

With a high population growth rate of 4.03% and rural-urban migration, Kampala is faced with traffic congestion especially in the morning (7:00am to 10:00am East African Time) and evening (4:00pm-8:00pm East African Time) peak hours (KCCA, 2019). In addition, the number of vehicles has steadily increased overtime as people's purchasing power of vehicles

has raised (Baertsch, 2020). A study by Baertsch (2020) quantified the cost of traffic congestion in Kampala and revealed that USD 1.5 million (4.2% of Kampala's daily GDP and 1.9% of Uganda's GDP) is lost per day due to traffic congestion.

Mwanje (2017) notes that severe traffic congestion is a big problem especially at intersections and affects mobility of people. The researcher further highlights the negative effects of traffic congestion in Kampala such as lost productive time, wastage of fuel, increased emissions to the environment, and disruption of businesses. According to respondents in the study, road infrastructure expansion especially at bottlenecks such as intersections could reduce the negative effects of traffic congestion.

Whilst the preceding paragraphs focussed on traffic congestion, road safety in Kampala is also a big challenge as discussed in the next paragraphs. First, the driving behavior in Kampala is characterised by reckless and careless actions as reported by Uganda Police (2020). Van der Griend and Siemonsma (2011) reported that motorcyclists do as they please and follow "law of the jungle" mentality. This condition is exhibited by the way drivers considerably neglect traffic rules and laws such as speed limits, motorcyclists sometimes ride on sidewalks and minibuses randomly stop (on call) at inappropriate places. In addition, their study pointed out that motorcyclists regularly drive in the wrong (opposite) direction, right of way belongs to he or she who claims it, and pedestrians cross wherever it is convenient. The same study states that drivers of motorised vehicles are not aware of the advantages of keeping to their own lanes and use the entire width of the road. The researchers concluded that taxi minibus drivers and motorcyclists were a serious traffic problem since they are aggressive and do not respect other road users. Such traits make the driving behavior in Kampala and other cities in developing countries different from cities in developed countries.

To be able to further understand the state of motorcycle safety in Uganda, the annual crime reports of the Uganda Police (2016, 2017, 2018, 2019, 2020) quantify traffic fatalities registered on both urban and rural roads. It is evident that the number of fatalities amongst motorcycle users (both the motorcyclists and passengers) was generally increasing over time (Figure 1) whilst fatalities in other road user groups were generally stagnant. With the available data, it is impossible to deduce that pedestrians started using motorcycles as the main transport mode and hence the exhibited trend. This trend suggests that motorcycle users as well as pedestrians are highly involved in fatal crashes in Uganda. In addition, more fatalities of motorcycle users than pedestrians were recorded in 2020.

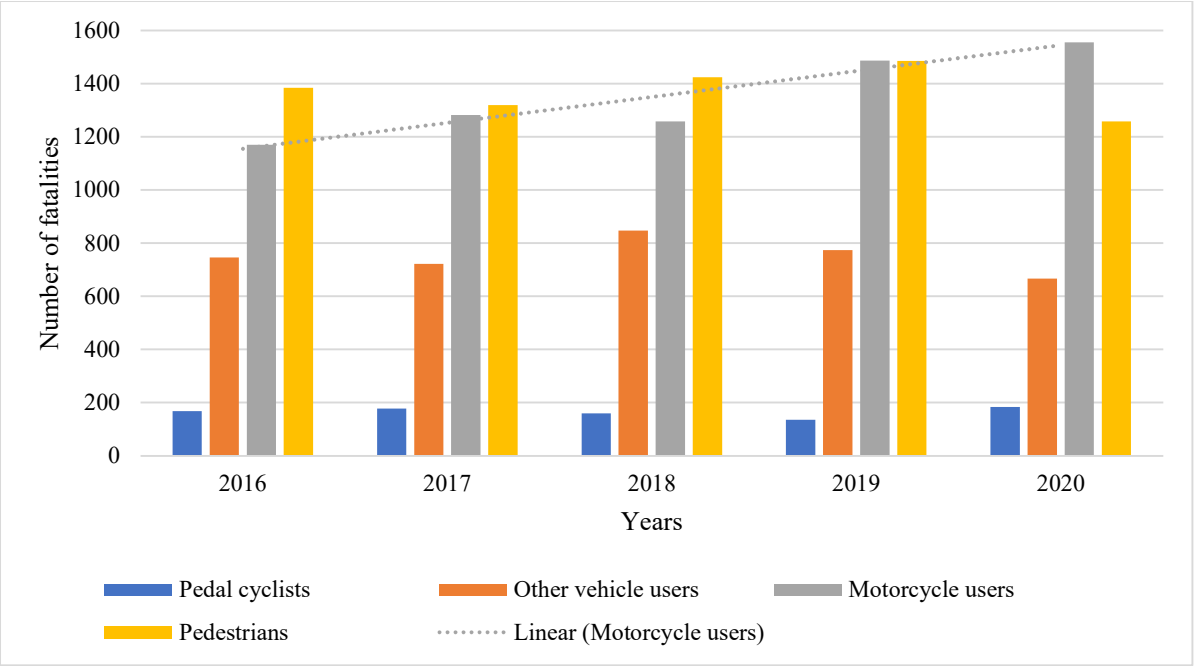

Figure 1: Trend of registered fatalities by road user group overtime

Evidently, more motorcycle users are seriously injured than other road user groups according to the Uganda Police records from 2016 to 2020. The trend of seriously injured pedestrians and other vehicle users decreased overtime whilst that of motorcycle users was largely stagnant as shown in Figure 2. Though, pedestrians and cyclists are more likely than motorcyclists to be fatally involved in a crash based on the fatalities to serious injury ratio. On average, about one pedestrian, cyclist and motorcyclist is fatally injured per one, two and three serious injuries, respectively. This assertion is attributed to higher vulnerability of both pedestrians and cyclists and thus necessitates interventions also for these categories. Importantly, these ratios are for the entire country and not Kampala where the fatality to serious injury ratio for motorcyclists is expected to be higher than in rural areas. Motorcyclists ride at high speeds especially along urban road sections in Kampala to make many trips thus increasing their daily earning (Siya et al., 2019). These over speeding motorcyclists are more exposed to fatal crashes in Kampala than in rural areas because of presence of other traffic in urban areas.

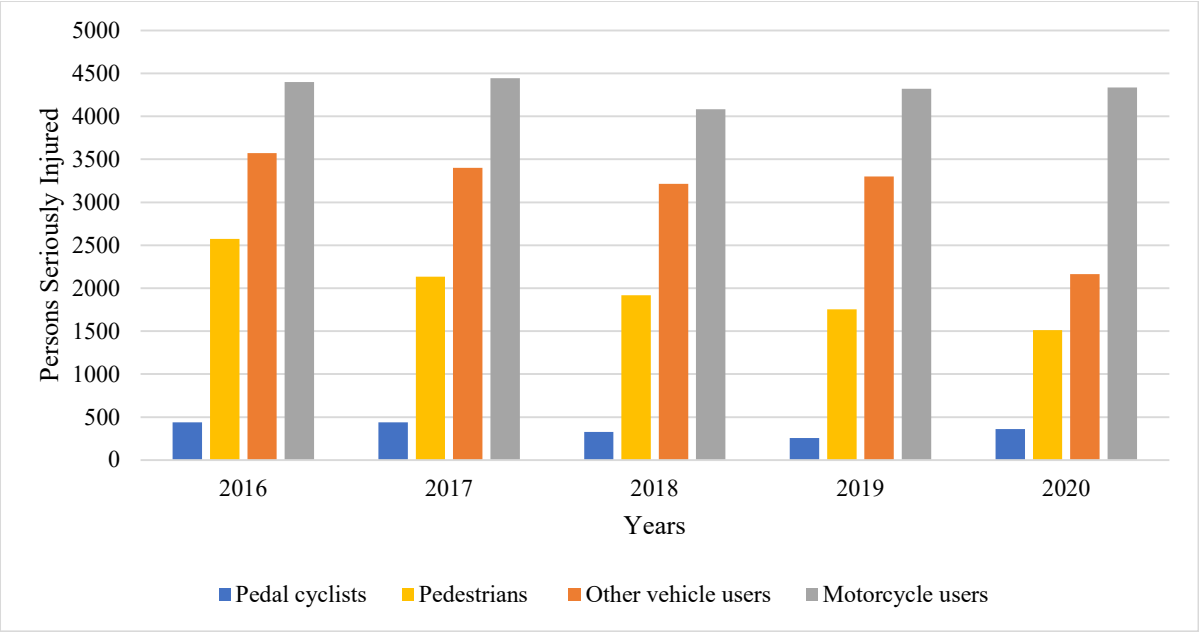

Figure 2: Trend of registered persons seriously injured per road user group overtime

Table 1 indicates the mortality rates per road user category computed for both fatalities and serious injuries based on yearly population estimates of Worldometers (2022). The number of crashes (fatalities or serious injuries) per road user type is divided by the population to determine the corresponding risk rate. On average over the 5-year period, 32 motorcycle users are involved in fatal crashes per one million people. In addition, 101 motorcycle users are seriously injured per year compared to 74 other vehicle users per one million people. The absence of detailed and realistic exposure data such as the number of vehicles in rural or urban areas, kilometres travelled per mode of transport hinder further in-depth understanding of the associated risk per transport mode/road user type. Therefore, it cannot be concluded that motorcycle users are exposed to greater risk for crashes compared to other road user categories.

Table 1: Mortality rates of registered fatalities and serious injuries in Uganda per 1 million people

Road User Category	**Fatalities**					**Serious Injuries**				
	2016	**2017**	**2018**	**2019**	**2020**	**2016**	**2017**	**2018**	**2019**	**2020**
Pedal cyclists	4.24	4.30	3.74	3.07	4.00	11.05	10.64	7.68	5.81	7.89
Other vehicle users	18.82	17.54	19.82	17.46	14.58	90.09	82.64	75.24	74.54	47.29
Motorcycle users	29.51	31.14	29.44	33.57	34.00	110.92	107.98	95.51	97.63	94.77
Pedestrians	34.91	32.04	33.33	33.54	27.50	64.89	51.86	44.86	39.67	33.03

In the above statistics, a fatality is defined as either occurring at the scene of a crash and/or within one year and one day as a result of injuries sustained in a crash (Uganda Police, 2020). This definition may not be critically adhered to while registering fatalities due to resource constraints (Segui-Gomez et al., 2021). In addition, the actual numbers of fatalities or serious injuries are highly likely to be more than the registered numbers considering that some people may not report such cases as stipulated by WHO (2018). Importantly, registered crash data per road user category were not available at regional or local level nor are they disaggregated to urban and rural. It is assumed that a major proportion of the total crashes involving motorcyclists occur in urban areas since most of these vehicles travel in these areas.

Considering the road safety situation in Kampala and not Uganda as a whole, Vaca et al. (2020) found that around 45% of road traffic injuries happened in the City. This trend is also evident in the annual crime report of Uganda Police (2020) in which the Kampala area had about 38% of the total crashes registered in the country. Balikuddembe et al. (2020) also pointed out that 50% of road traffic injuries in Uganda occurred in Kampala and its suburbs. Therefore, providing appropriate interventions for road traffic crashes in Kampala could yield tangible and significant safety and traffic flow results.

At the same time, Balikuddembe et al. (2020) established that 42.1% of crashes among motorists occurred at intersections in Kampala. The study was based on a review of crash data from Uganda police. In that study, unsignalized and signalized intersections were not differentiated. Other international studies in Tanzania, Sri Lanka and India have pointed out that unsignalized intersections are more common than signalized ones and therefore more relevant to this study. For example, almost 60% of the 46 black spots for motorcycle crashes in the city of Dar es salaam, Tanzania were unsignalized (Francis et al. 2021). A study by De Silva et al. (2018) in Sri Lanka noted that 63% of road traffic injuries happened at intersections of which 85% were unsignalized. The same study indicated that most of the road traffic injuries (33%) involved motorcyclists. Similarly, Paul et al. (2018) pointed out that 85% of 176,004 crashes in India happened at unsignalized intersections.

In short, traffic congestion for all vehicles and high crash risk for motorcyclists form the basis of this study. Due to high traffic demand, road users loose productive time in traffic congestion. Motorcycles which are means for (public) transport in Kampala and can percolate through the congested traffic are exposed to high crash risk due to non-adherence to traffic rules and regulations. Above all, the crash risk is much higher for both motorcyclists and their passengers in Kampala at unsignalized intersections than road sections.

1.6 Research gaps and contributions

The research gaps presented in this section were established following the identified problems of motorcyclists in the previous section. Therefore, this study aimed to scientifically contribute to finding a feasible solution to the eminent road safety and traffic flow concerns of motorcyclists at unsignalized intersections.

First, most of the previous investigations of road safety in Kampala but also in other African cities focussed on driving behavior, crash numbers and crash trends. None of these specifically evaluated the effect of introducing new infrastructure measures such as dedicated motorcycle lanes on both safety and traffic flow. Therefore, this study is a first attempt to investigate the potential benefits of implementing dedicated motorcycle lanes in not only Kampala but also cities in other developing countries. A framework for application of these lanes was developed in this study to improve both traffic efficiency and road safety.

Secondly, qualitative studies based on interviews and some quantitative studies using questionnaires have been performed in Uganda and specifically urban roads. Contrarywise, no quantitative study using either traditional approaches such as before and after analysis or microsimulation for an unsignalized junction in urban areas has been implemented. Traffic performance parameters such as acceleration/deceleration distributions, speed distributions of existing traffic in Kampala have thus not been factored into safety assessment. In addition, the effect of safety measures into traffic flow is ignored. Therefore, the road safety problem is not

comprehensively understood which results into varied estimates. The quantitative results of this study can therefore be a basis to segregate traffic to improve both traffic flow and safety.

Regarding data sources, most traffic congestion or road safety studies carried out have relied more on questionnaires and interviews as source of information. More accurate and driver behavior centred sources like video images have not been used to analyse road safety at unsignalized intersections and associated impact on traffic flow of urban roads in Uganda despite the installation of cameras on all key road sections and intersections by the Uganda Police. This study provides an additional use for the available video data at the Uganda Police. For example, the Ministry of Works and Transport (MOWT) can collaborate with the Uganda Police to share data for traffic flow and road safety research.

While a study commissioned by ADB on motorcycle safety in Africa recommended the application of separate lanes dedicated for motorcycle use as one of the interventions, the impacts of the interventions on both traffic flow and safety were not estimated/assessed (Tripodi et al., 2020). The recommendation was derived from a comprehensive review of international guidelines and practices. In that study, traffic counts were conducted on sampled road sections in Kampala, which showed that there were more motorcycles than other vehicles. The study concentrated on the driver behavior and how behavior could be impacted by motorcycle dedicated lanes. The actual proportions of motorcycles as well as other vehicles such as taxis (matatus) were not considered in the study hence ignoring the traffic flow aspect. Thus, the current study is a first attempt to investigate the effects of separating motorcycles from traffic on both traffic efficiency and road safety.

Surrogate safety measures such as PET and TTC have been applied to a limited extent in road safety evaluation of road sections and intersections in Uganda. Yet these safety indicators are robust for safety assessment of road infrastructure even before implementation of an infrastructure measure on a road network like dedicated motorcycle lanes. Therefore, this study is the first to use surrogate safety measures for safety evaluation of unsignalized intersections in Kampala and can be used by researchers for reference.

Lastly, earlier studies simulating traffic conditions at road sections or intersections in developing countries have relied on a Genetic Algorithm (GA) to calibrate the driving behavior. However, GA applies common rules of selection, crossover, mutation at each step and therefore can converge prematurely to a solution. On the other hand, there is limited application of Particle Swarm Optimization (PSO) to calibrate VISSIM driving behavior parameters of an unsignalized intersection in developing countries. Thus, there are less detailed sets of optimum values that can replicate such traffic conditions in microsimulation. The study builds on existing methods to further show their strength in finding scientific solutions to traffic congestion and road safety problems. The optimum values of driver behavior parameters can be used in other scientific studies in developing countries.

This study, therefore, uses microsimulation and surrogate safety measures to develop a framework for introduction of dedicated motorcycle lanes at unsignalized intersections. The effects of these lanes to both safety and traffic flow are quantitatively determined. The framework is further explained in the next section starting with introduction of the motorcycle lanes up to addressing the global challenges of road safety and congestion.

1.7 Conceptual framework

The conceptual framework indicated in Figure 3 depicts the relationships between key dimensions of road safety that are relevant for motorcyclists. The study aims to mainly improve the safety of motorcyclists at unsignalized intersections but at the same time enhance traffic flow. The focus of this study is on the encircled dimensions in a blue box in respect to the impact on traffic flow. The framework envisions a causal relationship and hence suggests one-way arrows from safe systems approach to road safety and traffic congestion which are global challenges. In contrast, Schepers (2013) used two-way arrows between crash risk on one hand and infrastructure, road user behavior and vehicles on the other hand. All the sub-questions are interlinked by the three contributing factors and crash risk concerning traffic and safety analysis of unsignalized intersections.

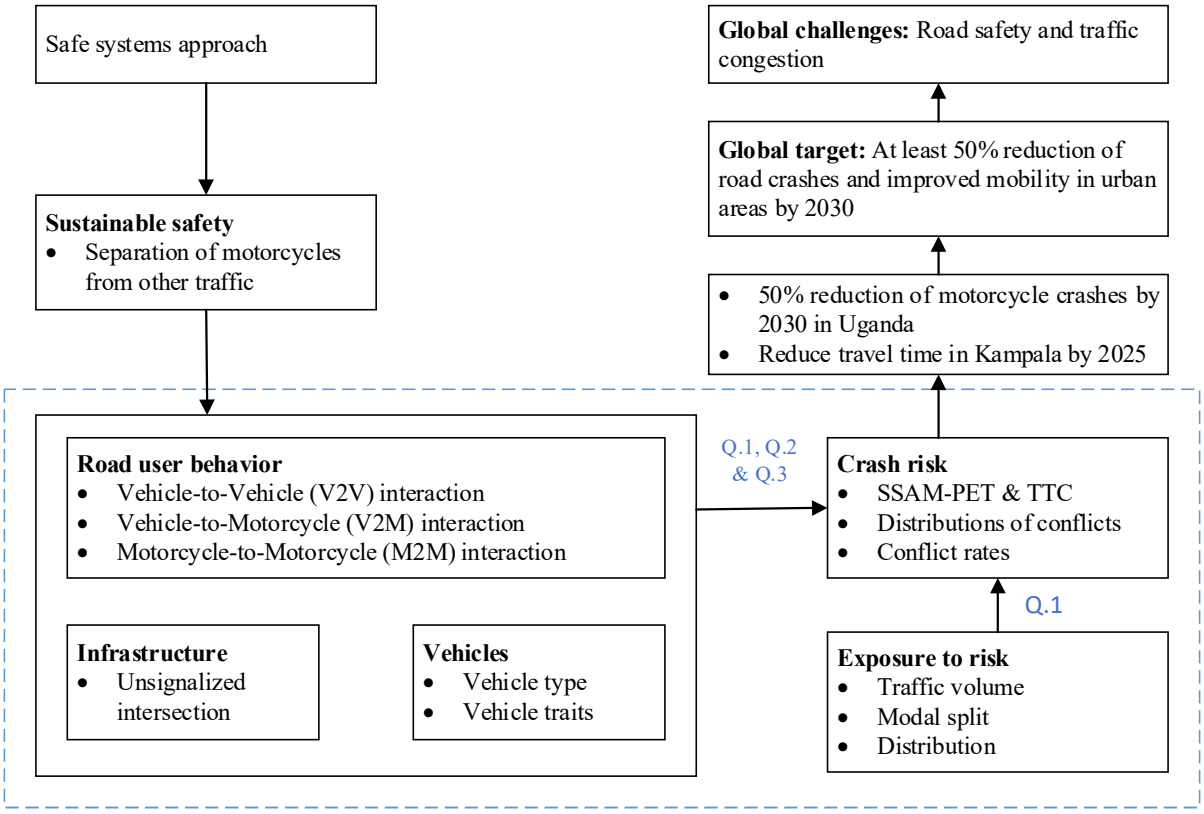

Figure 3: Conceptual framework for this study

First, sustainable safety in the Netherlands is an example of the safe systems approach that has been successful especially with separation of cyclists from vehicles under the homogeneity principle. Suitable lessons and challenges in respect to cyclists are drawn in order to evaluate the traffic flow and safety potential of dedicated motorcycle lanes in Kampala at unsignalized intersections. These lessons are further discussed in the literature review.

In order to introduce dedicated motorcycle lanes, road infrastructure has to be redesigned. Thus, intersection design forms the cornerstone of the study with a base model of the prevailing situation at the target location. This model was further changed to include motorcycle lanes that separate the motorcycle users from other traffic at the intersection. These motorcycle users are susceptible to the kinetic energy of the passenger and more to heavy vehicles that have higher mass and speed. In addition, according to Haddon (1973) these motorcycle users qualify as targets while passenger and heavy vehicles are hazards. His (Haddon) model proposes the

introduction of a barrier to stop or mitigate flow of unwanted energy from a hazard to a vulnerable target thus separation of motorcycles from other traffic.

Thirdly, the framework considers the other two contributing factors (vehicles and road user behavior) than infrastructure to crash risk as well as exposure. The interactions between the main traffic participants of vehicles, motorcycles and pedestrians are taken into account whilst cyclists are not because of the low volume as observed in the video data. Road user traits such as experience, culture, age, gender, training among others influence behavior. The influence of these traits is modelled by determining key parameters that affect car following, lane changing and lateral behavior. For example, variation of driver attributes is taken into account by applying desired speed, acceleration and deceleration distributions in VISSIM using field data. Additionally, different vehicle types such as taxis or matatus which are used in Kampala are considered in addition to the common ones like passenger cars. Vehicle types perform differently on the road due to inherent traits as well as the prevailing conditions. These vehicles as observed at the intersection in Kampala and are incorporated in the microsimulation. Therefore, the interplay between infrastructure, vehicle and road users in microsimulation is critical to determine the traffic flow and crash risk for different road users and thus, applicable to all the study questions.

Regarding exposure to risk, three issues of traffic volume, modal split, distribution are included to reflect the existing traffic conditions and hence accurately estimate the associated risk at the intersection. Traffic volume per road user category yields modal split or traffic composition and the directional split of traffic (approaches and/or exits) at the intersection forms its distribution. The relationship between crash risk and exposure is considered in VISSIM while applying required modifications such as traffic volume in tandem with the first research question about replication of driver behavior by microsimulation.

With proper microsimulation modelling, traffic flow is determined using fundamental diagrams and delay whilst crash risk is determined in terms of distributions of conflicts as well as their conflict rates. Fundamental diagrams are developed using data collected in microsimulation such as speed and number of vehicles per specified time interval. Conflicts are computed using PET, a surrogate safety measure which is suitable for evaluation of transversal conflicts at unsignalized intersections (Goyani et al., 2021; Tarko, 2018). In addition, TTC was also applied to assess occurrence of rear-end conflicts at the intersection. The study applies the Surrogate Safety Assessment Model (SSAM) to determine the conflicts whose distributions and rates are determined for comparison between scenarios. The software processes trajectory data of vehicles driving through a traffic facility in VISSIM and then calculates surrogate measures of each vehicle to vehicle interaction following a certain thresholds (Gettman et al., 2008) such as critical conflicts having a maximum PET and TTC equal to 1.5 seconds.

Finally, the target is to reduce road crashes by at least 50% by 2030 following the the recent global action plan for road safety for the decade 2021–2030 (WHO & UN, 2021). Additionally, the study aimed to reduce the travel time in Kampala from 3.98minutes/km in 2020 to 3.5minutes/km in 2025 (National Planning Authority, 2020). This travel time reduction is a step towards achieving the Uganda Vision 2040 which foresees a capital city (Kampala) with eased congestion and improved traffic flow. Therefore, the study contributes to solving the global challenges of road safety and traffic congestion.

2|Literature Review

Literature review was the basis for formulation of the research questions and conceptual framework. Firstly, section 2.1 presents the core principles of sustainable safety and impact in the Netherlands especially separation of cyclists from traffic to improve their safety. These principles are important for the formulation of the conceptual framework. This concept aligns with the introduction of motorcycle lanes whose effect on both traffic flow and safety (second and third research questions) is introduced in section 2.2. In section 2.3, the nature of motorcyclists in developing countries is discussed to create an understanding of their motives and how they (motorcyclists) behave in traffic. Thereafter, the three contributing factors (road user, vehicle, and infrastructure) to occurrence of crashes in general and traits of motorcycle safety are explored in section 2.4. Lastly, literature about the suitability and use of microsimulation to replicate traffic in developing countries for motorcycle safety studies is examined in section 2.5. This section contributes to the first research question. The section also discusses the use of surrogate safety measures in assessment of motorcycle safety in developing countries.

Specifically for the section 2.5, a systematic review of relevant literature was carried out in this study by searching on google scholar and Scopus whilst only relevant studies were used in other sections. A search query to return only road safety studies using microsimulation of mixed traffic in developing countries and at urban unsignalized intersections was used. In addition, some key studies with significant information such as a microsimulation study at unsignalized intersections in Italy by Caliendo and Guida (2012) and others were used to reinforce the findings.

2.1 Sustainable safety

While the sustainable safety concept has been used in countries like the Netherlands to improve road safety, it can as well be applied in other countries. It forms a building block in the conceptual framework for this study. The current global action plan for road safety supports the incorporation of sustainable safety in infrastructure design to address road safety as a global challenge (WHO & UN, 2021).

Sustainable safety is tailored to the fact that human beings make errors and therefore the objective is to eliminate road crashes from happening and if that is not possible, to minimize the severity outcomes. The approach is proactive and human characteristics are used as the starting point (Wegman et al., 2008). What this means in practice is that road designs must take into account the fallibility of humans and should be both self-explaining and forgiving. The five sustainable safety principles summarized in Table 2 form the cornerstone of discussion for motorcyclists' safety. Recently, the principles have been reformulated into three design and two organizational principles (SWOV, 2018). The design principles are functionality of roads, (bio)mechanics: limiting differences in speed, direction, mass, and size, and giving road users appropriate protection, and psychologics: aligning the design of the road traffic environment with road user competencies. In addition, the organization principles are effectively allocating responsibility, learning and innovating in the traffic system. An earlier version of advancing sustainable safety as indicated in a report by SWOV (2008) is preferred for this study since the stated principles are clearer and more direct for road infrastructure.

Table 2: The five sustainable safety principles (Wegman et al., 2008)

Sustainable Safety Principle	Description
Functionality of roads	Mono-functionality of roads as flow/motorway roads, distributor roads or access roads, in a hierarchically structured road network
Homogeneity of masses and/or speed and direction	Equity in speed, direction, and masses at medium and high speeds
Forgivingness of the environment and of road users	Injury limitation through a forgiving road environment and anticipation of road user behavior
Predictability of road course and road user behavior by a recognizable road design	Road environment and road user behavior that support road user expectations through consistency and continuity in road design
State awareness by the road user	Ability to assess one's task capability to handle the driving task

With sustainable safety, the Dutch use cycle paths which are physically separated from the carriageway and cycle lanes which provide a visibly delineated space on roads as shown in Figure 4 and Figure 5, respectively (Schepers et al., 2017).

Figure 4: On street two–way cycle path in the Netherlands (Bicycle Dutch, 2015)

Figure 5: On street cycle lane in the Netherlands (Bicycle Dutch, 2020)

For instance, Schepers et al. (2017) found out that deflecting a one-way bicycle path by 2-5m from the intersection yielded a 45% lower likelihood of cyclists' crashes at unsignalized intersections. In this study, it was not specified whether cyclists had right-of-way indicated or only traffic from the right had priority. On the other hand, two-way bicycle paths are associated with an elevated risk of about 75% compared to one-way paths. This assertion is because, in the case of right-hand driving, drivers coming from minor roads do not expect cyclists approaching from the right (please note that road users in the Netherlands keep right while in Uganda it's the left). Nonetheless, two-way cycle paths were found to have a net safety benefit by other scholars as indicated in the same study. Above all, in the Netherlands more than three-quarters of the bicycle paths are one-way and hence this contributes immensely to the safety of cyclists. However, cycling in two directions on these one-way bicycle facilities is unsafe as the offending cyclist is least expected. These lessons are important for designing of safe motorcycle lanes.

With regard to homogeneity, the Dutch advancing sustainable safety programme outlines the fundamental risk factors in traffic as speed, mass and direction (Wegman et al., 2008). Speed increases both crash risk and severity since the higher absolute speeds and speed differences of vehicles result in an exponential increase of risk. Increased speeds lead to increased kinetic

energy release at impact which in turn increases severity. Kinetic energy is also dependent on mass of the crash participants as a lighter party absorbs more kinetic energy. Considering protection, motor vehicles like cars and heavy traffic offer much more protection to vehicle occupants whilst they pose significant injury risk to VRUs but also to occupants of other vehicles and motorcycles. They noted that motorcyclists and their passengers have the highest fatality and injury risk in road traffic which is justified by the fundamental risk factors. Furthermore, it was recommended that motorized two wheelers should be separated from other vehicles (Wegman et al., 2008).

Importantly, a principle on homogeneity promotes separation of traffic in term of mass, direction, and speed. Therefore, the safety of motorcyclists in Kampala and other cities in developing countries can be improved with introduction of dedicated motorcycle lanes.

2.2 Effects of dedicated motorcycle lanes

The previous section regarding sustainable safety supported the introduction of dedicated motorcycle lanes. It is, therefore, of interest to understand their effects on both road safety and traffic flow. The effects of dedicated motorcycle lanes at unsignalized intersections on traffic flow and/or safety have to a less extent been studied. In this section, reference is made to the Malaysian guidelines for exclusive motorcycle lanes and other relevant studies.

According to the studies carried out in Malaysia, two distinct concepts related to headway and space define roadway capacity for motorcycles (Kerajaan Malaysia, 2018). The headway concept assumes a lane width of 1.7m and all motorcycles following one another in a queue. With the headway concept, capacity is determined by the number of 1.7m lanes with each lane having a capacity of 3060veh/h. However, in practice motorcycles tend to pass each other even when there is not a full 1.7m lane available and therefore the space concept is applied. With the space concept, capacity is dependent on lane width and as shown in Table 3.

Table 3: Capacity for motorcycle lane widths (Kerajaan Malaysia, 2018)

Motorcycle Lane Width (m)	**Headway Concept:** Capacity=3060 motorcycle/h/lane	**Space Concept:** Capacity=2207 motorcycle/h/lane
	Capacity (motorcycle/h/lane)	Capacity (motorcycle/h/lane)
1.4–1.7	3,060	-
1.8	-	3,973
1.9	-	4,193
2.0	-	4,414
2.1	-	4,635
2.2	-	4,855
2.3	-	5,076
2.4	-	5,297
2.5	-	5,518
2.6	-	5,738
2.7	-	5,959
2.8–3.4	6,120	

Regarding the width of motorcycle lanes, Saini et al. (2022) highlight that lanes are adopted to motorcycle characteristics and rider behavior and so 1.7-4.0m lanes have been used. The researchers emphasize that narrower lanes may compromise the comfort, safety, and performance of the infrastructure whilst wider lanes may be uneconomical and encourage other

vehicles to use the motorcycle facilities. The latter can increase crash risk for motorists and thus is undesirable.

Concerning traffic flow, motorcycle lanes in Indonesia increased traffic volume by approximately 25% while travel speed increased by 10km/h (Saini et al., 2022). Relatedly, Chaipanha et al. (2019) studied the impact of motorcycles and shoulder width on road capacity and attributed the increase in capacity to the ability of motorcycles to use wider shoulders.

Radin Umar (2006) reviewed literature about the safety effectiveness of exclusive motorcycle lanes along road sections in Malaysia. The researcher notes that the motorcycle lanes significantly reduced motorcycle fatalities by 600% while motorcycle crashes reduced significantly by about 39%. In addition, Saini et al. (2022) note that motorcycle lanes can improve road safety by reducing conflicts due to lane changes.

In all the above studies, none focused on unsignalized intersections and so the impacts of motorcycle lanes on both traffic flow and safety at unsignalized intersections have not been explored. For instance, Radin Umar (2006) recommends that further research should be undertaken to understand the safety impact of motorcycle lanes at intersections.

2.3 Motorcyclist safety in developing countries

While dedicated motorcycle lanes have been applied in countries like Malaysia as seen in the preceding section, motorcyclists in Kampala share the same lanes with other traffic. Their crash risk is high and so many researchers have tried to find out the causes, trends and suggested potential solutions. In this section, the state of motorcyclist safety in not only Uganda but also other developing countries is studied. Table 4 summarizes the main finds of relevant and selected studies.

Table 4: Status of motorcycle safety in developing countries

Study	Location	Study description	Main finding(s)
Oporia et al. (2018)	Uganda	Retrospective study-trends and distribution of Road Traffic Injuries (RTIs)	RTIs increased from 37,219 in 2011 to 222,267 in 2014 and were the highest in Kampala (18.3% and 22.6% for injuries and fatalities, respectively)
Ndagire et al. (2019)	Kampala	Cross sectional study on compliance to safety regulations among motorcyclists	0.9% and 24.4% of 340 motorcyclists interviewed were compliant to all the considered safety measures (helmet use, reflector jackets, licences and no pillion driving) and at least three-quarters of the measures, respectively
Siya et al. (2019)	Kampala	Perceived factors associated with motorcycle crashes including competition for passengers to make more money per day, helmet use among others	76% of 200 respondents perceived themselves to be at risk of crashes
Kiwango et al. (2020)	Dar es Salaam, Tanzania	Perception of unsafe driving behavior and reported driving behavior among commercial motorcyclists	19.5% of 400 motorcyclists were often or very often driving fast because of pressure from the passengers.
Tripodi et al. (2020).	Africa including Kampala	General motorcycle safety and carried out some traffic counts	Sampled roads in Kampala had more motorcycles than cars during the peak hours. Motorcycles form approximately 44% of the Annual Average Daily Traffic (AADT) in Uganda
Ghazwan and Lindskog (2005)	10 developing countries in Asia	Behavior and risks of motorcyclists	Motorcyclists had the highest risk when compared to all other modes and between 80-200 times higher than that of bus users

It can be seen from the above analysis that motorcyclists in developing countries are less complaint with traffic rules and are at a relatively high risk especially at unsignalized intersections in urban areas. Damani and Vedagiri (2021) notes that motorcycles have very different behavior compared to cars in terms of physical and dynamic parameters. They further emphasize that heterogeneous traffic patterns in developing countries pose an additional challenge to the researchers who normally tend to focus on the conventional and homogeneous car-based traffic. According to Van der Griend and Siemonsma (2011), motorcyclists in Kampala do not respect other road users and traffic rules. They (motorcyclists) repeatedly overlook traffic lights and drive in the wrong direction. Motorcyclists use all available road space due to the flexibility of the motorcycles. In addition, the same researchers note that

motorcyclists in Kampala usually use shoulders of the roads for overtaking other vehicles and drive on sidewalks in order to pass the highly dense and slow-moving traffic during congestion.

There is also, however, a further point to be taken into account, that is, the differences in the use of motorcycles between developed and developing countries as studied by Nguyen (2013) and summarized in Table 5. This disparity clearly shows the context to consider while designing infrastructure measures for motorcycle safety.

Table 5: Variations of motorcycling between developed and developing Countries (Nguyen, 2013)

Factor	Developed Countries	Developing Countries
Purpose/ use	Commuting, recreational	Main form of transport (mobility)
Engine size	Mainly high engine capacity motorcycles	Predominantly low and medium engine capacity motorcycles
Way of use	Normally single rider	Normally carry passengers, attachments for carriage, delivery, and vending
Intrinsic value	Leisure, and economic reasons	Employment/ entrepreneurship

Notwithstanding the above context, many factors exacerbate the risks for motorcyclists such as the road environment comprised of the presence of mixed traffic, road infrastructure design and the actual state of the roadways. This is further intensified by the motorcycles themselves which are unstable, lack protection from crashes and are influenced by the behavior of road users (PAHO & WHO, 2014). Nguyen (2013) also points out the noticeable characteristics of motorcycles including increased flexibility, accessibility and ease of operation, instability, less visible, lack of physical protection and personal danger in Asian developing countries. In respect to enforcement, Tripodi et al. (2020) identified limited use of helmets, lack of rider licences, over speeding and pillion riding as key issues to motorcycle safety in Africa.

In summary, low-power motorcycles are used as a form of public transport in developing countries and hence are a livelihood. Motorcyclists compete to earn more money and consequently do not adhere to traffic rules. The question whether motorcyclists with such behavior can stick to separate lanes was not answered by this research. As discussed in this section, the dynamics of motorcyclists are complex with many unexpected movements and defined by high crash risk. Secondly, mainly qualitative studies have been carried out and none has even focussed on the quantitative impact of motorcycle lanes at unsignalized intersections.

2.4 Contributing factors to motorcycle crashes

In order to understand the high crash risk of motorcyclists in developing countries, the contributing factors to crashes (human factor/road user, vehicles and the environment/ infrastructure) must be contextualized. These factors are interdependent in nature though they have been studied as standalone in many studies as explained in this section. However, some studies on safety of motorized traffic in general were included in case of limited information specific to developing countries. In addition, no studies were specific to contributory factors to motorcycle crashes on dedicated motorcycle lanes or even at unsignalized intersections in developing countries.

2.4.1 Human factors/road user

Human factors are related to the traffic participant and in this case the motorcyclist. However, the motorcyclists use the same facilities as other road users such as car drivers, cyclists, and pedestrians. Relevant studies were thus reviewed and safety concerns for motorcyclists pointed out.

A study by Chen (2010) concluded that human behavior and impairment (visual and fatigue) account for more than 85% of registered road traffic crashes in Africa. It is thus important to have clearly visible and forgiving motorcycle lanes. The study further identified that speeding is a key contributing factor in 75% of the fatal traffic crashes in South Africa and 25% in Dar-es-Salam, Tanzania. This assertion was attributed to the fact that higher speed reduces the time in which the rider can respond and increases crash severity. Motorcycles were included in the vehicles since they used the same roads as other vehicles.

Pakgohar et al. (2011) studied the role of human factor in the occurrence and severity of all road crashes in Iran and not motorcycles in particular. The study applied accident severity as the dependent variable and four independent variables of age, gender, safety belt and driving license. Whilst gender of drivers had no significant impact on accident severity, a negative relationship between age and rate of fatal accidents in Iran was established. The results also indicated that driving license and safety belt have relationships with severity of crashes in Iran. For example, the rates of injury and fatal crashes increased from 28% and 3% for the participants without a fully registered driving license to 52% and 6%, respectively, if car passengers did not fasten their safety belts. In the study, the contribution of human factor, environmental factor and vehicle factor to all crashes was established as 97.5%, 70.5% and 31.5%, respectively.

The above results for the human factor were comparable to those in a study by Gopalakrishnan (2012) in India. The researcher confirmed that 81.9% of road traffic crashes were due to faults of the road users including motorcyclists, drivers, pedestrians, and cyclists. However, Gichaga (2017) studied crashes along an international highway in Kenya and discovered that human factors/drivers accounted for over 50% of the road crashes and so should be adequately trained to attain sufficient skills. This percentage was specific to the highway and not for all crashes in Kenya.

Based on these studies, the human factor contributes at least 81.9% to occurrence of road traffic crashes. This percentage is not entirely to human factors but rather in combination with the other two factors of road infrastructure and vehicle. This explains why total percentage for all the factors in some of the studies was more than 100%.

2.4.2 Road infrastructure

Road infrastructure includes both paved and unpaved roads and both have intersections of different kinds. According to Chen (2010), infrastructure design and maintenance contributed to less than 5% of the total road crashes. The researcher emphasized that the combined effects of infrastructure and other factors have a devastating effect and hence should not be ignored. On the other hand, Wang et al. (2013) concluded that improved road infrastructure would reduce crashes after studying the effects of traffic characteristics of speed, density and flow on crashes.

Furthermore, Pembuain et al. (2019) reviewed relevant literature in Indonesia to establish the correlation of each road element with crashes. The road elements of geometry (lane width, horizontal curves, vertical curves), road surface condition, roadside hazards, sidewalks, and bus bays, and marking, signs and lights had significant effects on crashes. The researchers advocated for proper design and construction of roads for safety. The same recommendation was made by Gichaga (2017) who emphasized that road design should discourage over-speeding by using traffic signs, road markings, and bumps.

Even when the contribution of infrastructure is seemingly negligible, that is, less than 5% as determined by Chen (2010), well designed and maintained road infrastructure is critical towards safer roads. The global action plan for road safety for the decade 2021–2030 highlights the need for safe road infrastructure for VRUs including motorcyclists (WHO & UN, 2021).

2.4.3 Vehicle or motorcycle

This section focusses on the general traits of a motorcycle as a vehicle and cross cutting issues related to behavior of motorcyclists. These traits explain the risks associated with using motorcycles and how best to improve their safety.

Wegman et al. (2008) in particular, emphasize that motorcyclists travel at high speeds with a relatively low mass and are essentially unprotected in case of a crash. This justifies the need for protective wear such as helmets for both the rider and passenger. More so, this affects design of road elements such as roadside and advancement of motor-friendly guard rails.

Furthermore, Lee et al. (2009) categorizes the characteristic movements of motorcycles into the following eight groups: travelling alongside another vehicle in the same lane, moving to the head of a queue, filtering, swerving or weaving, tailgating, oblique following, maintaining a shorter headway when aligning with the lateral edge of the preceding vehicle and traveling according to the virtual lanes formed dynamically by the surrounding vehicles. These researchers consider all the mentioned traits in the development of a new approach to modelling mixed traffic containing motorcycles in urban areas. Furthermore, Correa (2017) explains that motorcycles can exploit the road space by filtering through a slow-moving flow using the clearance between two (parallel) lanes of slow moving cars or the possibility to weave in and out of a stationary flow of vehicles.

With more focus on a motorcycle as a vehicle, the Transport for London (2016) urban design manual points out additional factors that influence motorcyclist's behavior. Firstly, a motorcycle has two relatively small points of contact with the road surface and so changes in the road surface condition can have a big impact on grip and stability. Secondly, since most braking and steering control is directed through the front tyre, riders try to avoid skidding and losing control by not braking and steering at the same time. Thirdly, anything that causes the tyre to lose grip can lead to a loss of control much more easily than with cars. Lastly, motorcyclists generally follow a different line to that of other motor vehicles in bends. They use the full width of the available traffic lane to minimize the amount of steering input required, maximize grip and their view of the road ahead.

Quantitatively, Chen (2010) determined that vehicle (inclusive of motorcycles) failure contributed 5% to 6% of the total crashes but this contribution increased to 10% once vehicle failure was combined with other contributing factors of road and human. This percentage is because of the different traits mentioned in this section.

Concluding, all the three factors contribute to motorcycle safety since crashes involve a vehicle which must be operated by a driver and on road infrastructure. This fact explains why all the three were included in the conceptual framework for this study. However, the contribution of the human factor is much higher compared to the other factors. Dedicated motorcycle lanes are planned to improve the infrastructure for motorcyclists but at the same time the benefits apply for all road users.

2.5 Microsimulation for motorcycle safety

Microsimulation allows the incorporation of all the three contributing factors in one environment to assess both traffic flow and safety impacts. Other traditional methods such as before and after studies are potential options but dedicated motorcycle lanes have not been implemented in Kampala. Therefore, the impacts of these lanes on traffic performance in terms of traffic flow and safety can best be assessed using microsimulation. The extent to which microsimulation has been used to study these impacts in developing countries is discussed in this section and later combined with findings of this study to answer the first research question.

2.5.1 Microsimulation modelling

Microsimulation is defined as a technique for representing road traffic flow, in which the actions of every individual vehicle are evaluated at sub second intervals by analyzing the interactions of all road users with the road network and traffic control systems (Sykes, 2007). Different microsimulation platforms such as VISSIM, PARAMICS, and AIMSUN have been used to simulate mixed traffic. These microsimulations have been carried out in various studies especially in India for both intersections, and roadway sections on urban roads but also highways. Key lessons and challenges drawn from literature are further explained in this section and are taken into account while developing a methodology for this study.

Microsimulation tools (based on psychophysical car following model) such as VISSIM and PARAMICS among others have been used in studies related to mixed traffic (Mahmud et al., 2019). The researchers further reviewed microsimulation modelling applications for traffic safety evaluation with respect to heterogenous traffic environment. They noted that VISSIM, PARAMICS and AIMSUN are the most used tools for safety evaluation because of they are comparatively more user friendly for development of non-lane based heterogenous traffic microsimulation. The vehicle and driver behavior can easily be modified and controlled hence facilitating road safety assessment.

Specifically, VISSIM uses the Wiedemann-74 psycho-physical model which uses both relative speed and relative distance to control the vehicle–following behavior of the follower to the leader. The four modes of free driving, approaching, following, and braking are considered in the model. The model includes the following parameters, the minimum distance headway in standstill condition (AX), the minimum desired following distance to avoid collision (ABX), the additive part of safety distance (bx_{Add}), and the multiplicative part of the safety distance (bx_{Mult}), speed of the slow-moving vehicle of either the leader or the follower (V_{slower}), z is a value of range [0.1], which is normally distributed around 0.5 with a standard deviation of 0.15. Equation [2-1] indicates a relationship between the parameters of Wiedemann–74 model for following behavior.

$$ABX = AX + (bx_{Add} + bx_{Mult} \times N[0.5,0.15]) \times \sqrt{V_{slower}} \quad [2\text{-}1]$$

ABX is identified as the minimum relative distance in the aggregated hysteresis plots of each vehicle category.

Given, the advantages of VISSIM stated in the previous paragraphs, Vuong et al. (2019) was able to simulate multimodal traffic flow (with motorcycles) on complex geometries of intersections. Additionally, VISSIM allows lateral behavior of motorcycles and so well suited for the mixed traffic condition in developing countries. The researchers also noted that the different parameters of fine-tuning driving behavior can be changed using conflict areas, priority rules and vehicle traits to simulate the existing traffic conditions.

A contrary explanation by Mahmud et al. (2019) is that, most microsimulation packages were developed to relate traffic environment in developed countries with lane based and homogenous traffic. This point is also sustained by the work of, Matcha et al. (2020) who highlighted that 2D traffic modelling using VISSIM of heterogenous traffic conditions is unsuccessful. This failure is mainly attributed to the following reasons: bottleneck formation due to low-speed vehicles in mixed traffic flow, high dependence on car following models which consider only one influential leader for the following vehicle, no traffic assignment algorithm and failure to model lateral displacement within a lane. However at the same time, Mahmud et al. (2019) revealed that microsimulation models have been applied to non-lane based heterogenous environments in developing countries. The same position was also maintained by Matcha et al. (2020) who indicated that only three modelling platforms: SUMO, VISSIM and AIMSUN can model lateral behavior that is prevalent and time discrete in mixed traffic. Therefore, the three platforms are successful in simulating the mixed traffic scenarios based on time-step frameworks. These frameworks are defined by simulation resolution that states the number of times road users move per simulation second.

Another limitation of microsimulation with VISSIM was pointed out during the validation of Surrogate Safety Assessment Model (SSAM) by U.S. Department of Transportation (2008). A high number of rear-end and lane change conflicts were noted. This discrepancy was associated to the deficiencies of microsimulation using VISSIM as trailing vehicles drove through stopped or slow-moving leader vehicles that partially completed lane changes. These tilted vehicles were not seen by trailing drivers especially during free lane changing. Additionally concerns included: increase of rear-end conflicts with increase of vehicle stops, abrupt changing of lanes and no variable driver reaction time in VISSIM and so drivers follow the same patterns.

Despite of the above weaknesses, microsimulation packages have been used to study the impact of human factors on safety. For example Baran et al. (2019) applied VISSIM to study both traffic performance and safety for an unsignalized T–intersection in the USA based on driver age and experience. Different scenarios with input of age and experience were executed but in a developed country. Regarding to road safety in developing countries, VISSIM has been successfully used in most studies in India as indicated in section 2.5.2.

Microsimulation models must be calibrated to identify optimum driving behavior parameters in respect to field data so that the model can correctly represent the observed traffic conditions. This optimization is more important for safety research than even capacity studies. Different studies have used either Genetic Algorithm (GA) or Particle Swarm Optimisation (PSO) as discussed below.

Proponents of GA as the first heuristic such as Paul et al. (2017) used the 85^{th} percentile gap time accepted by the least prioritized minor road vehicles (microscopic) at an unsignalized

intersection as performance measure during calibration. GA aims at generating a high-quality optimization solution through natural selection and survival of the fittest. However, this study did not consider a high volume of motorcycles that are not compliant with traffic rules such as when to yield for another movement. Additionally, GA applies common rules of selection, crossover, mutation at each step and therefore can converge prematurely to a solution (Majeed & Kumar, 2014). Other studies have also used GA to calibrate VISSIM parameters (Bhattacharyya et al., 2020; Dadashzadeh et al., 2019; Siddharth & Ramadurai, 2013; Tettamanti et al., 2015).

Another meta heuristic known as PSO has been used to calibrate driver behavior for mixed traffic. PSO is based on social behavior of particles for example bird flocking and fish schooling. The method has been applied in calibration of VISSIM parameters at signalized intersections and highways. Specifically, Dabiri and Abbas (2016) used a PSO algorithm to generate arterial traffic signal timing parameters. The study revealed that the method is promising and outperforms other optimization methods (e.g., VISTRO-a commercial optimization tool) for various traffic states.

Likewise, PSO is regarded to be a computationally inexpensive approach in terms of both memory requirements and speed (Russell Eberhart & Kennedy, 1995). In addition, the researchers identified other advantages of PSO over GA and which include: interaction in the group enhances as the optimization progresses towards the solution; particles in the swarm have memory unlike in GA where changes in the population result into destruction of previous knowledge of the problem (expect with elitism where a few of the particles retain their identities); all particles retain knowledge of good solutions; and particles that bypass the best solutions are compelled to return towards the optima.

Tran et al. (2013) highlight the importance of having good quality data for calibration. The researchers associated the discrepancy between the observed and simulated traffic conditions to the difference in behavior and flexibility of vehicle categories. In addition, they concluded that microsimulation can best be applied using different sets of parameters for motorcycles and car traffic. This recommendation had earlier been applied by Kumar et al. (2012) who used different driving behavior parameters for an urban lane and a motorcycle lane.

From the above literature, microsimulation has potential to simulate non-lane based and mixed traffic in developing countries for both traffic flow and safety assessment. With calibration, the driver behavior parameters are optimized to reflect the field traffic conditions. However, it is also noted that microsimulation was mainly developed for traffic efficiency than safety.

2.5.2 Use of surrogate safety measures

Microsimulation is further enhanced by surrogate safety measures to ably evaluate traffic conflicts. Vehicle trajectories from microsimulation are used to generate conflicts with defined values for safety indicators such as Post Enchronchment Time (PET) and Time to Collision (TTC).

Due to the fact that crashes are random, rare, not well reported and go through an unclear process up to final crash outcome, the use of surrogate safety measures can be an alternative in safety analysis (Laureshyn & Varhelyi, 2018). The researchers also emphasized that the use of traffic conflicts is based on the concept of the safety pyramid with a few interconnected elementary events with differing degree of severity. These events include encounters at the lower level, potential conflicts, slight conflicts, serious conflicts and finally crashes on the top

of the pyramid. Crashes are further sub-divided into damage only, slight injury, severe injury, and fatalities. So, the frequency of rare crashes can be predicted based on known frequency of conflicts if the relationship between the severity and frequency of events is also known.

Different safety assessment methods of unsignalized intersections using surrogate safety measures are detailed in this section. The main measure is PET which is the time difference when the first vehicle leaves the conflict area, and a conflicting vehicle enters the same conflict area (Goyani et al., 2021). On the other hand, TTC is the remaining time to collision between two vehicles if they remain on their paths and with the constant speeds (Tarko, 2018).These methods generally evaluate safety of the intersection using field data and thereafter apply a microsimulation model to study the safety effects as indicated in Table 6. The conflicts in the simulated model are assessed mainly using the Surrogate Safety Assessment Model (SSAM).

Table 6: VISSIM microsimulation studies using PET from field data at unsignalized intersections in India

Study	**Data collection**	**Safety Indicators**	**Safety assessment method**	**Main finding**
Killi and Vedagiri (2014)	Area occupancy criteria to extract PET from field data	PET (all values were considered)	C++ code to extract PET for a VISSIM file	• Higher increase in conflict frequencies due to changes in volume of heavy vehiucles • Changing speed had no great effect on conflcit frequencies
Srinivasula et al. (2020)	PET from field data	PET=8s, Critical speeds	SSAM	• The model was reasonably replicating field conditions • Number of conflcits was decreased by decreasing speed and volume
Sowjanya and Kumar (2018)	PET from field data	PET	SSAM	• Microsimulation tools are reliable for assessment of mixed traffic • Increase in traffic volume on any approach results in decrease of the mean PET values
Goyani et al. (2021)	Manual extraction PET from field data	PET=6s	Generalised Extreme Value (GEV) distribution	• Right turn vehicles from the minor roads are at a higher risk of conflicts • Higher proportion of two-whelers results into higher critical crossing conflicts
Paul et al. (2018)	Manual extraction PET from field data	PET=1s, critical speed	Field data to determine critical conflicts and SSAM	• Increase in overall traffic volume, reduction in heavy vehicle volume, increase in grade up to 4% gradient resulted into increased safety level • Speed humps and speed tables were effective

In all the above studies, VISSIM was used to develop microsimulation models for different scenarios and then trajectories were generated as input to SSAM. However, Goyani et al. (2021) used manually calculated PET values for safety analysis in which distributions were developed. The studies used different PET thresholds to as low as one second as applied Paul et al. (2018). Furthermore, critical review of the traffic data and sites selected for these studies revealed that less busy sections were not used. At the same time, none of the studies focussed

on the impact of motorcycle lanes on road safety but instead on the general safety of mixed traffic.

Mahmud et al. (2019) discussed why PET is more appropriate than TTC for intersection conflicts even when some studies apply different indicators. According to the researchers, the use of only TTC has limitations because TTC does not consider many potential conflicts due to acceleration or deceleration discrepancies. Furthermore, TTC assumes that consecutive vehicles maintain constant speed which may not necessarily be true especially in mixed traffic conditions. Additionally, Caliendo and Guida (2012) established that PET was useful for evaluating transverse collisions/ conflicts at unsignalized intersections with varying traffic volume and speed limits. They insisted that other surrogate safety measures like TTC are necessary to examine other types of collisions/ conflicts such as rear-end and converging collisions/ conflicts. TTC and PET values below the thresholds of 1.5s and 5.0s, respectively, were classified as critical conflicts and hence further analyzed. In their study, conflicts with TTC=0 and PET=0 were excluded as they are collisions. Conflict types (crossing, rear-end, lane change) were also differentiated using SSAM based on the absolute value of the conflict angle as shown in Table 7. However, analysis was only based on the total number of conflicts and not the conflict types. This was due to the absence of field-based crash types as registered by urban police.

Table 7: Conflict types and absolute conflict angle

Conflict type	**Conflict angle**
Rear-end	$<30^0$
Crossing	$>85^0$
Lane changing	Between or equal to 30^0 and 85^0

Relating to manual extraction of PET from field data, Paul et al. (2018) divided the primary conflict area of the 4-legged and 3-legged unsignalized intersections into grids of 3.5m by 3.5m. They further edited the video recordings to include the grids and thereafter extracted traffic volume with composition, the speed of conflicting through moving vehicles, time headway, and PET. Right turning vehicles from the major or minor and through vehicles along the major road formed the key conflicts in the grids and were used to determine PET. The speed of vehicles on the major road was determined using a trap length of 20m. The start and end points of the trap length were fixed per approach and entry time and exit time of a vehicle were noted to compute speed. Time headway data for in the field and well as in the microsimulation environment was obtained based on the first reference line of the trap length. The location of this line was maintained in the microsimulation to minimise errors in simulations. In addition, time headway data was obtained for 2 hours of which the first hour was used for calibration and the second hour for validation.

Bulla-Cruz et al. (2020) validated a roundabout model by statistically testing the TTC and PET distributions from VISSIM/SSAM and the video based distribution of conflicts. The same approach was applied by Baran et al. (2019) who used SSAM to determine traffic conflicts for the considered scenarios and thereafter compared the obtained conflicts with real-life crash data for validation.

A combination of both microsimulation using VISSIM and surrogate safety measures can be used to study safety at unsignalized intersections in developing countries. In addition, traffic flow can be assessed since microsimulation models are basically developed first for traffic efficiency. The methodology in the next section discusses the step taken to actualize the study

and details from literature review such as microsimulation and surrogate safety measures are considered.

3|Methodology

This chapter aims to develop a methodology for determining the traffic efficiency and safety effectiveness of introducing new motorcycle dedicated lanes in non–lane based and mixed traffic conditions at unsignalized intersections. The proposed methodology can be summarized into seven stages: (i) field data collection using video cameras installed at the study intersection, (ii) processing and preparation of video data, (iii) creating a base (virtual) model of the intersection in VISSIM, (iv) microsimulation of traffic at the calibrated and validated virtual intersection, (v) development of alternative scenarios with dedicated motorcycle lanes, (vi) extraction of surrogate safety measures such as PET and TTC, and (vii) comparing the base and alternative scenarios in terms of traffic and safety. These steps are discussed thoroughly in the following sections.

3.1 Study Intersection

The 4–legged unsignalized intersection along the Kampala–Jinja Highway, Ntinda road and Nakawa–Jinja road was selected as a use case for this study. The intersection is commonly known as "Spear Junction" and is found in Nakawa Division of Kampala. The location of the intersection is depicted in Figure 6. Due to high traffic demands in peak periods, traffic police are deployed to regulate the traffic during these times.

A list of site selection criteria was compiled to typify unsignalized intersections in Kampala. This list was qualitative and focused on the volume of both motorized and non-motorized traffic, distance to the nearest intersection, street parking, alignment of approaches, availability of road reserve and Uganda Police cameras. Applying these criteria in the site selection process would ensure that results would be applicable and transferable to other unsignalized intersections in Kampala. Therefore, the study intersection was selected from a representative list of unsignalized intersections in Kampala because of the following reasons:

- The layout favors the construction of motorcycle dedicated lanes since enough road reserve is available
- Straight approaches that provide adequate sight distances for drivers
- High traffic demand including all vehicular categories such as cars, buses, heavy vehicles, and motorcycles with potential for large numbers of traffic conflicts in a limited period
- There are no on street–parking and formal bus stops within the functional area of the intersection
- Very limited volumes of pedestrians (crossing) and cyclists
- No dedicated infrastructure for vulnerable road users

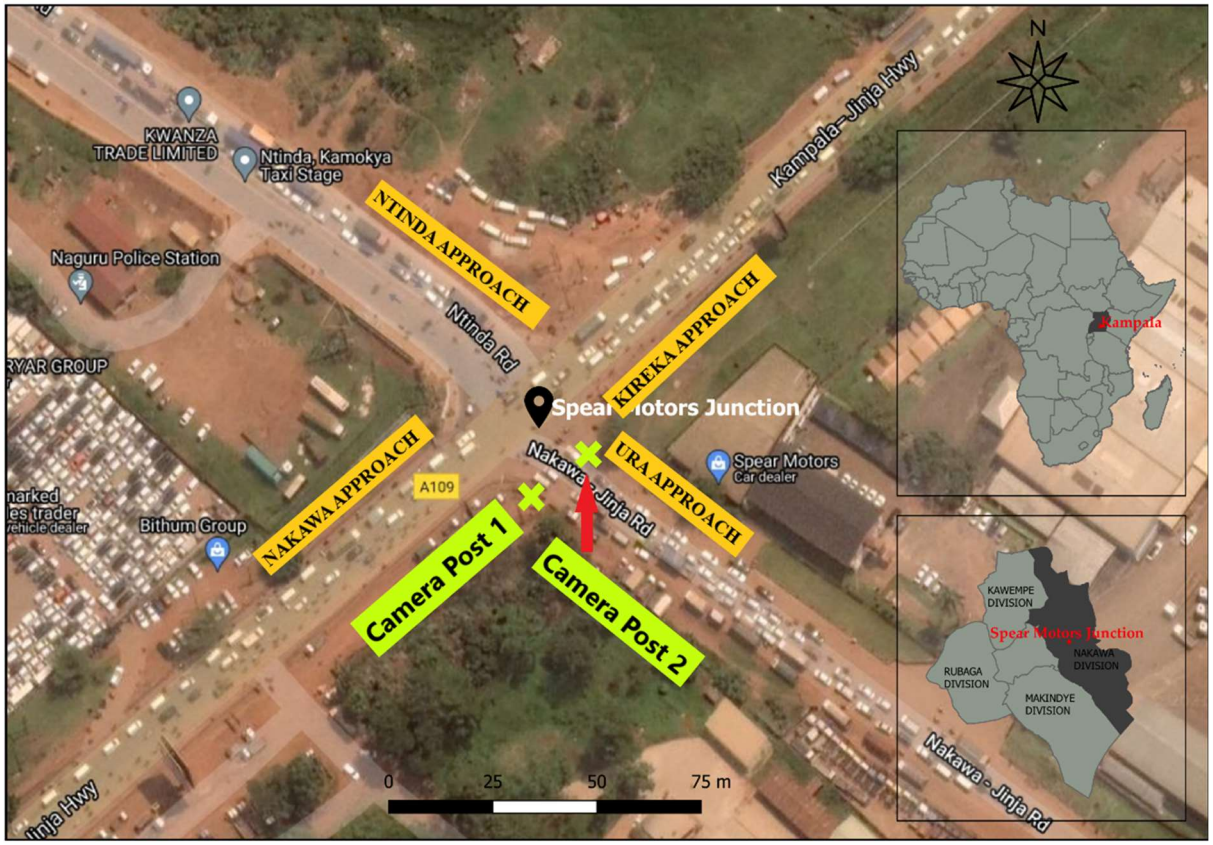

Figure 6: Location of the study intersection and camera locations

To study the impact of motorcycle lanes on the above intersection, microsimulation is needed to make changes onto the intersection since the lanes are non-existent. Thereafter, traffic can be added into the microsimulation to further obtain relevant traffic flow and safety results.

3.2 Research design

Different methods have been used to study driver behavior. According to Glendon (2007), these methods can be summarized into real-time (direct and indirect), simulation, indirect (post hoc) and experimental. In real time methods, data are collected by an observer who is either physically present (naturalistic observations) or recorded by an instrumented vehicle, instrumented driver, or video camera. In contrast, indirect (post hoc) methods rely on crash data and people's experiences from crashes that can be extracted using either questionnaires or interviews whilst experimental methods whether in the field or laboratory focus on limited variables to understand particular structural relationships. On the other hand, simulation methods including microsimulation apply mainly computer data capture. Real-time and indirect methods are more realistic (high ecological validity) but are generally expensive and guarantee less control over the study compared to simulations and experiments. In addition, the former methods and field experiments require the infrastructure (roads) to be in place.

From the above methods, microsimulation of motorcycle traffic in the target location is one way of evaluating the safety impact of a newly introduced measure i.e., dedicated motorcycle lanes in this study. There are several advantages that motivate the use of microsimulation to answer the research questions in this study:

First of all, the road infrastructure measures to be evaluated have not been experimented or even put in place in Kampala. This fact does not favor other options like post hoc-before and

after studies which require a measure to have been implemented or piloted. Therefore, microsimulation is best suited for the case of the non-existent motorcycle lanes in Kampala as the measure can be modelled in perspective of how it would be implemented in the future. This issue was further pointed out by Siddharth and Ramadurai (2013) who emphasized that microsimulations are used to evaluate proposed improvements and alternatives to the extent that their effect can be found before implementation. The same advantage was highlighted by Mahmud et al. (2019) in a review of the microsimulation application to heterogenous traffic environment.

Secondly, the absence of crash data before and after an intervention for at least three years in each case, implies that microsimulation is best suited for this study. This advantage emphasizes the prolonged time aspect for post hoc-before and after studies which is a traditional impact assessment method. Microsimulation makes it possible to carry out safety analysis of a measure as individual elements in the traffic system are critically studied thus no need to wait for a long period of time.

The third benefit is related to its implementation. Siddharth and Ramadurai (2013) note that microsimulations are safer, less expensive and faster than field implementation and testing. With microsimulation, the researchers conduct the study using both hardware and software and not field experiments. In addition, the costs that would be incurred to monitor the study location for a specified duration are saved. With respect to time, microsimulation can be executed at increased speed with the help of a software and hence it is a faster option.

The methodological approach used in the study is indicated in Figure 7. The first phase focusses on data collection and preparation and then the model is developed in VISSIM. VISSIM was the preferred microsimulation tool for the study because of reasons highlighted in section 2.5. Looping arrows provided for both model calibration and validation indicate interactive processes between the different stages. For instance, the model was valid when the GEH statistic was less than 5.0 and p-value of a t-test was more than 0.05, respectively. Thereafter, the model is modified to include dedicated motorcycle lanes that are evaluated based on conflicts. The study relied on Post Encroachment Time (PET) as a surrogate safety measure for evaluation of the safety impact of the different scenarios. In addition, Time to Collision (TTC) was applied to study rear-end conflicts at the intersection. These indicators were determined using Surrogate Safety Assessment Model (SSAM) as explained in section 3.8.3.

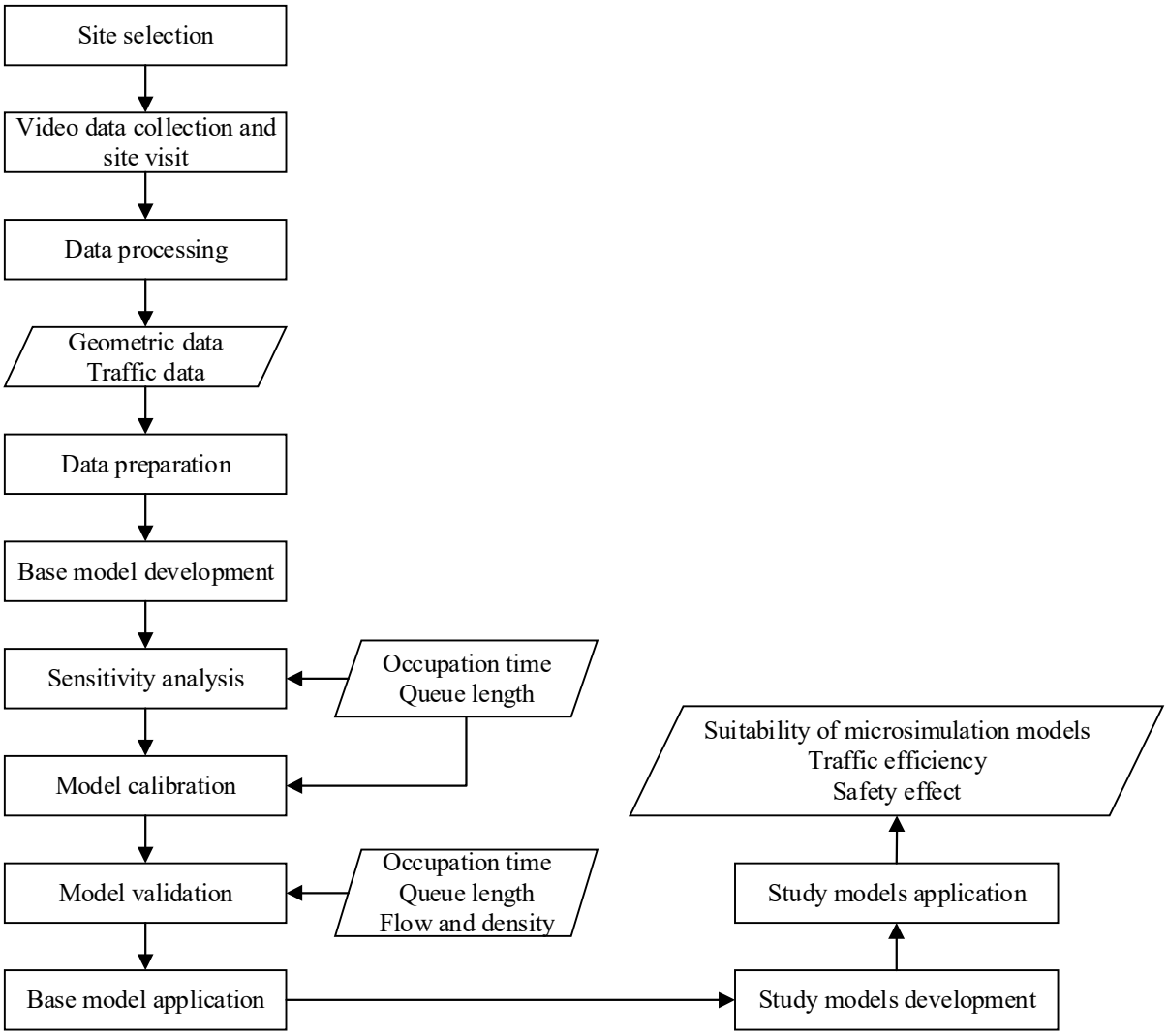

Figure 7: Methodological approach of the study

Microsimulation was used to mimic the traffic conditions at the intersection. However, data such as geometric and traffic is important to reflect the actual driver behavior. Therefore, the next section describes the relevant data as well as how it was collected.

3.3 Data collection

The required data to successfully carry out the study and the respective data collection methods are discussed in this section.

3.3.1 Data

Traffic and geometric data were key for the study. The data were to be used in the development of a realistic microsimulation model. This model would form a basis for both traffic flow and safety analysis in line with the second and third research questions as discussed below.

Traffic data such as traffic volume and composition per direction was a direct input in the microsimulation tool (VISSIM). This data impacts on the driver behavior that is simulated. For example, vehicles are added onto the interface following a negative exponential distribution with an average value equal to the average gap between two consecutive vehicles. Therefore, the higher the volume, the lower the average gap (more vehicles per input). Furthermore,

vehicle inputs influence interactions between road users and hence trajectories are formed in reaction to the users. These trajectories were significant for conflicts assessment in the study.

Geometric data were also used to develop the microsimulation model. For example, the size of the intersection had to approximate site conditions such as lane width, number of lanes and slope. Since distance is directly related to time then vehicle travel time can significantly change with variation of geometric dimensions. Secondly, vehicles require a minimum width or space in order to make lateral movements and adopt some speeds. Therefore, geometric data highly affect the extent to which a model replicates the observed behavior.

3.3.2 Data collection methods

With the use of the existing cameras at the study intersection by Uganda police, traffic data were obtained while geometric data were collected physically during a site visit. Two cameras are fixed on each of the two posts at the intersection shown in Table 8. The existing cameras were preferred in order to save time and money while collecting data. Data was collected from two random weekdays and two weekends under good visibility conditions and weather as indicated in Table 8.

Table 8: Dates and duration for video data collection

Date	**Time (East African Time–EAT)**	**Duration (hrs)**
Friday, 21st January, 2022	8:00am–18:00pm	10
Sunday, 6th February, 2022	10:00am-3:00pm	5
Tuesday, 22nd February, 2022	8:00am–18:00pm	10
Saturday, 26th February, 2022	10:00am-3:00pm	5
Total recorded duration		**30**

The video images were viewed to determine quality and whether all road user types could be identified. In addition, a site visit was organized in the presence of the Traffic Police to obtain the geometric data of the intersection. As-built drawings were unavailable, and thus a site visit was preferred since it yields actual dimensions. The data included road widths on all approaches, dimensions of the conflict area including the diagonals, slope of the major road, length of approaches, location of key features such as access points and median width on the Ntinda approach. Both a steel tape and measuring wheel were used to measure the above details. The slope was determined using a combination of dumpy level, staff, and a duo-frequency Global Positioning System (GPS) receiver. Finally, spot speeds of each vehicle category were determined using a laser speed gum (LTI 20/20-CAM II) on each approach and at about 50-100m from the study intersection.

Video image analysis software requires homography/defining the intersection for the image software and for that, coordinates and aerial pictures of the intersection are needed. These pictures were taken using a drone at an adequate height to obtain a clear view of the entire intersection and its approaches. Coordinates of camera posts and key points that can be viewed in the video data such as manholes, road edges, posts, electric poles were obtained using a duo-frequency GPS receiver. Vehicle characteristics such as the vehicle dimensions were retrieved from websites of either car manufacturers or importers. The most common vehicle brands were noted during review of the video images.

3.4 Video data preparation

At this stage, raw data was available for the study. Video images were collected but cannot be directly used in microsimulation while geometric data can be used. Therefore, the collected data and specifically video data was further prepared as discussed in this section.

The video recordings were viewed to establish peak, near peak and off-peak time periods. Peak periods were characterized by congested approaches to the intersection as well as the presence of traffic police who control the flow of traffic. Since the microsimulation model cannot simulate traffic while a policeman (or two) is on duty, peak period traffic was discounted from further analysis. The descriptive analysis of traffic data at this intersection was carried out using video image data for the off–peak and near peak time periods. Near peak data were used purely for descriptive purposes. For the detailed further analysis only the off–peak time period was used. Consequently, the traffic simulations in the study were based on traffic conditions during off-peak periods only. This choice is further motivated by the fact the speeds in off-peak periods are likely to be higher yielding more serious conflicts than during peak periods.

Two of the four cameras viewed a bigger section of the conflict area and longer stretches of two approaches and hence their recordings were further processed using TrafxSAFE software of Transoft solutions. TrafxSAFE uses technologies developed by Brisk Synergies that was acquired by Transoft Solutions in 2020 (Transoft Solutions, 2020). TrafxSAFE utilizes deep and machine learning object detection algorithms for traffic safety analysis (Guerrero-Ibañez et al., 2021; P. B. Silva et al., 2020). The video was first calibrated by matching points in the video with those on the actual intersection. This process is known as homography (Inter-American Development Bank, 2019). TrafxSAFE detects, classifies, and tracks road users in the video to generate output data (see below). Quality control per road user type and conflicts was also done in order to correct the data of mainly obstruction of vehicles by other vehicles. This defect resulted into more traffic volume and conflicts at the intersection and so the correction factors were used to reduce the reported data.

The software had the following output data that were relevant to the study as explained in section 3.3.1:

- Traffic movement counts per each different road user types (classified into bicycles, motorcyclists, passenger cars, pick-ups, work vans, buses, heavy equipment, farming equipment, rigid trucks and articulated trucks)
- Detailed speed data and speed distribution per road user type for the conflict area and per movement
- Movement trajectories per road user type per movement
- PET and TTC conflict indicators per road user type for the conflict area and per movement

From the above observed data, some traffic flow parameters such as occupation time, number of vehicles per interval, and speed were determined. Specifically, occupation time in seconds was calculated by subtracting entry time from exit time per vehicle for the conflict zone. Based on entry time, the number of vehicles in a particular interval were counted and the corresponding flow calculated. Median speed values in the conflict area were also included in

traffic movement counts. These inputs were used in not only calibration and validation but as well for the traffic flow analysis.

Concerning queue length, the parameters were manually extracted from the video images. Queue length was determined by considering the dimensions of known points along the approaches. These points were noted during the site visit. The maximum queue observed per approach and time interval was considered for field data as well as simulations. This extraction was done only for 2 hours of video data selected for calibration and validation. Frame by frame analysis of the video data was performed using Avidemux 2.8 software. This software is a video player and is freely available on the market.

TrafxSAFE generates PET based on a generic, scenario-independent, volumetric-compliant form just like SSAM does. Similarly, TrafxSAFE also uses a generic, constant-velocity-collision-course-estimation-based, volumetric-compliant form to generate the TTC (Transoft Solutions, 2022). Therefore, the PET and TTC values based on video data (observed) were compared with the simulated SSAM results for both the base model and the scenarios since both TrafxSAFE and SSAM are based on the same principles. PET and TTC were used to cluster conflicts that were critical based on a maximum threshold of 1.5s for field and simulated data. On the other hand, a threshold of 0.5s was used for severe critical conflicts. Differences in the distributions of PET and TTC for the simulated and field data were used to analyze the conflicts. As well, percentage reductions of conflicts per scenario were determined based on conflict rates for Vehicle-to-Vehicle (V2V), Vehicle-to-Motorcycle (V2M) and Motorcycle-to-Motorcycle (M2M) interactions. In this analysis, conflict types of crossing, rear-end and lane change were considered and based on absolute conflict angles indicated in section 2.5.2, Table 7.

For calibration, two performance measures, namely maximum occupation time of all vehicles and motorcycles alone on the minor roads for critical movements (through and right turn) in the conflict area and maximum queue length on the minor roads were applied. Occupation time was derived from the observed vehicle data and trajectories per approach by subtracting entry time from exit time. For a 2-minute interval, the maximum occupation time of either all vehicles or motorcycles alone was determined. Maximum queue length observed in video images at an approach in 2-minute intervals was also considered. Left turn conflicts were not considered for determination of occupation time as these are associated with lower risk compared to through and right turning conflicts. It should be noted that drivers in Uganda drive on the left side of the road which was taken into account in VISSIM. Notably, delay on the approaches due to traffic congestion was not directly considered since off-peak periods were simulated. Since the current intersection is uncontrolled, vehicles are not expected to make stops on the approaches but rather in and near the intersection. Regarding the stops made in the conflict area during negotiations, the associated delay was included in occupation time which was an input in calibration. This behavior was observed in the video data. Additionally, the behavior of pedestrians was not calibrated but their effect on intersection performance was considered based on their volume.

3.5 Base model development

A collection of both geometric and prepared video data was used to develop a representation of actual traffic conditions at the intersection. This base model was developed using PTV VISSIM 21 to simulate field observations. VISSIM was used because it is suitable for this study and used to study heterogenous and non-lane based, and mixed traffic as discussed in

section 2.5.1. This software is associated with versatility in modelling both vehicle and driver characteristics and behavior. Key parameters were calibrated and validated as discussed in Section 3.7. VISSIM has been used in different studies to model traffic in developing countries such as India, Vietnam, Thailand, and Colombia (Bulla-Cruz et al., 2020; Caliendo & Guida, 2012; Chaipanha et al., 2019; Singh et al., 2020; Tran et al., 2013; Vuong et al., 2019).

In VISSIM, some key adjustments of desired speed distributions for approach roads per vehicle category and per approach were made using cumulative distribution functions. However, the speed distributions per vehicle type were developed for the entire conflict area but not per approach. These distributions affect link traffic flow and travel times by influencing speed choices of the drivers (PTV, 2021b). In addition, default desired acceleration and deceleration functions were maintained for existing vehicle types and functions for car were used for both taxi and SUVs as new vehicle types. These functions accounted for differences in the driving behavior and vehicle performance. The maximum deceleration for reduced areas per vehicle type was computed using trajectory data per second. The kinematic formula indicated in Equation [3-1] was used since the input data was all given in the trajectory file. Both acceleration and deceleration were determined for all vehicle types and per approach and negative values filtered to develop relevant distributions.

$$a = \frac{5(v-u)}{18t} \qquad [3\text{-}1]$$

where:

a=acceleration/deceleration (m/s^2)

v=final velocity of a vehicle obtained from the trajectory data (km/h)

u=Initial velocity of a vehicle obtained from the trajectory data (km/h)

t=change in time between v and u also obtained from the trajectory data (s)

While determining the distributions and number of simulations, the number of observations had to be above the minimum n, determined using Equation [3-2] as stipulated by Chen et al. (2019). The formula is based on the standard deviation σ, reliability of the inference being made (1-α) $Z_{\alpha/2}$ and d, the desired accuracy. Reliability was determined at 95% confidence and a desired accuracy of 10% of the mean was adopted in this study.

$$n \geq \frac{z_{\alpha/2}^2 \, \sigma^2}{d^2} \qquad [3\text{-}2]$$

3.6 Sensitivity approach

The elementary effect approach was adopted for sensitivity analysis of key parameters used in microsimulation. The approach is further discussed in this section. Driving behavior parameters were subjected to sensitivity analysis following the procedure indicated in Figure 8.

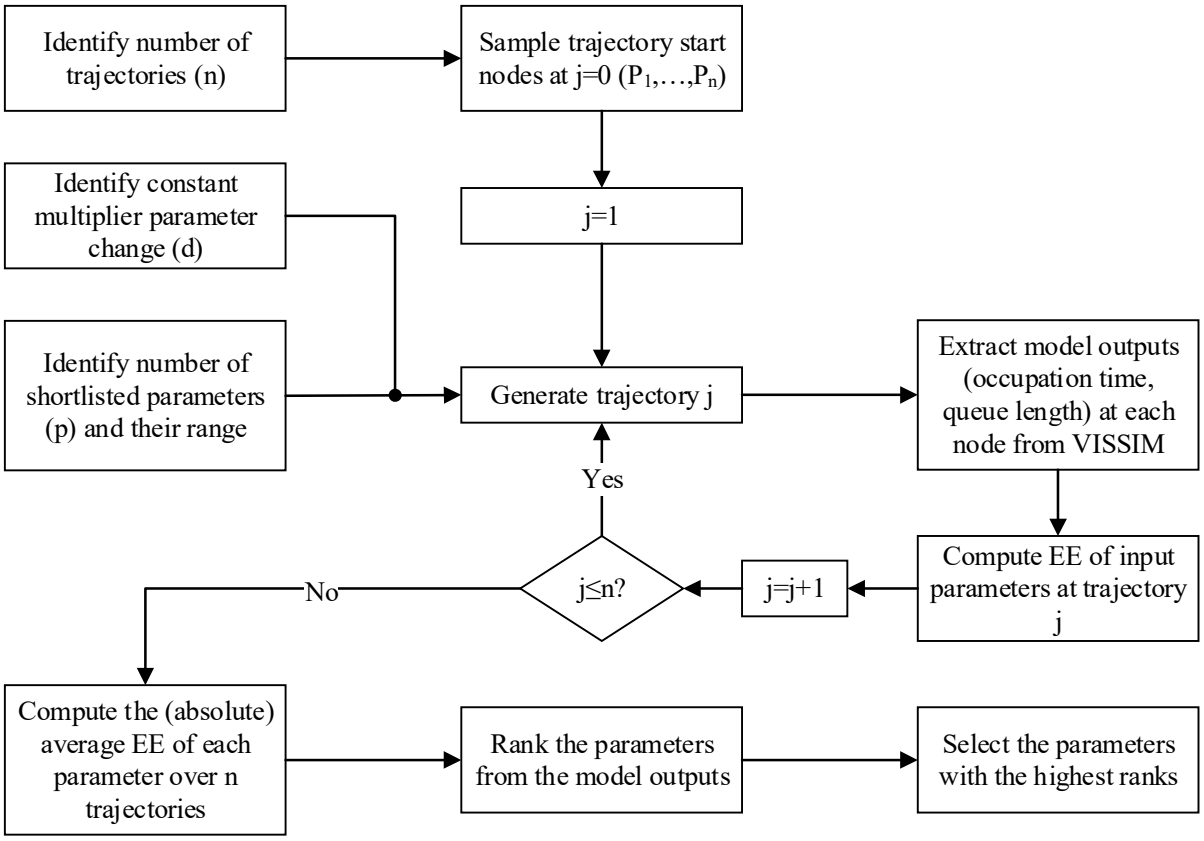

Figure 8: Sensitivity approach for the study

With this approach, the elementary effect of each input parameter is evaluated n times, where n is the number of trajectories. It is important to note that these trajectories are not from observed data but rather a MATLAB input to facilitate computation of sensitivity indices. This evaluation is possible by using a sufficient number of trajectories that is between 10 and 50 (Campolongo et al., 2007; Khavas et al., 2017). The model output Y(X) is computed at every node of a trajectory consisting of (p+1) nodes where p is the number of parameters. The total number of nodes is equal to n(p+1) and all these must be simulated in VISSIM using the base model. Every node of P_i has a complete set of input parameters $X_i,\ldots,X_k$ and the value of only one parameter changes by Δ_i from the previous value to the new one. It must be noted that for higher number of trajectories such as 300, the strategy can result into a non-optimal coverage of the input space (Campolongo et al., 2007). The researchers proposed an improved sampling strategy by limiting the maximum Euclidian distance between the trajectories.

In this study, the constant multiplier for all parameters, d was set at 0.1 as also done by Khavas et al. (2017) while n was adopted as 10 in order to limit computational time and memory required for sensitivity analysis. Since each parameter has its own range then the magnitude of change per parameter was calculated using Equation [3-3]. The sample trajectory start nodes at j=0 ($P_1,\ldots,P_n$) were chosen using Latin Hypercube Sampling (LHS). Saliby and Pacheco (2002) emphasized that LHS is a variance reduction technique with controlled selection of sample values within a subspace defined by different variables or dimensions. Random samples of all parameters were generated using this technique. These initial parameter values were then adjusted according to their range and change step along a specific trajectory in MATLAB.

$$\Delta_i = d.r_i \quad [3\text{-}3]$$

where:

Δ_i=change step value of parameter i,

d=constant multiplier for all parameters, and

r_i–range of parameter i.

The elementary effects were used to further determine the sensitivity index of absolute mean since the higher the absolute mean, the more sensitive is a parameter. The change step value for a parameter in Equation [3-3] is added to only that parameter and the elementary effect calculated using Equation [3-4] as developed by Morris (1991). This equation was implemented in a study to identify VISSIM parameters for microsimulation in inclement weather (Khavas et al., 2017).

$$EE_i = \frac{Y(X_i, \dots, X_{i-1}, X_i + \Delta_i, X_{i+1}, \dots, X_k) - Y(X_i, \dots, X_{i-1}, X_i, X_{i+1}, \dots, X_k)}{\Delta_i} \quad [3\text{-}4]$$

where:

EE_i=elementary effect of parameter i,

X_i=input parameter i, and

Y(X)=model output.

The model outputs (average occupation time of vehicles on the minor approaches and maximum queue length) were determined by running VISSIM for every input file from MATLAB at a node. The process was computationally demanding but necessary to reduce the number of parameters for calibration. The absolute mean was computed for the obtained elementary effects per parameter considering separate model outputs (average occupation time, maximum queue length). Driver behavior parameters were then ranked based on the calculated absolute mean. Finally, sensitive parameters were identified as those with high absolute mean (Ge & Menendez, 2014; Siddharth & Ramadurai, 2013).

3.7 Calibration and validation

The methods for calibrating and validating the model are elaborated in this section. Calibration focusses on optimizing the driver behavior in terms of the following, lane changing and lateral behaviors to simulate the same traffic conditions as observed in the field. The performance of the simulation is confirmed through validation.

3.7.1 Calibration

In this study, the base model was calibrated using both maximum occupation time and maximum queue length of vehicles on the minor roads. Occupation time is a proxy of accepted time gap, and it considers the numerous stops made by drivers while negotiating an unsignalized intersection. The general Particle Swarm Optimization (PSO) approach as summarized in Figure 9 was used in this study. PSO capitalizes on swarm intelligence by allowing information flow between the particles (communication) and hence learning of particles from one another (Russell Eberhart & Kennedy, 1995). In this way, the researchers emphasized that PSO does not converge prematurely as the case for Genetic Algorithm (GA)

and above all the method is computationally inexpensive in terms of both memory requirements and speed.

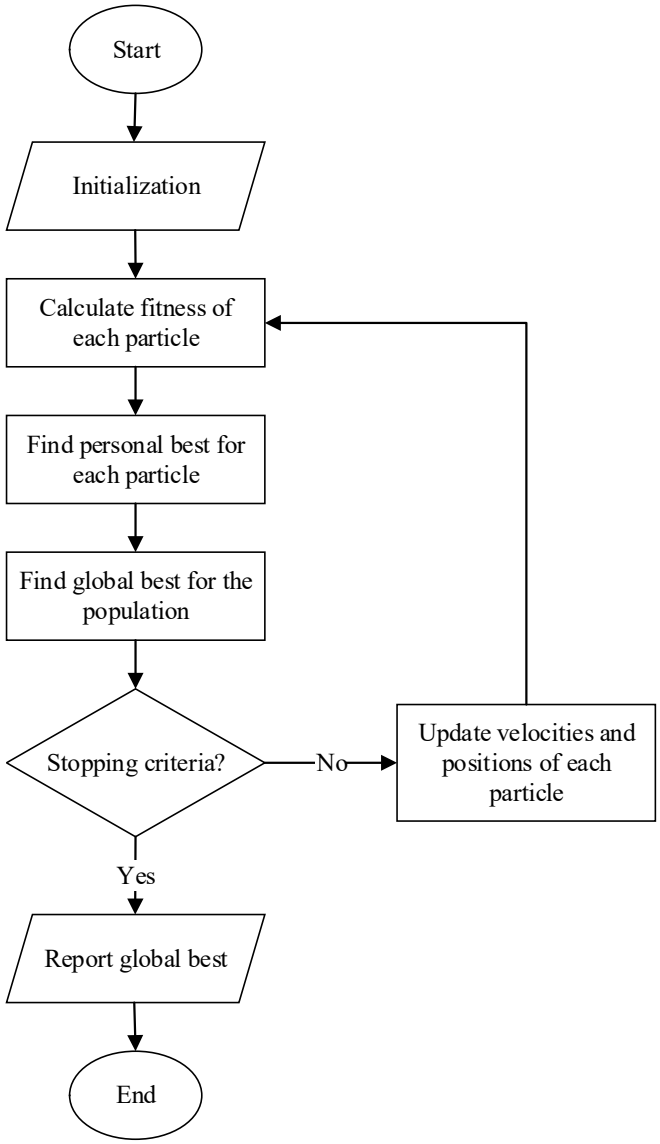

Figure 9: Flow chart of the general PSO algorithm

From section 3.6, sensitive driving behavior parameters were considered as optimization indicators and calibrated using PSO as guided by Dadashzadeh et al. (2019). The approach used in this study is illustrated in Figure 10. The parameters were initialized using Latin Hypercube Sampling (LHS) as the case during sensitivity analysis. The optimization was performed in MATLAB by integrating VISSIM with the help of COM interface in order to automate the calibration process. In this study, both maximum occupation time of the conflict area and maximum queue length of minor road vehicles were used to optimize the key performance measures. The two parameters were separately analyzed for motorcycles and other vehicles. Motorcycles (two-wheelers) were separated because of high volume and totally different behavior at the intersection. For example, motorcycles weave through traffic and rarely stop at the intersection as observed in the video data. The average parameter values for a time interval, per vehicle category for both occupation time and queue length computed for the simulation results and the corresponding video-based results (field) were used in the absolute normalized error function as shown in Equation [3-5]. Multiple VISSIM runs were

conducted to attain a higher fitness between the simulation and field traffic conditions. A maximum number of iterations equal to 50 was adopted in the study as the stopping criteria as well as a t-test. The optimum values of sensitive parameters were then applied in the simulation to get base results as well as to run all the scenarios in VISSIM.

$$Minimize\ Z = \frac{1}{N}\sum_{j=1}^{N}\left(\frac{\left|O_{obsj} - O_{simj}\right|}{O_{obsj}} + \frac{\left|Q_{obsj} - Q_{simj}\right|}{Q_{obsj}}\right) \quad [3\text{-}5]$$
$$w.r.t\ the\ constraints\ Lb_{Xi} \le X_i \le Ub_{Xi}$$

where:

Z–Objective function in terms of occupation time and queue length

N-total number of data collection intervals. For example, for one hour observation of detection with two-minute intervals, N=60/2=30

O_{obsj}, Q_{obsj}–observed maximum occupation time of vehicles in the conflict area and maximum queue length of vehicles. Queue length was manually extracted from the video data using Avidemux 2.8 software as elaborated in section 3.4 while occupation time was calculated from the trajectory data.

O_{simj}, Q_{simj} -simulated maximum occupation time of vehicles in the conflict area and maximum queue length of vehicles by VISSIM (extracted using detectors)

X_i-vector of parameters for driving behavior in VISSIM

Lb_{Xi}, Ub_{Xi}–lower and upper value of parameter X_i as obtained from VISSIM

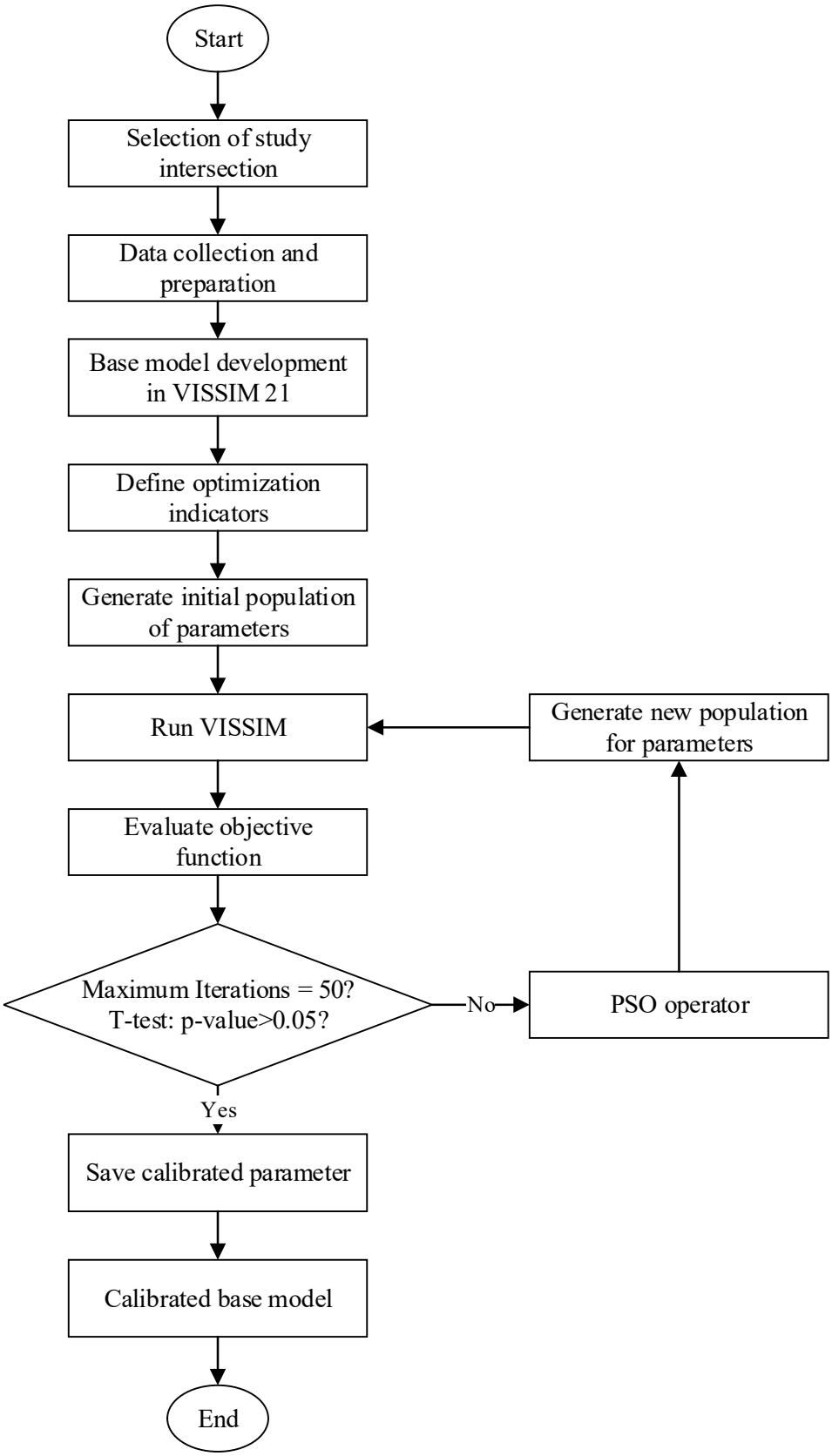

Figure 10: Calibration procedure for the study

In this study, the original PSO as proposed by Eberhart and Kennedy (1995) and later modified to include the constriction factor χ was used to calculate the velocity of particles (Clerc & Kennedy, 2002; R Eberhart & Shi, 2000). The adopted PSO main function is indicated in

Equation [3-6]. In a study by Eberhart and Shi (2000), particles were defined as potential solutions with randomised velocity through the problem space.

$$\boldsymbol{V}_{t+1} = \chi[V_t + r_i c_1(\boldsymbol{p} - \boldsymbol{x}) + r_2 c_2(\boldsymbol{g} - \boldsymbol{x})] \quad [3\text{-}6]$$

where:

c_1 and c_2 are learning constants which are usually equal and greater than 1.

r_1 and r_2 are random numbers

The current velocity of a particle $\mathbf{V}_{t+1}$ is determined by adding three terms. The first one is the inertia component with the previous velocity a particle $\mathbf{V}_t$. This was earlier suggested in a study by Shi and Eberhart (1998) in which an inertia factor was introduced to limit the velocity of the particles. In this study the inertia factor is equal to the constriction factor. Secondly, the cognitive component relates to the difference between the current position of a particle **x** and the best position attained by a particle **p**. The third part is known as a social component, and it is the difference between the best-known position of all particles in the swarm **g** and the current position of a particle **x**.

The constriction factor χ was calculated using Equation [3-7] and it balances between exploration and exploitation as it attempts to limit the velocity of the particles (Barrera et al., 2016).

$$\chi = \frac{2\kappa}{|2 - \phi - \sqrt{\phi^2 - 4\phi}\,|} \quad [3\text{-}7]$$

where κ is an arbitrary constant in the range [0,1] and ϕ is the sum of the learning constants $\phi = c_1 + c_2$.

The next position of a particle x_{t+1} was computed using Equation [3-8] based on the calculated velocity in Equation [3-6].

$$x_{t+1} = x_t + V_{t+1} \quad [3\text{-}8]$$

The PSO was further reinforced by limiting the position and velocity of the particles using the ranges of the decision variables from VISSIM. For each iteration, the upper L_d and lower S_d bounds of the positions of all particles and variables were fixed using Equation [3-9] and used to determine the range.

$$x_{max} = L_d;\ x_{min} = S_d \quad [3\text{-}9]$$

The maximum and minimum limits of particle velocity in each iteration were determined using Equation [3-10]. The parameter μ is a velocity clamping percentage that also reduces the velocity of the particles within the solution space as proposed by Adewumi and Arasomwan (2015).

$$V_{max} = \mu(L_d - S_d)\ ; V_{min} = -\mu(L_d - S_d) \quad [3\text{-}10]$$

Generally, two methods were used to limit the velocity and position of the particles in the PSO that is the constriction factor method as well as the dynamic adjusted position and velocity

limits. Since the constriction factor is equal to the inertia factor, one can arguably state that three velocity and position methods were applied in this study. The factors adopted in this study were μ=0.15, c_1 and c_2 were equal to 2.0 while r_1 and r_2 were randomly generated using a uniform random number generator in MATLAB. These values for the parameters were used because they have been proved to be usually good and efficient (Adewumi & Arasomwan, 2015). The calibration methods were used in MATLAB and VISSIM through a COM interface based on the selected one-hour field data during off-peak time.

3.7.2 Validation

The model was validated using different parameters at both a microscopic as well as macroscopic levels. These are explained in this section.

Microscopically, another one-hour field data set (collected on 26/02/2022 from 10:30h to 11:30h) was used to determine maximum occupation time and maximum queue length of motorcycles and all vehicles for validation of the calibrated model. The determined values of the measures were compared with the corresponding simulated occupation time as well as queue length for the minor approaches. An independent samples t-test was carried out to confirm the extent to which simulated data conforms to the observed data.

At a macroscopic level, the simulated density and flow rate for each time interval of 5 seconds was compared with the real values obtained from the video data using fundamental diagrams. The Geoffrey E. Havers (GEH) statistic was computed using Equation [3-11]for 5-minute intervals of both observed and simulated traffic counts and a threshold of 5.0 for at least 85% of the points was applied. Caliendo and Guida (2012) and Kumar et al. (2012) adopted the same threshold in their respective studies.

$$GEH = \sqrt{\frac{2(M-C)^2}{M+C}} \qquad [3\text{-}11]$$

where M is the simulated hourly traffic volume and C is the hourly traffic volume measured in the field and different parameters can be used.

3.8 Study models

This section discusses the development of scenarios or proposals for new, safer design and the assessment procedure of traffic flow and safety impact.

3.8.1 Scenario development

Different design alternatives (scenarios) were considered to evaluate the impact of introducing dedicated motorcycle lanes at the current intersection. These designs were based on the provisions of CROW (2019) for cyclists in built-up areas in the Netherlands. These provisions include use of roundabouts as well as deflected crossings at intersections. Introducing these changes to the layout of the current intersection necessitated building separate traffic models for each of these. A separate model was developed for each scenario as further explained in this section. In all the scenarios, dedicated motorcycle lanes were physically separated from the normal carriageway other than at the crossing points of the intersection. The width of a dedicated motorcycle lane was adopted as 1.7m as indicated in the Malaysian (2018) guidelines for exclusive motorcycle lanes. This width is compliant with the motorcycle design requirements that recommend a minimum width of 1.52m (motorcycle width of 0.77m and two

safety margins of 0.375m each) as highlighted in the Transport for London (2016) urban design manual. These geometric parameters were adopted from Malaysia because of similar motorcycle conditions. In addition, a motorcycle is not considered as a design vehicle in Uganda and so comparison was made with other countries. During the review of video images, it was found that over 95% of the motorcycle population in Kampala comprises of small and medium sized type-motorcycles with engine sizes of 150c.c and below. According to Bajaj (2022), these motorcycles are 1,970mm long, 770mm wide, 1,065mm high and with a wheelbase of 1,235mm.

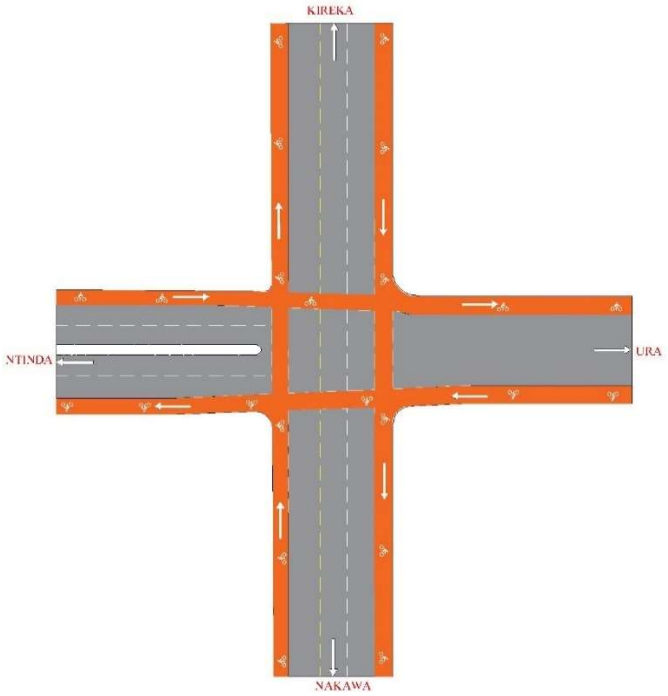

Figure 11: Scenario 1-inclusion of dedicated motorcycle lanes (straight crossings)

In this scenario dedicated one-way motorcycle lanes are provided on the outside of the carraigeway (Figure 11) with a demarcated crossing area in the intersection itself. This alternative considered the shortest path of crossing the intersection.

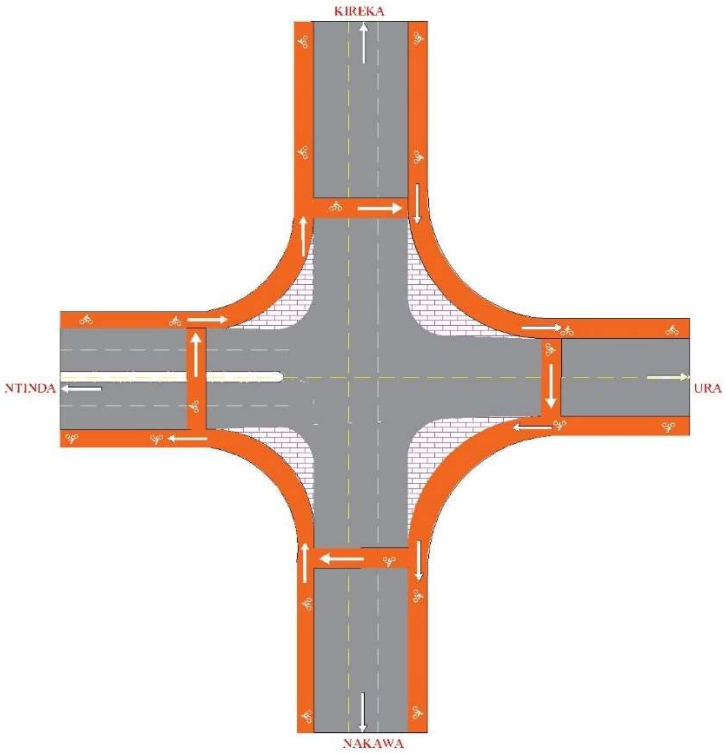

Figure 12: Scenario 2-inclusion of dedicated motorcycle lanes (deflected crossings)

In scenario 2, the dedicated motorcycle lanes were deflected by not less than 5m for the crossing point to be far away from the intersection as demonstrated in Figure 12. Similarly, a minimum turning radius of 3.0m as specified by the Malaysian (2018) guidelines for exclusive motorcycle lanes was maintained for the splitter island in order to guarantee stability of motorcyclists.

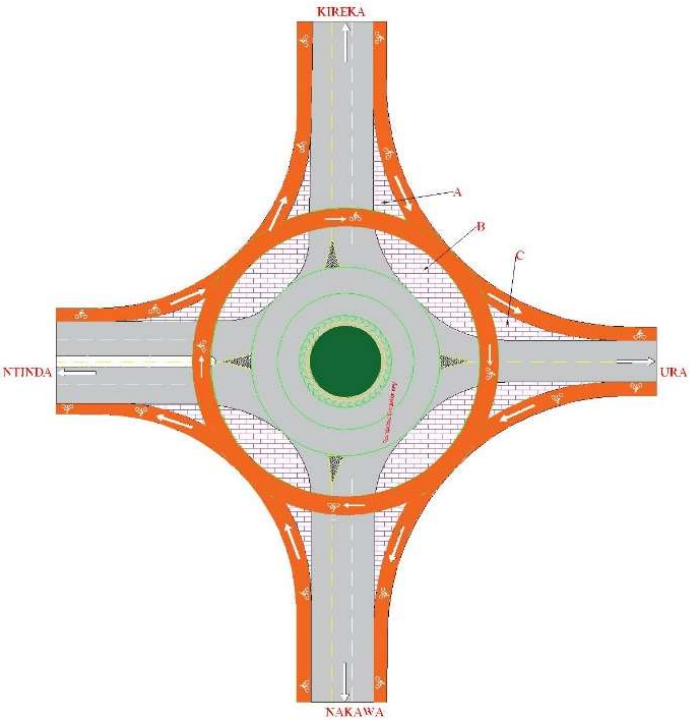

Figure 13: Scenario 3-inclusion of dedicated motorcycle lanes (roundabout)

In scenario 3, a roundabout with separate lanes for main traffic and motorcycles was introduced at the intersection as illustrated in Figure 13. This option allowed only one-way movement of motorists. The design followed Ugandan guidelines that specify a Central Island Diameter (CID) between 20m and 50m for safety and Inscribed Circle Diameter (ICD) or carriageway diameter between 42m and 68m for normal two-lane roundabouts. The dimensions of the roundabout were fitted within the specified ranges with consideration of site geometric limitations. Splitter islands A, B and C were designed with a minimum entry radius greater than 15m and entry width of 6.0m for a semi-trailer as a design vehicle (MOWT, 2010). The same minimum entry radius was maintained for motorcycles since it is above a minimum turning radius of 3.0m as stipulated by the Malaysian (2018) guidelines. However, the width of the motorcycle lane was maintained as 1.7m.

3.8.2 Traffic flow assessment

In this study, the traffic flow assessment was performed based on Level of Service (LoS) and fundamental diagrams per approach.

First, the Level of Service (LoS) was determined using a rectangular node in VISSIM which was added to include all the approaches and the conflict area. The levels of transport quality from A to F based on average vehicle delay at the unsignalized intersection are allocated per direction and specific time interval in VISSIM (PTV, 2021b). The limits in VISSIM per level are comparable to the LoS defined in the 2010 American Highway Capacity Manual (HCM) and are indicated in Table 9. Distribution charts of LoS per approach were developed and used to assess traffic flow in the study. The distribution of LoS per scenario was compared with only the base model.

Table 9: LoS limits for unsignalized Intersections in VISSIM (PTV, 2021b)

Level	**Average Delay Limits(seconds)**
LoS A	Delay <10
LoS B	> 10 to 15
LoS C	> 15 to 25
LoS D	> 25 to 35
LoS E	> 35 to 50
LoS F	> 50

Secondly, fundamental diagrams per approach were generated to indicate the impact on traffic flow. As with the LoS component, comparisons were made with both the base model and field data. Both observed speed and number of vehicles per interval were obtained from the observed data. These diagrams were developed using a MATLAB code to extract both harmonic speed of the vehicles and their corresponding volume per time interval of 5s. Hourly flow was calculated by dividing the number of vehicles to the time interval in seconds and then multiplying by 3600. In addition, harmonic speed was determined using Equation [3-12] while density was computed using Equation [3-13]. Harmonic speed allocates greater weightage to smaller speed observations and minimizes the effect of outliers. Thus, the resulting fundamental diagrams are smoother and can easily be interpreted.

$$V = \frac{n}{\frac{1}{\sum_1^n(\frac{1}{S_n})}} \quad [3\text{-}12]$$

where:

V=harmonic speed (km/h)

n=number of vehicles in a time interval with measured speeds

S_n=observed or measured speed per n^{th} vehicle (km/h)

$$K = \frac{Q}{V} \quad [3\text{-}13]$$

where:

K=Density (veh/km)

Q=flow of vehicles (veh/h)

3.8.3 Safety assessment

The traffic conflicts were assessed using Post Encroachment Time (PET) as a surrogate safety measure which is suitable for evaluation of transversal conflicts at unsignalized intersections (Goyani et al., 2021; Tarko, 2018). In addition, TTC was also considered since rear-end conflicts can also occur at the intersection (Transoft Solutions, 2022). These two indicators were explained in section 2.5.2. The assessment was done for every scenario except scenario 1 using the SSAM. This assessment used the two metrics of distribution of number of conflicts and conflict rates. The conflicts were further categorized using conflict types of crossing, rear-end and lane change based on absolute angles in section 2.5.2, Table 7. In addition to conflict types, interactions based on conflicting vehicles were considered and these included Vehicle–to-Vehicle (V2V), Vehicle-to-Motorcycle (V2M) and Motorcycle-to-Motorcycle (M2M). Pedestrian to anything interactions were not considered because their trajectories are not generated by the microsimulation platform. As well, bicycle to anything interactions were not considered in this study because of low bicycle volume.

The distributions of observed and base simulated conflicts were statistically tested using chi-squared goodness-of-fit test as explained by Zeng et al. (2015) to ensure that they (distributions) were comparable. The conflicts of scenarios 2 and 3 were then compared to those of the base scenario in order to determine the percentage reduction of each measure. Regarding conflict rates, the average conflict rates were checked using paired samples t-tests as described by Gerald (2018). Importantly, the chi-squared goodness-of-fit test is applicable to frequencies (non-continuous data) while the paired samples t-test can be used for continuous data such as conflict rates. A scenario that highly reduced the conflicts or their rates was deemed the most effective.

With regard to SSAM, the software processes the trajectory data of vehicles driving through a traffic facility and then calculates surrogate measures of each vehicle to vehicle interaction following a certain criteria (Vasconcelos et al., 2014). For example, less than 5 and 1.5 seconds for PET and TTC, respectively. PET is determined as the time between the departure of the encroaching vehicle from the conflict point and the arrival of the vehicle with the right-of-way

at the conflict point (Gettman & Head, 2003). The same study clarified that TTC is the difference between the encroachment end time of the turning vehicle and the projected arrival time of the through vehicle with the right-of-way at the conflict point if the vehicle had continued at the same speed at which it was travelling at the time of initial deceleration to avoid collision. The model was validated for unsignalized and urban intersections (Gettman & Head, 2003). Furthermore, a final report to U.S Department of Transportation by Gettman et al. (2008) details the four steps of conflicts identification algorithms and further validation. Firstly, the software determines the dimensions of the analysis area based on the header name in the trajectory file. Secondly, a single time step of the trajectory file is analysed. Thirdly, the rectangular perimeter delineating the current and future locations of each vehicle is established. Lastly, more detailed processing of each V2V, V2M and M2M interactions for the current time step is performed.

3.9 Ethical Issues

Ethical issues in the study were dealt as detailed in this section. First and foremost, video images make it possible to derive identities of people and personal information from vehicle registration plates. Henceforth ethical approvals from both SWOV and TU Delft (see Appendix E) were sought before receipt of data and further data processing. A data transfer agreement was signed between Uganda Police and the University stipulating the obligations of either party and security issues to be addressed. Furthermore, a standard data processing agreement was signed between the University and Transoft Solutions following the General Data Protection Regulation (GDPR) 2016/679 of the European Union. All these measures were taken to guarantee safe handling of the data by all parties.

Secondly, the data collection team was exposed to fast moving traffic and associated risks during field measurements. All participants in field work wore personal protective equipment especially reflectors, and the activities were well coordinated to minimize exposure time. Reflectors did not influence driver behavior since drivers mainly take note of traffic police uniform but not ordinary people with reflectors. The use of a measuring wheel fastened the measurement of the approach length while a steel tape was used to measure lane width and other smaller dimensions. These tools were readily available and easy to use. Spot speeds were collected at a safe distance from the intersection and all field work was carried out in the presence of Traffic Police. The main role of the police was to secure the enumerators from errant traffic especially motorcycles.

After data processing and analysis, the video data was permanently erased from the clouds of both the University and Transoft Solutions in accordance with the agreements. In addition, the data was not shared with any other person during the study, video images including means to identify people were not used in any report.

4|Implementation

In this section, the details of the steps followed to execute the study are described. First, section 4.1 explains how the base model was developed. Sensitivity analysis is detailed in section 4.2 while section 4.3 discusses the steps for both calibration and validation. Lastly, section 4.4 describes how the scenarios were developed and assessed.

4.1 Base model development

4.1.1 VISSIM

Firstly, the intersection was created with a background extracted from PTV VISSIM Maps and supplemented with aerial pictures of the study intersection. The developed model as depicted in Figure 14 was then improved based on the actual and measured details of the intersection (road geometry) including lane width, shoulder width, slope, and width of medians. A short video of the base model is also available on YouTube (Mwine, 2022a). The base model Traffic properties of volume, composition and characteristics were incorporated in the VISSIM model. More general and evaluation modifications made in VISSIM are included in Appendix A.

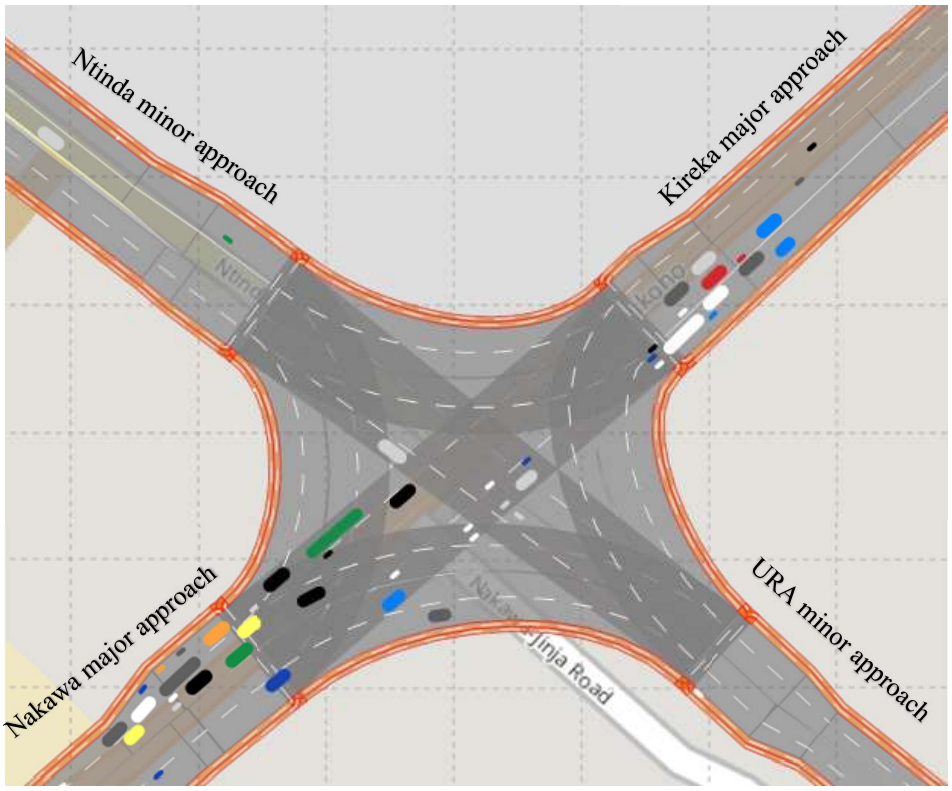

Figure 14: Base model of the unsignalized intersection in VISSIM

3D models of the existing vehicle types in Uganda were obtained from 3D warehouse and then imported into VISSIM. Care was taken to ensure that the dimensions of 3D models are comparable to those of the existing vehicles in Uganda. The latter was achieved based on websites of different car manufacturers and importers. For example, a 3D model of a minibus (taxi for public transport in Kampala) licensed to carry at most 16 people including the driver was imported into VISSIM. In addition, the carrying capacity of the vehicles was set according to the practice as observed in the field and not according to the laws or vehicle specifications.

This is because of low adherence to traffic laws in Uganda. For instance, capacity of a motorcycle was increased from two to three since this (and overloading) is common practice in Uganda. These traits make the traffic conditions in Kampala entirely heterogenous.

Desired speed distributions of vehicles approaching the intersection at about 50-100m were developed using spot speeds per vehicle category and approach. These graphs are illustrated in Appendix A, for all the approaches as well as Heavy Good Vehicles (HGV) and buses. These distributions were updated in VISSIM per approach for the vehicle categories of motorcycles, Sport Utility Vehicles (SUVs), passenger cars and taxis or matatu. HGVs were combined for all the approaches including buses, trailers, and semi-trailers in order to obtain the minimum number of observations based on variation at a confidence of 95% and desired accuracy of 10%. Not enough data was obtained in the field for bicycles and Light Good Vehicles (LGVs) on either separate approaches or combined for the intersection. Thus, bicycles were ignored entirely in the study while LGVs used a speed distribution of HGVs. Speed distributions per vehicle type in the conflict area were developed and for each vehicle class included in the simulation (see Appendix A).

Importantly, VISSIM parameters for driver behavior were set to model the heterogenous traffic conditions. Vehicles were allowed to place anywhere in the lane by setting the Wiedemann 74 (W-74) driving behavior parameter 'desired position at free flow' to 'any'. In addition, vehicles could overtake along the right or left of the slower vehicle after. Reduced speed areas were also applied near the intersection to exhibit field traffic conditions. Detectors for data collection in VISSIM were placed at the exact location where field observations were made to ensure consistency while extracting data. For the case of reduced speed areas, maximum deceleration rates for each vehicle type as shown in Table 10 were used to model traffic behavior as also observed in the field. The maximum deceleration was determined using box plots as shown in Appendix A to ignore outliers.

Table 10: Maximum deceleration of vehicle types in the conflict area

Vehicle type	Minimum number of measurements (n_{min})	Number of observations (n)	Maximum deceleration (m/s^2)
Passenger car	403	6506	1.41
Taxi or matatu	398	1285	1.46
SUVs	173	197	2.04
Bus	104	121	1.44
HGV	460	9488	2.16
Motorcycle	425	956	2.06

4.1.2 Data

Regarding the use of observed data in the study, the following adjustments were made to either the observed data or to the base model:

First, it was observed from the observed data and videos that some motorcycles were using sidewalks instead of the normal carriageway. This situation was replicated in the base model by using vehicle compositions in VISSIM specific to sidewalks and including both pedestrians and motorcyclist. However, motorcycles were not observed at crosswalks but only pedestrians.

At the same time, some motorcycles were observed as bicycles during video data processing. Their (bicycles) speed distribution was close to that of motorcycles (see Appendix A) and in actual sense bicycles cannot be faster than even passenger cars. Additionally, it was observed

during the site visit as well as in the video images that there were very few bicycles using the intersection. Consequently, the reported volume of bicycles was added to motorcycles.

On the other hand, the volume for Heavy Good Vehicles (HGV) included both rigid trucks and articulated trucks as obtained from observed data. Camera data revealed that the volume of articulated trucks was lower than that of rigid trucks.

Due to limitations of the camera view, no data was obtained for the Nakawa crosswalk (CW1), Nakawa-Ntinda sidewalk (SW1) and Nakawa-URA sidewalk (SW4). However, their corresponding values were corrected and assumed to be equal to Kireka crosswalk (CW3), Ntinda-Kireka sidewalk (SW2) and URA-Kireka sidewalk (SW3), respectively. These crosswalks and sidewalks are indicated in Appendix A.

Observed traffic data were checked by Transoft to correct for double counts which are possible when road user types are for example obstructed from view. Also, vehicles with extremely low occupation times were removed from the dataset

The observed data was sorted to obtain off-peak time periods after review of video images to determine the same periods without congestion and traffic police at the intersection. Furthermore, any conflicts with either TTC or PET equal to zero were deleted since these are collisions and not conflicts. The considered thresholds for PET and TTC were 5.0s and 1.5s, respectively, as best practice according to Mahmud et al. (2019). Subsequently, conflict rate per 1000 road users and per 1000 motorcyclists were calculated and are indicated in Figure 15 and Figure 16, respectively.

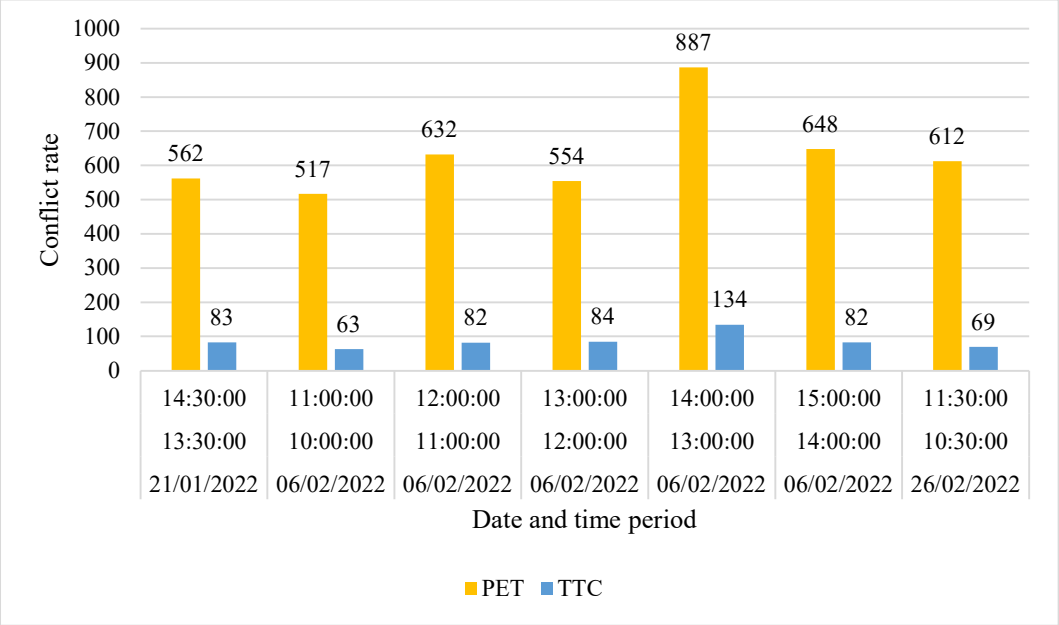

Figure 15: Conflict rates per 1000 road users (all) over the off-peak time periods

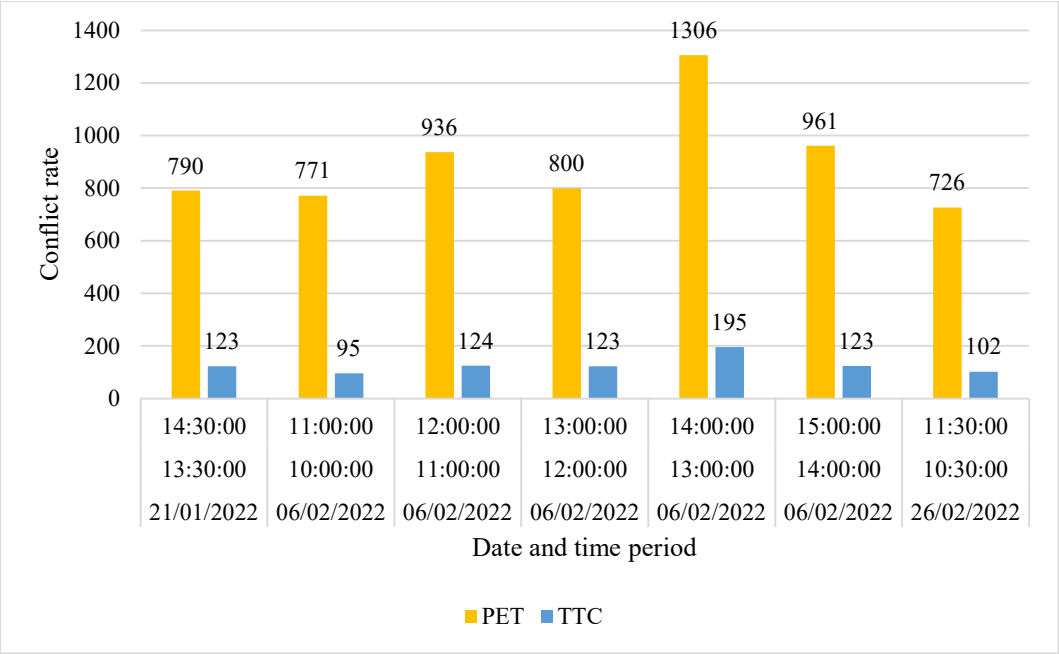

Figure 16: Motorcycle conflict rate per 1000 motorcycles over selected off-peak time periods

Based on the above results, data for 06/02/2022 between 13:00 and 14:00 were selected to represent the off peak at this intersection. These data reveal the highest conflict risk for all road users, and specifically motorcyclists, and therefore were used as input for building the base model and calibrating it. A pie chart of traffic volumes by road users for this period is illustrated in Figure 17 with more than 50% being motorcyclists.

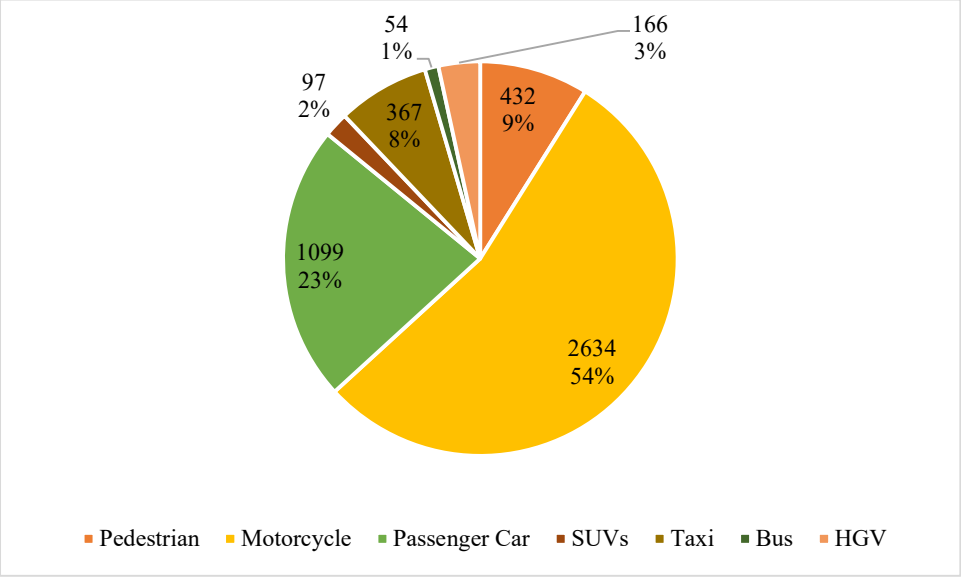

Figure 17: Pie chart of traffic volumes (corrected) by road users-06/02/2022 from 13.00 to 14.00[1]

Secondly, data on 26/02/2022 from 10:30 to 11:30 was used to validate the model as well as for scenario development. This decision aimed at increasing time variability since data was collected in the morning hours whilst data for model development was collected in the afternoon hours. Moreover, the conflict rate (for all road users and also motorcyclists only) was in the same range as other off-peak periods.

1. Cyclists were excluded due to low counts

4.2 Sensitivity analysis

Sensitivity analysis was carried out considering driving behavior parameters indicated in Table 11 that have identified in previous research studies and not using all the parameters that affect behavior in VISSIM modelling. The parameters are further detailed in Appendix B. The studies included were also for VISSIM modeling for mixed flow conditions (Bandi & George, 2020; Dadashzadeh et al., 2019; Paul et al., 2017; Siddharth & Ramadurai, 2013). The parameters are for car–following, lane changing and lateral behaviors. Additional lateral behavior parameters for specifically motorcycles and taxi were included to cater for exceptional maneuverability in traffic as observed in the video images. A code was set up in MATLAB to automate the process using a Component Object Model (COM) interface with VISSIM. Since the base model was built using field data such as geometry, speed distributions, traffic volume, traffic composition and visually checked, the model outputs (average occupation time and maximum queue length for minor approaches) were not compared with corresponding observed data. The average occupation time for all vehicles and maximum queue length per minor road and per time interval were considered during this analysis.

Table 11: Parameters and corresponding default Values in VISSIM 21

Behavior	ID	Model Parameters	Description	Default value	Adopted Range
Following	1	W74ax	Average standstill distance	2.0m	0.50 ~ 2.50
	2	W74bxAdd	Additive part of safety distance	2.0	0.10 ~ 2.00
	3	W74bxMult	Multiplicative part of the safety distance	3.0	0.00 ~ 3.00
	4	LookAheadDistMin	Look ahead distance-min	0m	0.00 ~ 30.00
	5	LookBackDistMin	Look back distance-min	0m	0.00 ~ 30.00
Lane change	6	MaxDEcelOwn	Maximum deceleration (own)	-4.0m/s^2	-5.00 ~ -1.00
	7	MaxDEcelTRail	Maximum deceleration (trailing vehicle)	-3.0m/s^2	-4.00 ~ -1.00
	8	DiffusTm	Diffusion time	60s	25.00 ~ 65.00
	9	MinFrontRearClear	Minimum clearance (front/rear)	0.5m	0.10 ~ 1.00
	10	SafDistFactLnChg	Safety distance reduction factor (lane change)	0.6	0.10 ~ 1.00
Lateral	11	LatDistStandDef	Default Lateral distance at standstill	1.0m	0.05 ~ 0.50
	12	LatDistDrivDef	Default Lateral distance at 50km/h	1.0m	0.50 ~ 1.0
	13	LatDistStand for motorcycles	Lateral distance at standstill	1.0m	0.05 ~ 0.20
	14	LatDistDriv for taxis	Lateral distance at 50km/h	1.0m	0.30 ~ 0.80
	15	LatDistDriv for motorcycles	Lateral distance at 50km/h	1.0m	0.20 ~ 0.70

The analysis was carried out using the elementary effects method as earlier stated in section 3.6. A COM interface facilitated the analysis by applying four random seeds. Six model outputs of average occupation time and maximum queue length on the two minor approaches for both the through and right turns were used to evaluate elementary effects of changes in model parameters. It should be noted that queue length was considered per minor approach and not a specific turn since there are no specific lanes for the various turning movements. In addition, outputs that returned any undefined values were not considered because they could not be compared with other data. The general ranking of model parameters is provided in Table 12 (details are provided in Appendix B). Variation of the ranks was checked using Equation [3-2]

to confirm that enough simulations were run to provide a 95% confidence interval and desired accuracy of 10% of the mean rank.

Table 12: Results of sensitivity analysis and general rank(descending)

Behavior	ID	Model Parameters	Description	Sensitive?	Rank
Following	1	W74ax	Average standstill distance	Yes	8
	2	W74bxAdd	Additive part of safety distance	Yes	9
	3	W74bxMult	Multiplicative part of the safety distance	Yes	7
	4	LookAheadDistMin	Look ahead distance-min	Yes	10
	5	LookBackDistMin	Look back distance-min	Yes	11
Lane change	6	MaxDEcelOwn	Maximum deceleration (own/leading)	No	12
	7	MaxDEcelTRail	Maximum deceleration (trailing vehicle)	No	13
	8	DiffusTm	Diffusion time	No	14
	9	MinFrontRearClear	Minimum clearance (front/rear)	No	15
	10	SafDistFactLnChg	Safety distance reduction factor (lane change)	Yes	6
Lateral	11	LatDistStandDef	Default Lateral distance at standstill	Yes	3
	12	LatDistDrivDef	Default Lateral distance at 50km/h	Yes	2
	13	LatDistStand for motorcycles	Lateral distance at standstill	Yes	1
	14	LatDistDriv for taxis	Lateral distance at 50km/h	Yes	5
	15	LatDistDriv for motorcycles	Lateral distance at 50km/h	Yes	4

Generally, lateral driving behavior parameters were established to be the most sensitive, followed by following behavior parameters and lastly lane changing behavior. Based on this result, only the sensitive parameters were further used in calibration whereas non-sensitive parameters were fixed using values obtained from earlier studies.

4.3 Calibration and validation

This section describes the steps applied particularly during calibration and validation of the model. Particle Swarm Optimization (PSO) was used to calibrate the base model as explained in section 3.7.1 while both microscopic and macroscopic were applied following the criteria in section 3.7.2.

4.3.1 Calibration

A MATLAB code to facilitate COM interface with VISSIM was developed to calibrate the base model using the objective function in Equation [3-5]. In the code, non-sensitive parameters and PSO factors were fixed based on a study by Paul et al (2017) for unsignalized intersections with mixed traffic and recommendations by Adewumi and Arasomwan (2015). The adopted values for the parameters and factors are indicated in Table 13.

Table 13: Fixed non-sensitive parameter values and other PSO values used in calibration

Parameter or factor	Value
Maximum deceleration (own/leading)	-3.341m/s^2
Maximum deceleration (trailing vehicle)	-3.025m/s^2
Diffusion time	60s
Minimum clearance (front/rear)	0.535m
Learning constants, c_1 and c_2	2.0
Velocity clamping factor, μ	0.15

During simulations, simulated data was collected using vehicle travel time measurement function in VISSIM for occupation time and queue counters for the maximum queue length. These detectors were placed at the beginning and end of the conflict areas as defined in the video analysis of the field data. Simulated data for eight model outputs was compared with field data (see Appendix C). These outputs show occupation time of all vehicles for both through and right turns of minor roads and only right turns for motorcycles. Additionally, the maximum queue length was considered for the only the minor approaches.

In this study, PSO was conducted with 10 particles running for a maximum of 50 iterations and the results are indicated in Figure 18. These constants were based on literature as other researchers had previous used the same trials. For example Dadashzadeh et al. (2019) used 10 particles and 40 iterations in PSO. Furthermore, five random seeds (42, 45, 47, 49 and 51) were employed and the corresponding results are in Appendix C. The least attained value of the objective function per seed ranged between 6.89 and 5.60 and so the values were close. Similarly, the differences between the values of each parameter per seed were generally low. As a result, optimum values for the calibrated parameters were adopted for the random seed that returned the least minimum value for the objective function are shown in Table 14. These calibrated parameters were thereafter utilized in validation and scenario development.

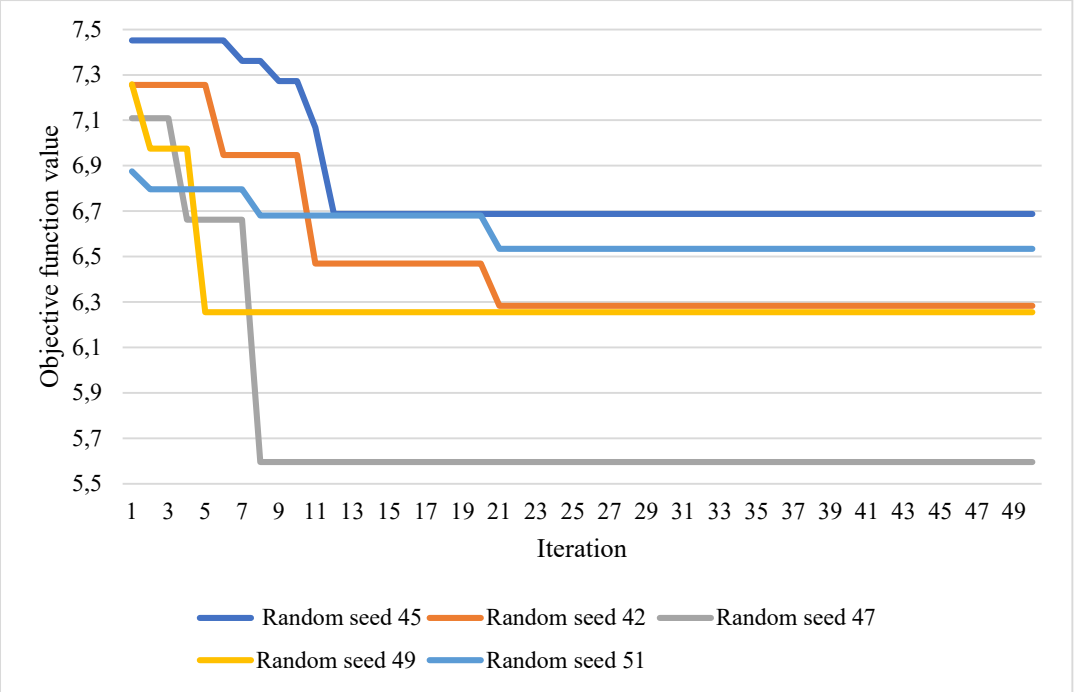

Figure 18: Variation of the objective function per random speed

Table 14: Optimum values after calibration

Behavior	ID	Parameter description	Optimum value
Following	1	Average standstill distance	1.66
	2	Additive part of safety distance	0.98
	3	Multiplicative part of the safety distance	1.79
	4	Look ahead distance-minimum	16.27
	5	Look back distance-minimum	9.61
Lane change	10	Safety distance reduction factor (lane change)	0.47
Lateral	11	Default Lateral distance at standstill	0.28
	12	Default Lateral distance at 50km/h	0.79
	13	Lateral distance at standstill for motorcycles	0.05
	14	Lateral distance at 50km/h for taxis	0.55
	15	Lateral distance at 50km/h for motorcycles	0.52
Objective function			**5.60**

Notably, the calibration process yielded a minimum value of the objective function of 5.60. This value could not accurately show the error between observed and simulated traffic conditions because the corresponding terms have equal weights in the objective function. Consequently, 8 independent samples t-tests were conducted using observed and simulated occupation time and queue length based on the optimum values (random seed=47). Simulated data for these tests is in Appendix C. This analysis resulted in p-values greater than 0.05 in all the cases. In this test, the null hypothesis was that the mean difference of the observed and simulated data is zero. This hypothesis was not rejected at 95% confidence interval in all the eight trials and thus the mean difference between the observed and simulated data was equal to zero. Therefore, the objective function converged, and the optimum values can be used for further analysis at this intersection.

4.3.2 Validation

Validation was done using both microscopic and macroscopic parameters as explained in section 3.7.2. Both occupation time and queue length of the minor approach vehicles were utilized in microscopic validation while flow and density were used for macroscopic validation. In addition, fundamental diagrams were used to illustrate the capability of the model to replicate traffic flow conditions. MATLAB codes were developed to input the calibrated driving behavior parameters as well as extract data from VISSIM. More so changes were made in VISSIM to include new traffic data, relative flows and vehicle composition as indicated Figure 19. Vehicle compositions were based on classified traffic data of 26/02/2022 from 10:30h to 11:30h is indicated in Appendix C.

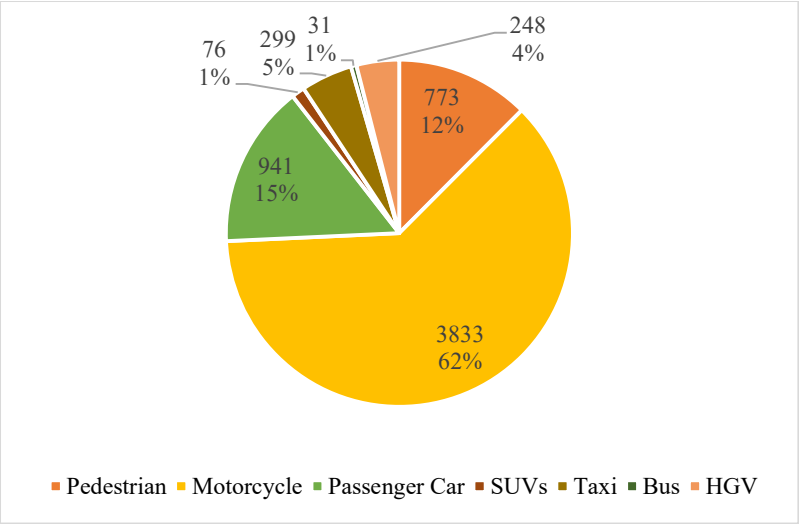

Figure 19: Corrected classified counts as applied in validation (26/02/2022 from 10:30h to 11:30h)[2]

In microscopic validation, maximum occupation time for all vehicles and motorcycles as well as queue length on the minor approaches of Ntinda and URA were used. The observed data per parameter in Appendix C (collected on 26/02/2022 from 10.30h to 11.30h was compared with simulated data per random seed (see Appendix C) using an independent samples t-tests. As indicated in Figure 20, the calculated p-values were greater than 0.05 for more than 85% of the 40 tests carried out. With p-values greater than 0.05, the null hypothesis that observed and simulated data had equal means was not rejected at 95% confidence interval. Therefore, the mean difference was zero between observed and simulated data, hence the model was valid.

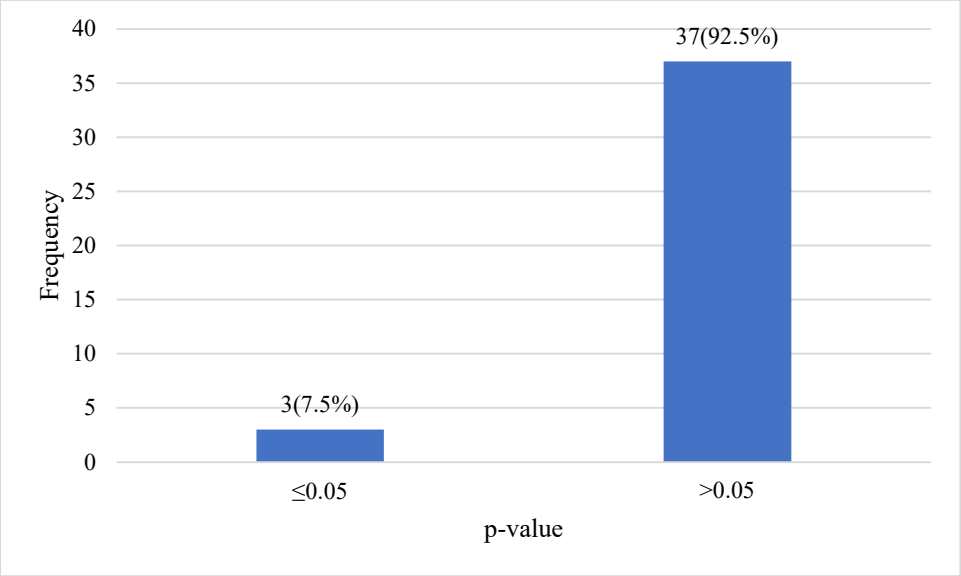

Figure 20: Bar chart of p-values for microscopic validation

For macroscopic validation, the GEH statistic was computed using Equation [3-11] for simulated and observed traffic counts shown in Appendix C. The traffic counts were initially collected using intervals of 5s but were aggregated to 5 minutes and then converted into hourly traffic volume. The same interval was used to input the traffic data in VISSIM. The bar chart in Figure 21 shows that all approaches had more than 85% of their corresponding GEH statistics less than or equal to a threshold of 5.0. The study had an acceptable goodness of fit

[2] Cyclists were excluded due to low counts

between the observed and simulated traffic counts. A maximum frequency of 60 was attainable since five random seeds were considered also with 5-minute intervals. The GEH statistic was only applied to traffic counts because according to Friedrich et al. (2019), the statistic is defined for hourly traffic volumes and is not suitable for other indicators.

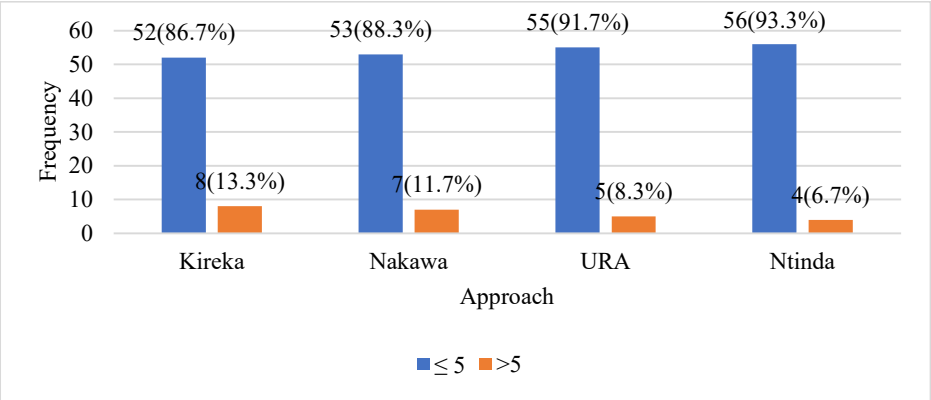

Figure 21: Bar chart of GEH statistic per approach

Furthermore, Fundamental Diagrams (FDs) were developed per approach and the t-test was performed for each seed, per simulated density and flow with corresponding observed density and flow. FDs for the major approaches are indicated in Figure 22 and Figure 23 for Kireka and Nakawa, respectively, while those for minor approaches are illustrated in Figure 24 and Figure 25 for URA and Ntinda. Harmonic speed and number of vehicles were extracted from VISSIM using a code and these were further processed to obtain both the flow and density as elaborated in section 3.8.2.

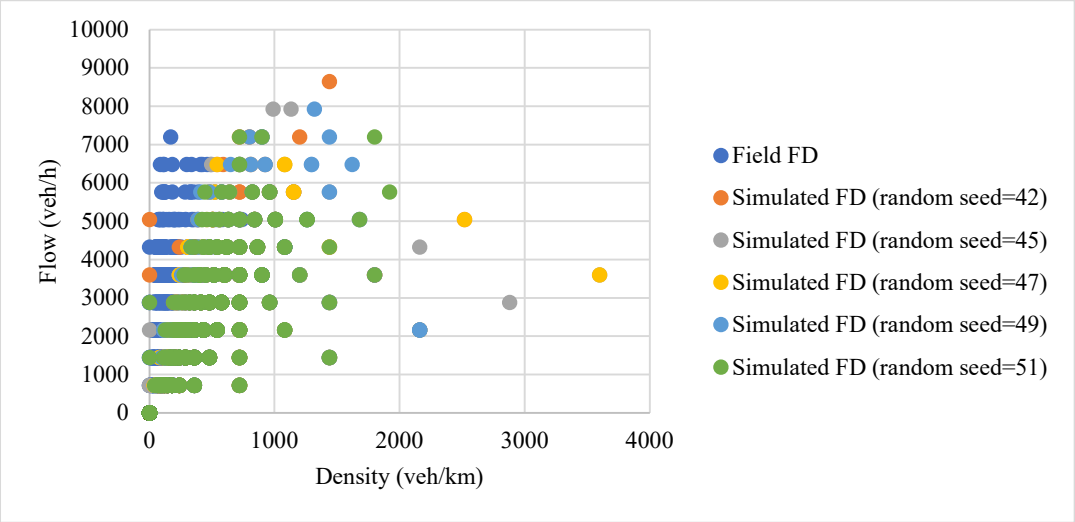

Figure 22: Fundamental diagram for observed and simulated traffic conditions-Kireka approach

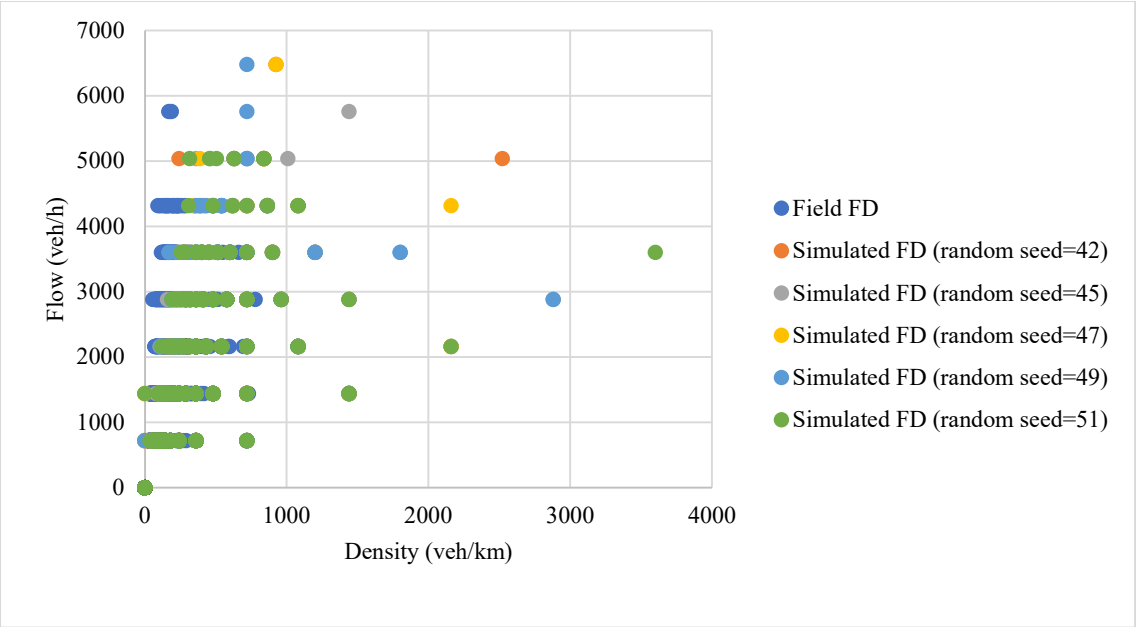

Figure 23: Fundamental diagram for observed and simulated traffic conditions-Nakawa approach

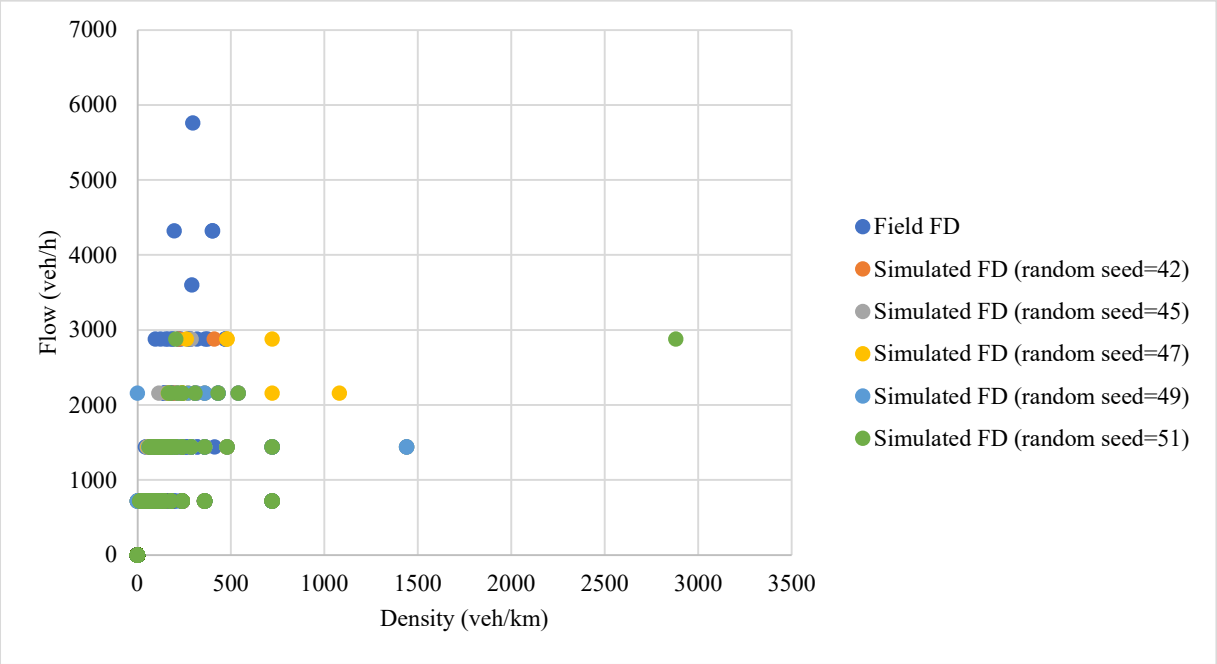

Figure 24: Fundamental diagram for observed and simulated traffic conditions-URA approach

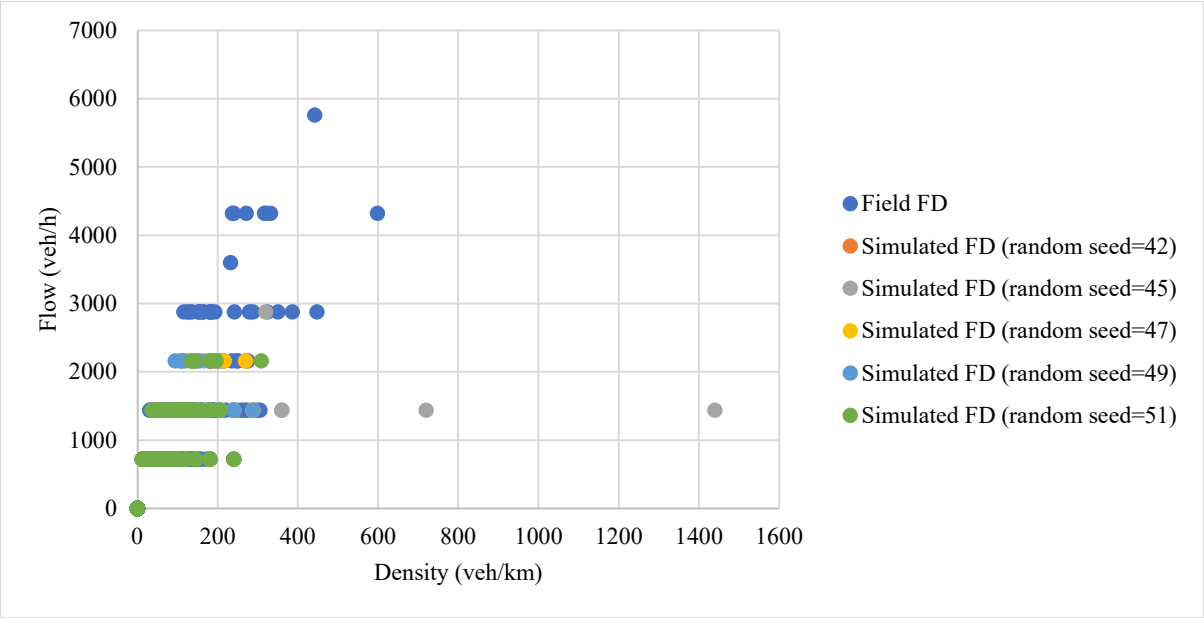

Figure 25: Fundamental diagram for observed and simulated traffic conditions-Ntinda approach

From the FDs, it is observed that simulated and observed points greatly overlap and mostly on the uncongested part. This observation is expected since simulations were performed for off-peak traffic conditions. The high flow rates above 2000veh/h are feasible on this intersection due to high inflow of motorcycles that arrive in batches and not one at a time. This occurrence is typical of intersections with non-lane based and mixed traffic.

4.4 Study models

4.4.1 Scenario development

During scenario development, a new driving behavior was introduced in VISSIM following the guidance of Kumar et al. (2012). For example, allowing diamond queueing for the motorcycles. This option allows motorcycles to be positioned offset and thus are represented not as a rectangle, but as a rhombus (PTV, 2021b). Dedicated motorcycle lanes were incorporated using the links function in VISSIM. These lanes were accorded separate vehicle inputs, routes, composition of only motorcycles and relative flows. The traffic volume was reduced for the normal carriageway based on the specific motorcycle volume per approach in the data previously utilized in validation. The volume of four-wheelers was therefore, maintained and motorcycles were allocated to the dedicated motorcycle lanes. In addition, conflict areas with other road users were resolved mainly to give right of way to the minor approach traffic or motorcycle lane in order to avoid blockage. This is because of the likelihood of blockage once major road traffic is favored. The impediment of minor traffic in VISSIM would result into a gridlock and hence field traffic conditions are not replicated. Important to note, the observed traffic does not follow priorities and hence this was considered by allowing all vehicles to approach the intersection at the same time. The performance of the intersection is enhanced by the stochasticity in VISSIM as road users find the right of way on a first come-first served basis. This randomness creates enough gap times for traffic and hence limits the development of congestion.

In order to obtain number of vehicles per 5-second intervals, data collection points were fitted on all approaches on both dedicated motorcycle lanes and the carriageway. Likewise, a node

and section were created in VISSIM to obtain Level of Service (LoS) and trajectories, respectively.

Figure 26 shows all scenarios developed in VISSIM for the study. In scenario 1, uni-directional motorcycle lanes on every approach and exit which allow motorcycles to cross within the conflict area. In scenario 2 the crossings are further offset so that they are further upstream of the intersection. In scenario 3 the intersection is converted to a 2-lane roundabout with separate motorcycle lanes Using a semi-trailer as a design vehicle, radius of central island, entry and exit radii etc, the roundabout was designed as stipulated in the Ugandan Road design manual, Ministry of Works and Transport (2010).

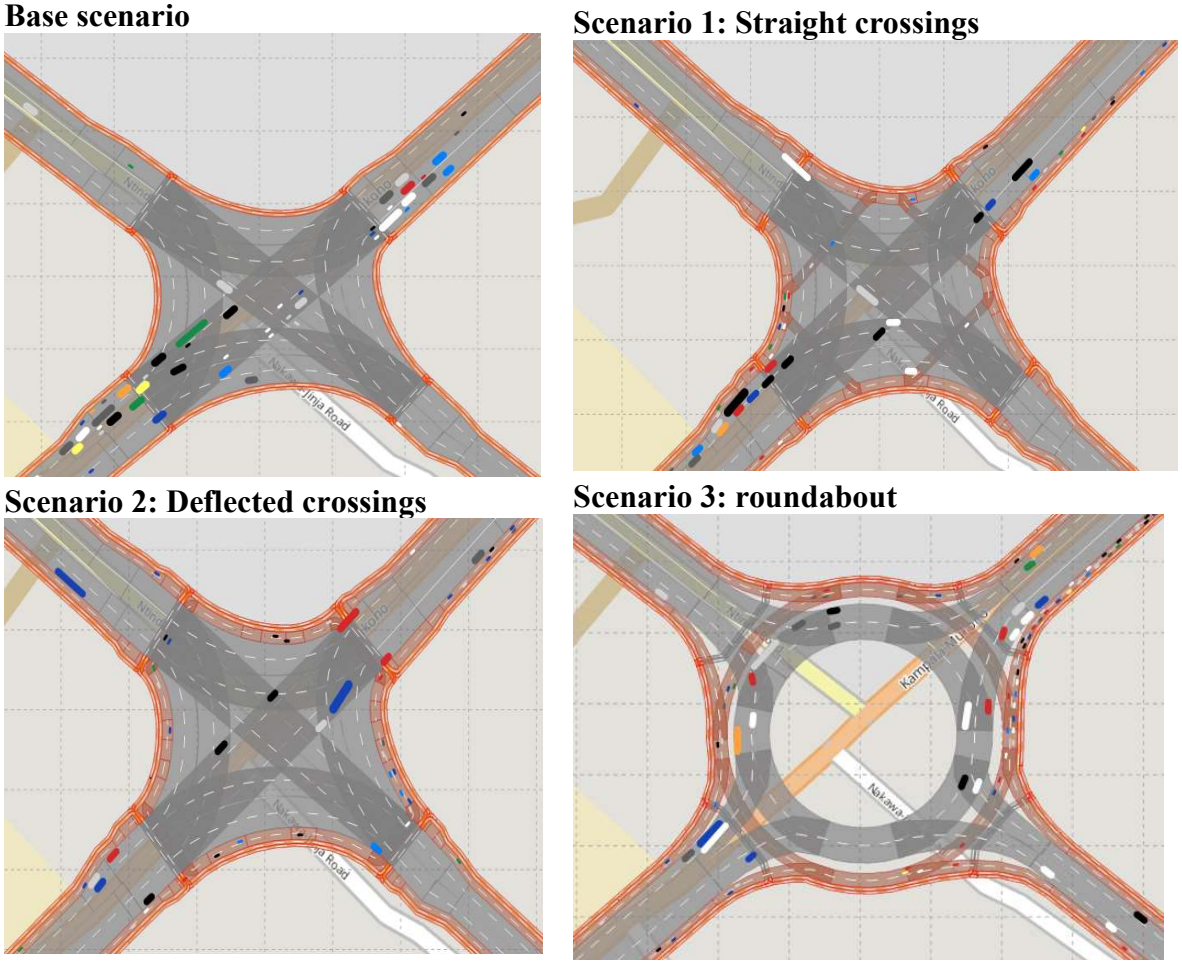

Figure 26: Developed scenarios in VISSIM

At the same time, driving behavior parameters were adjusted within VISSIM to optimum values since a code was not used to automatically control the software. The results were carefully configured to generate the required data (LoS, trajectories, speed, number of vehicles). The node results were obtained per 2-minute interval while speed and number of vehicles were collected per 5-second interval.

4.4.2 Safety assessment

In addition to the safety assessment methods mentioned in section 3.8.3, more steps were taken in order to harmonise between observed and simulated critical conflicts. Five random seeds were run but the seed with the highest number of conflicts (worst case) was considered for further analysis. The critical simulated conflicts were lower than the observed. These steps aimed at having comparable and realistic critical or severe critical conflicts that could be

analysed based on the study findings. In addition, simulated critical conflicts had both PET and TTC while observed critical conflicts had only PET. These steps are described in this section.

First, critical conflicts for through and right turn movements at the intersection were maintained for further analsysis because they were well controlled during video processing. The quality control results from Transoft clearly indicated the conflicts that had fewer errors due to the camera angle and obstruction. Consquently, critical conflicts that occurred only on the corresponding links in VISSIM were filtered from observed conflicts for the base case and scenarios 2 and 3.

VISSIM does not yield pedestrian trajectories and again these were not completely observed using video images. Therefore, pedestrian conflicts and interactions were excluded from further analysis.

Thirdly, PET and TTC thresholds for critical conflicts were adjusted according to the ones adopted by Transoft especially during quality control. These adjustments were made to ensure consitency in the study. Therefore, conflicts with TTC and PET ranging from 0 to 1.5s were extracted using SSAM. All conflicts with either TTC or PET equal to zero were deleted in both observed and simulated data. A chi-squared goodness-of-fit test was carried out using number of critical conflicts per 0.25s interval of PET for both the observed data and base scenario. Details on how the chi-squared goodness-of-fit test was performed are explained by Zeng et al. (2015). Both the actual and expected critical conflicts are indicated in Appendix D. With a p-value less than 0.05, the null hypothesis was rejected that is the distributions of the number of observed and simulated critical conflicts for the base using PET are the same. The alternative hypothesis was thus accepted and therefore, the distributions of the number of observed and simulated base critical conflicts over the applied intervals were different. Therefore, the base critical conflicts could not be compared with those critical conflicts generated from scenario 2 and 3.

The rejection of the null hypothesis for the critical conflicts implied that more evidence is required to further study the critical conflicts. Therefore, severe critical conflicts were filtered using a PET threshold of 0.5s. Such low thresholds are suggested by Paul and Ghosh (2020) who recommdend a PET threshold of 1.0s for critical conflicts invloving motorcycles and at unsignalized intersections in developing countries. The use of 0.5s as a PET threshold for severe critical conflicts in this study is hence justified.

The extent to which the distributions of severe critical conflicts for observed and simulated base case per interval (0.10) were the same was again tested using a chi-squared goodness-of-fit test. Both the actual and expected severe critical conflicts are indicated in Appendix D. With a p-value more than 0.05 (degrees of freedom, df=4; test statistic, χ^2=8.479; critical statistic, χ^2=9.488), the null hypothesis was not rejected at 95% confidence, that is, the distributions of the number of observed and simulated conflicts for the base using PET were the similar.

The severe critical conflicts were further categorized according to interaction and conflict type and the corresponding reductions computed with respect to the simulated base severe critical conflicts. Interaction types of Vehicle-to-Vehicle (V2V), Vehicle-to-Motorcycle (V2M) and Motorcycle-to-Motorcycle (M2M) were extracted from the observed and simulated data for the conflicting vehicles.

The distributions of severe critical conflicts shown in Appendix D were further used to determine severe critical conflict rates. These rates were calculated by dividing the distribution

(frequencies) by the exposure data of total simulated traffic per scenario as indicated in Appendix D. Furthermore, the severe critical conflict rates were categorized according to interaction and conflict types. The corresponding reductions of conflict rates for the simulated scenarios 2 and 3 in respect to the simulated base case were also determined. The significance/p-values were calculated using paired samples t-tests as explained by Gerald, (2018). This test did not justify the reduction of conflict rates but rather the difference between average rates for the base and simulated scenarios. Despite the use of only 3 observations per test which are lower than the minimum of 30 observations for normal distribution, this microsimulation study included more than 3,500 vehicles per simulation (see Appendix D) and hence robust conclusions can be made.

5|Traffic flow and safety results

Based on the observed traffic data, traffic flow and safety results were generated from VISSIM and further analyzed in order to assess the potential improvement to the current intersection. Traffic flow results are discussed in section 5.1 including the Level of Service (LoS), while safety related results are described in section 5.2.

5.1 Traffic Flow

Traffic flow results of all the three scenarios are discussed in this section in terms of flow, density, average speed, and delay. Important to note, flow is reported in vehicles per hour (veh/h) per approach but not per lane. Secondly, vehicles are summed up without application of conversion factors to Passenger Car Units (PCUs) because the percentage of Heavy Good Vehicles (HGVs) and buses was about 5%. This percentage was low compared to other vehicles whose conversion factor to PCU is one according to the Ugandan design guidelines by MOWT (2010).

5.1.1 Base

First the base scenario with no changes in the existing provisions for motorcycles at the intersection was considered. Five random seeds were used in VISSIM to account for stochasticity and the results are demonstrated in Figure 27.

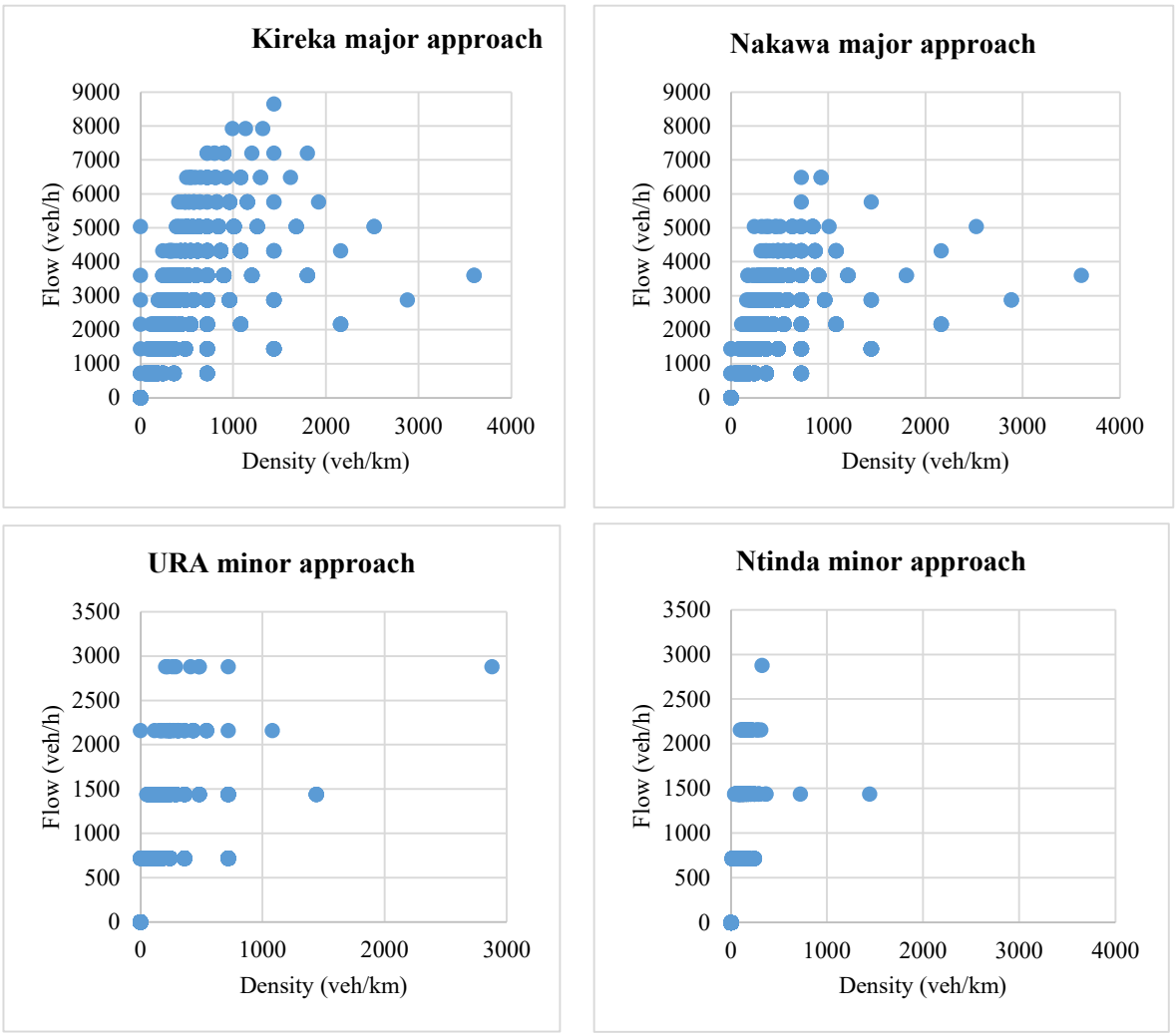

Figure 27: Fundamental diagrams of simulated traffic for the base scenario per approach

Generally, most simulated traffic operated on the uncongested part of the fundamental diagram for all approaches as illustrated in Figure 27. The Kireka approach registered a highest flow of about 8,000veh/h at a critical density of 1,000veh/km and this is in tandem with the traffic volume during the morning hours. This was followed by the Nakawa approach with a highest flow of approximately 6,500veh/h at a critical density of 600veh/km. These values result into average speed of 8km/h and 10.8km/h for Kireka and Nakawa approaches, respectively. This is based on the Daganzo bi-linear fundamental diagram that assumes a straight line for the uncongested part of a macroscopic fundamental diagram whose gradient is the free-flow speed/ average speed (Seo et al., 2019). In contrast, low flows and densities are observed on the minor approaches. For instance, the URA approach recorded the highest flow of approximately 3,000veh/h at a critical density of 300veh/km. These values translate into an average speed of 10km/h which is expected towards an intersection. In addition, a highest flow of about 2,500veh/h is noted for the Ntinda approach at a critical density of 200veh/km which yields an average speed of 12.5km/h.

5.1.2 Scenario 1-straight crossings

The first scenario with straight crossing points for motorcycles within the intersection was run for 5 random seeds and the results are further discussed in this section.

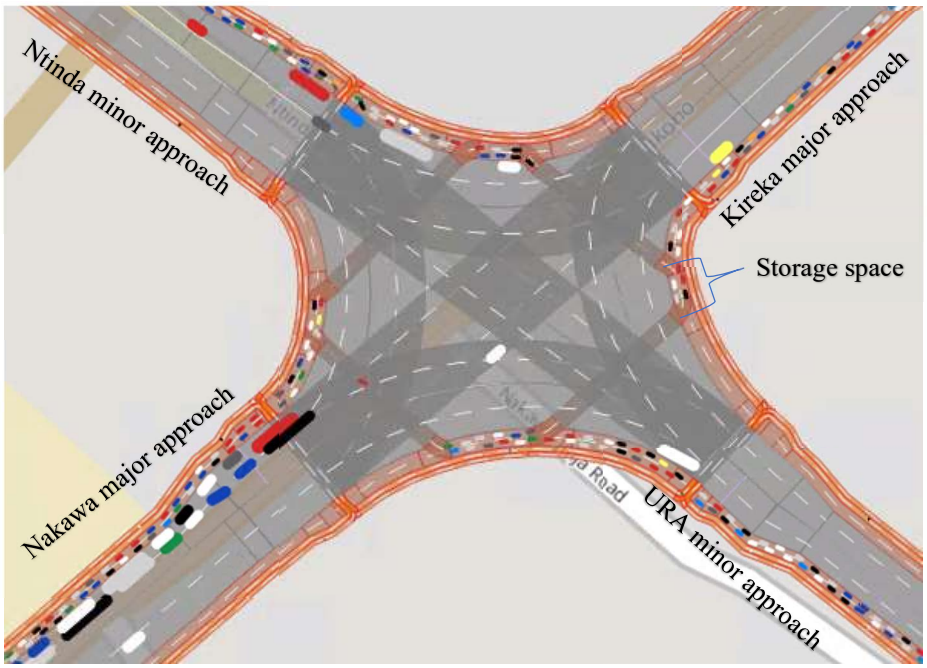

Figure 28: Blocked motorcycle (all) and Nakawa approaches for scenario 1-straight crossings

It was established that the approaches for all motorcycle dedicated lanes were blocked due to less storage space even before the end of startup duration (600s) as indicated in Figure 28. The blockage can be watched in a YouTube short video (Mwine, 2022d). Storage was constrained by the small gap distance between two conflicting areas especially on the major approach. This constraint resulted in blockage on the Kireka motorcycle approach which subsequently spilled over to other motorcycle approaches. Crossing motorcycles did not have any space downstream and so they stopped. Consequently, one of the four main approaches was also blocked in each run resulting into less observations per random seed. Fundamental diagrams were developed per main approach for vehicles excluding motorcycles as shown in Figure 29. No fundamental diagram was drawn for motorcycles since they were not recorded by the data collection points on the dedicated motorcycle lanes.

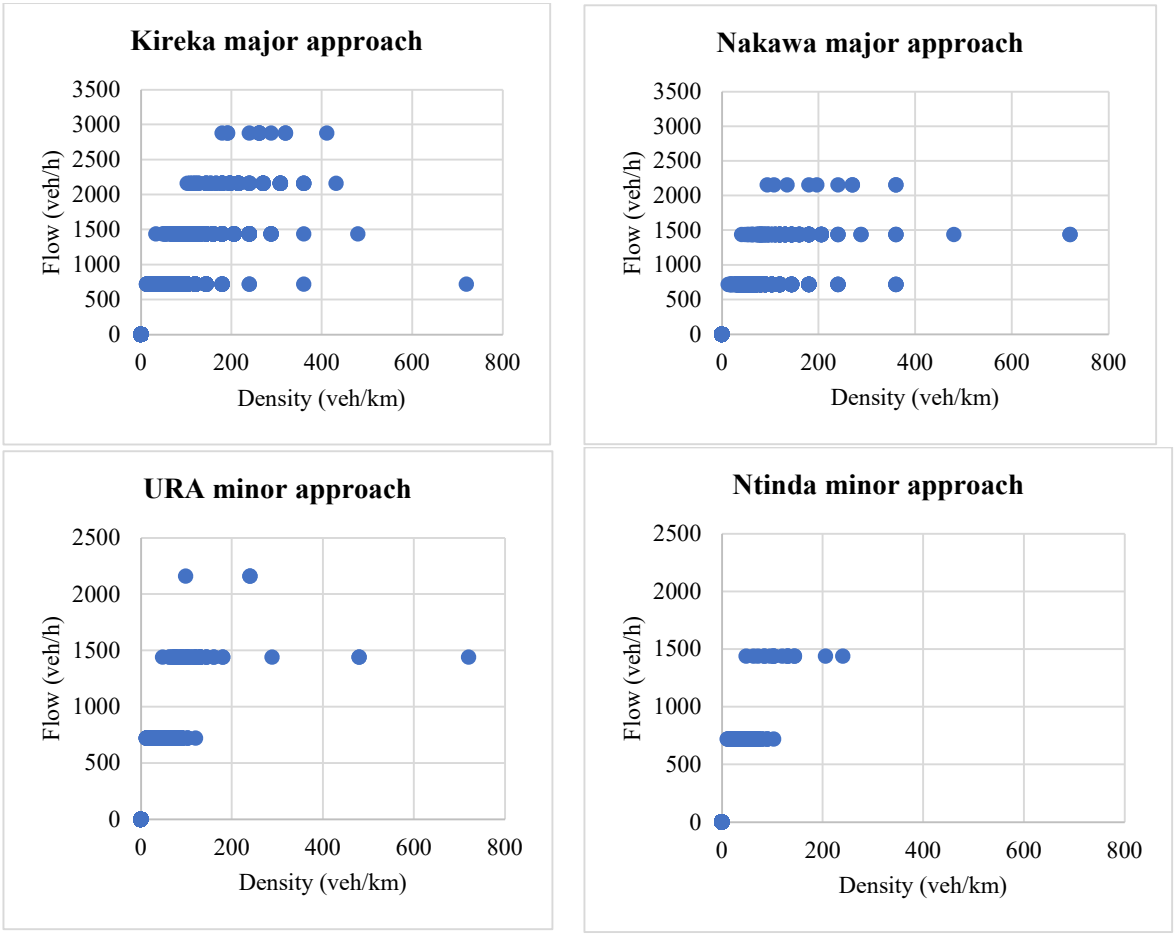

Figure 29: Fundamental diagram of simulated traffic per main approach for scenario 1-straight crossings

Approximate values for key traffic flow parameters based on the above fundamental diagrams are summarised in Table 15 for scenario 1.

Table 15: Traffic flow parameters for scenario 1-straight crossings

Approach	Maximum flow (veh/h)	Critical density (veh/km)	Average speed (km/h)
Kireka	3,100	250	12.4
Nakawa	2,500	200	12.5
URA	1,600	150	10.7
Ntinda	1,600	100	16.0

Both flow and critical density were higher on the major approaches of Kireka and Nakawa than on the minor (Ntinda and URA) approaches. It must be noted that these parameters are not conclusive since part of the intersection was blocked and hence vehicles were not observing normal behavior such as giving way to motorcycles. This behavior would greatly influence the performance of the intersection but is ignored. For this reason, scenario 1 was not considered a realistic alternative to the current situation.

5.1.3 Scenario 2-deflected crossings

In this scenario, separate dedicated motorcycle lanes are provided at the intersection and deflected further upstream of an approach to create a staggered crossing. As seen from Figure 30, scenario 2 allows smooth flow of traffic on the main approaches and motorcycles but some congestion is observed on the Kireka approach.

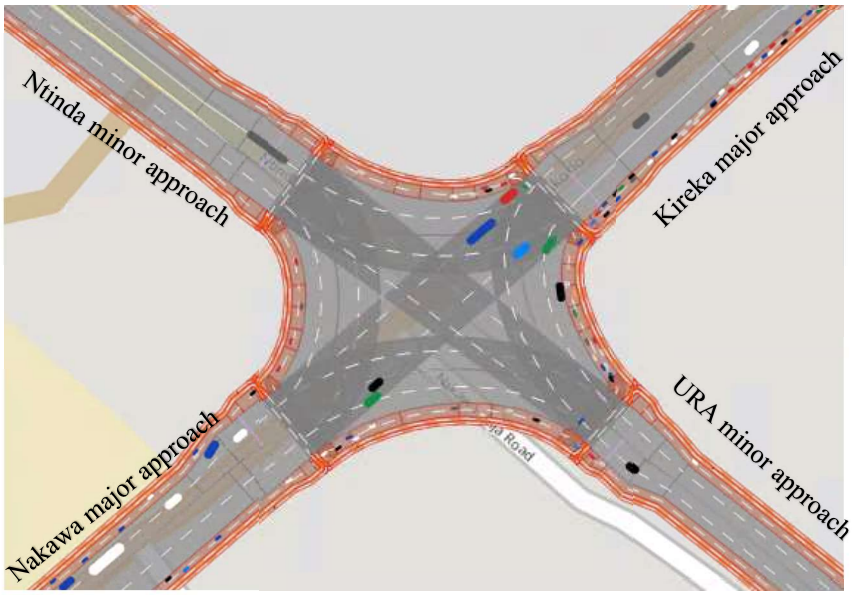

Figure 30: Snapshot of the microsimulation-scenario 2 (deflected crossings)

The fundamental diagrams of simulated traffic on the main approaches excluding motorcycles and dedicated motorcycle lanes per approach are indicated in Figure 31 and Figure 32, respectively. These were developed using traffic data of all the five random seeds and for 5-second time intervals of the one-hour simulation. Data for the start-up periods of 600s were not considered.

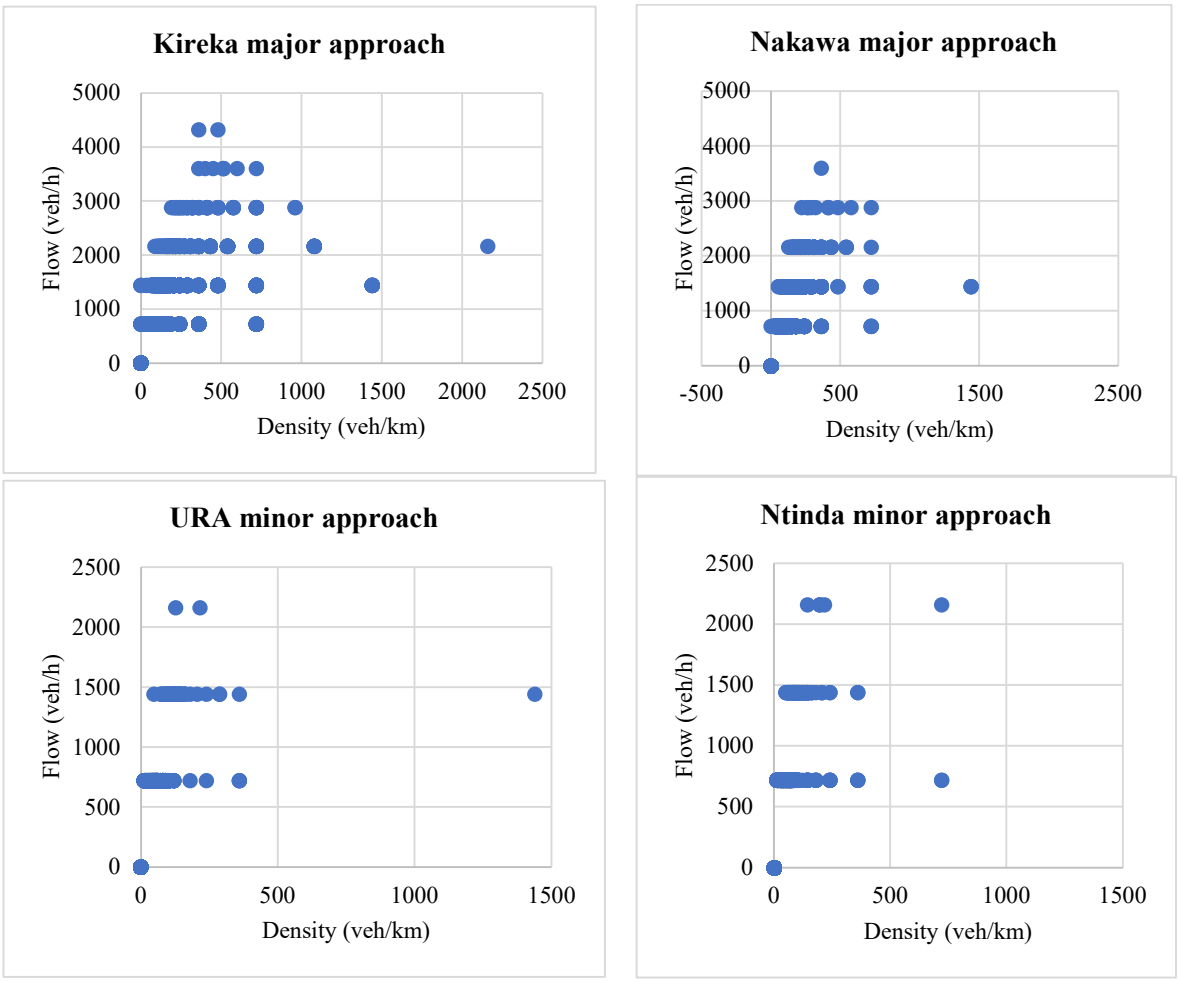

Figure 31: Fundamental diagrams of simulated traffic for the main approaches in scenario 2-deflected crossings

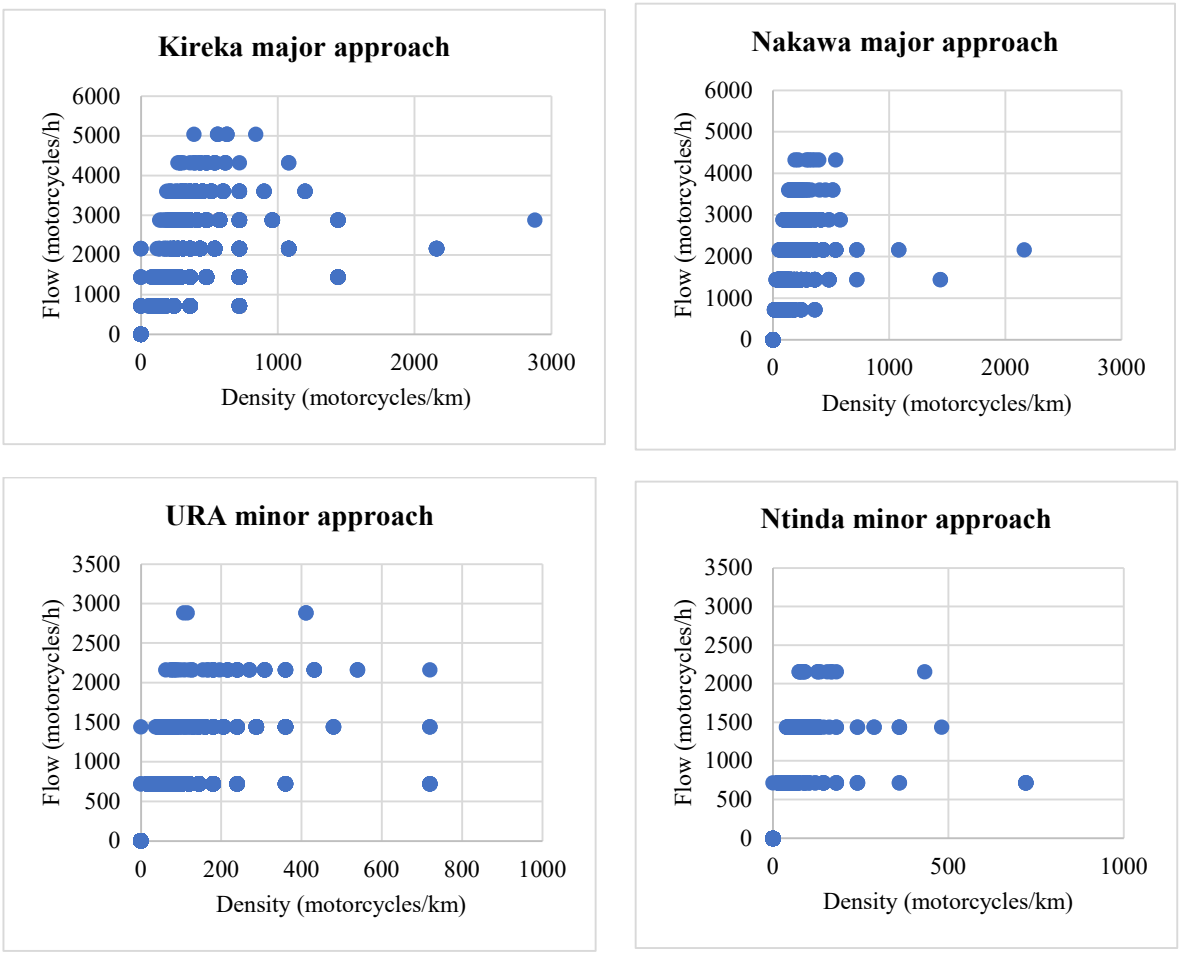

Figure 32: Fundamental diagrams of simulated traffic for the motorcycle approaches in scenario 2-deflected crossings

From the above fundamental diagrams, approximate values of key macroscopic traffic flow parameters are shown in Table 16.

Table 16: Traffic flow parameters for scenario 2-deflected crossings

Approach	**Maximum flow (veh/h)**		**Critical density (veh/km)**		**Average speed (km/h)**		**Total flow (maximum) (veh/h)**
Facility	Main	Motorcycle	Main	Motorcycle	Main	Motorcycle	
Kireka	4,500	5,500	500	600	9.0	9.2	10,000
Nakawa	3,500	4,600	400	400	8.8	11.5	8,100
URA	2,000	2,700	180	220	11.1	12.3	4,700
Ntinda	2,000	2,400	120	120	16.7	20.0	4,400

Generally, the highest flow of all the approaches increased compared to the base scenario. The highest flow for the major approaches of Kireka and Nakawa increased by about 25% while it increased by 56.7% and 76% for the URA and Ntinda minor approaches, respectively. Using traffic volume per approach in the base case as weights, the highest flow increased by 31%. In addition, less congestion was experienced on all approaches since the critical density decreased for both main road traffic (without motorcycles) and motorcycles on their own lanes. On the Kireka approach, 50% less vehicles occupied 1km while traffic on other approaches reduced by 33% to 40%. However, the speed in both the base and second scenario remained in the same range of average speed (8.0-20km/h). On all approaches, motorcycles had slightly higher average speed than traffic on the main road. The average speed of Ntinda approach was the

highest for both main traffic and motorcycles. With improved traffic conditions, the scenario was subjected to safety analysis. The performance of this scenario is shown in a YouTube short video (Mwine, 2022b).

5.1.4 Scenario 3-roundabout

Just like in scenario 2, some congestion is formed along the Kireka motorcycle approach as seen in Figure 33.

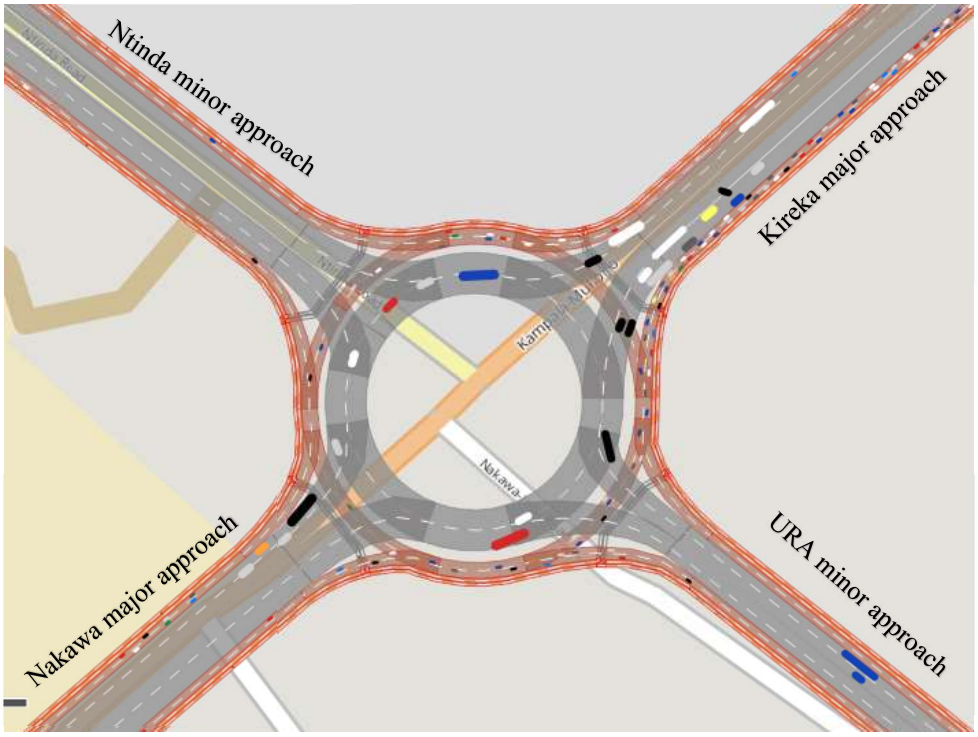

Figure 33: Snapshot of the microsimulation-scenario 3(roundabout)

In order to understand the traffic flow conditions, fundamental diagrams were developed for the main road approaches as well as the dedicated motorcycle approaches to the study intersection. These diagrams are clearly indicated in Figure 34 and Figure 35.

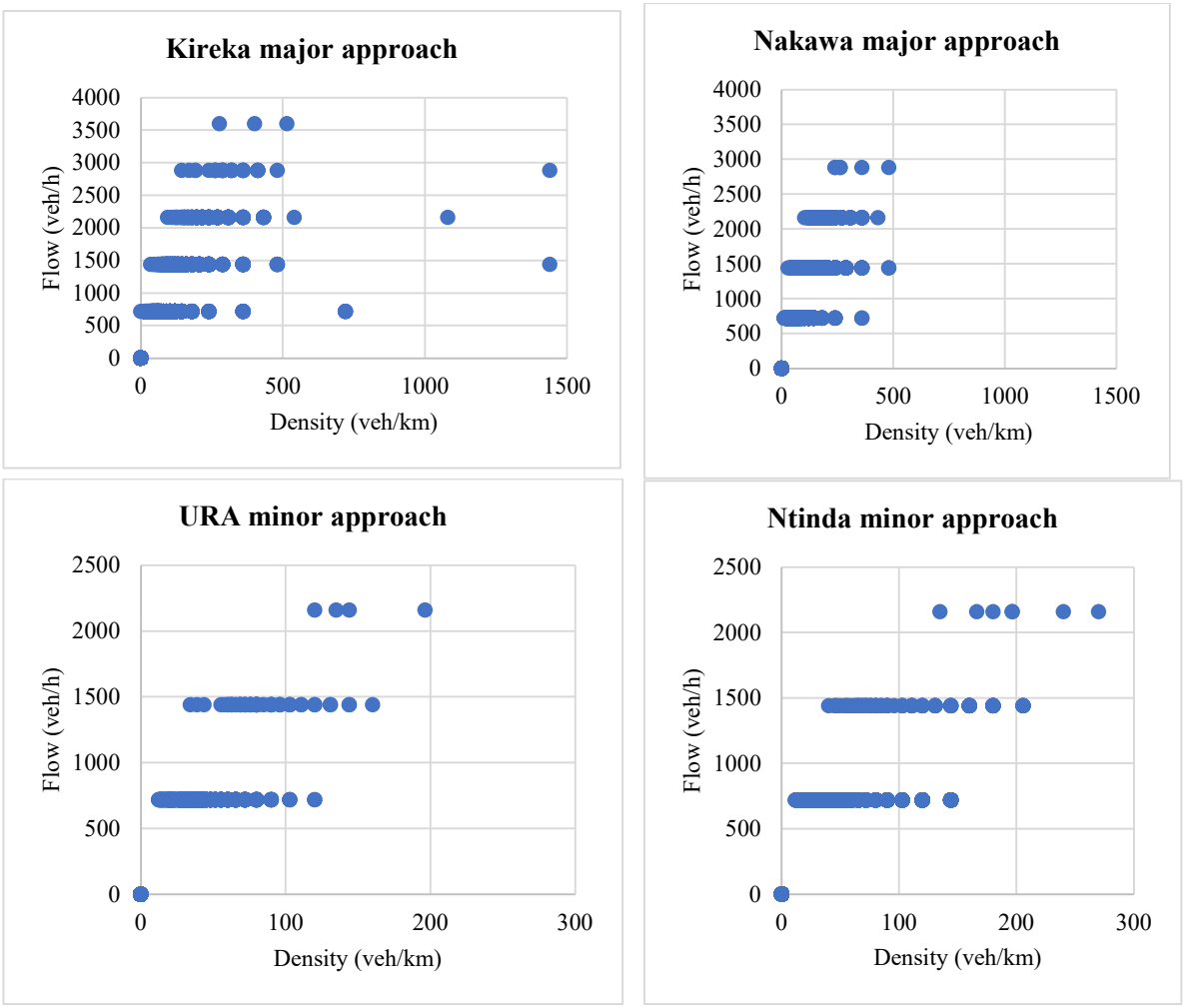

Figure 34: Fundamental diagrams of simulated traffic for the main approaches in scenario 3-roundabout

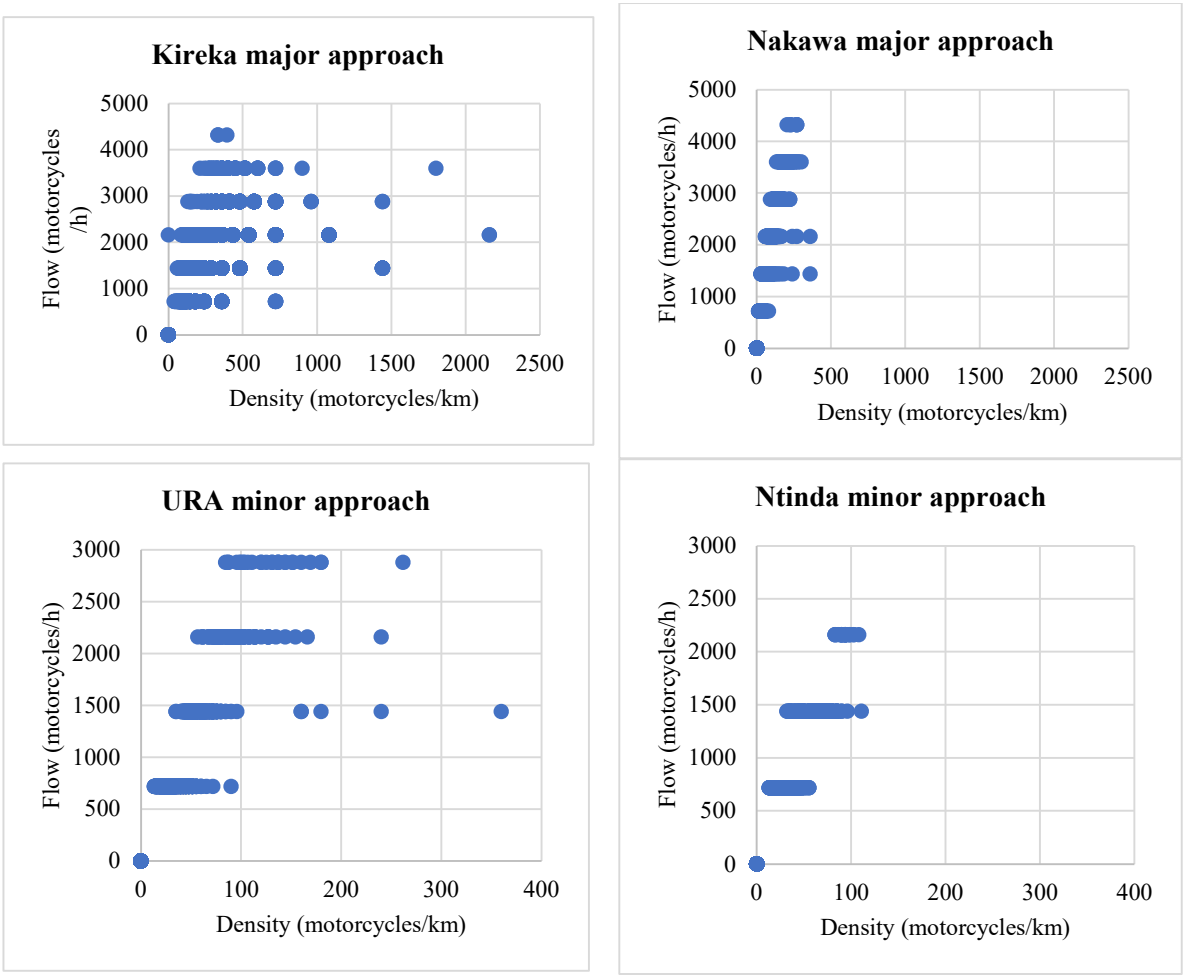

Figure 35: Fundamental diagrams of simulated traffic for the motorcycle approaches in scenario 3-roundabout

With reference to the above fundamental diagrams, approximate values of key macroscopic traffic flow parameters are illustrated in Table 17.

Table 17: Traffic flow parameters for scenario 3-roundabout

Approach	**Maximum (veh/h)**		**Critical density (veh/km)**		**Average speed (km/h)**		**Total flow (maximum) (veh/h)**
Facility	Main	Motorcycle	Main	Motorcycle	Main	Motorcycle	
Kireka	3,700	4,500	400	250	9.3	18.0	8,200
Nakawa	3,000	5,000	250	250	12.0	20.0	8,000
URA	2,200	3,100	120	125	18.3	24.8	5,300
Ntinda	2,100	2,200	150	90	14.0	24.8	4,300

Notably, all approaches had higher total flow (maximum) compared to the base case. While the highest flow of the Kireka major approach increased slightly by 2.5%, the highest flow of the Nakawa approach increased by 23.1%. Furthermore, the maximum flow of the minor approaches greatly increased by 76.6% and 72.0% for URA and Ntinda approaches, respectively. Based on traffic volume per approach in the base case as weights, the highest flow increased by 20%.

Regarding congestion, the critical density was much lower on both the main road and the motorcycle lanes as compared to both the based case and scenario 2. Generally, the critical density reduced by about 60% for the two major approaches and URA minor approach on the main road. However, the critical density reduced by only 25% on the Ntinda minor approach.

For motorcycles, the improvement was slightly better than that for the main road. The performance of this scenario is shown in a YouTube short video (Mwine, 2022c).

On the other hand, scenario 3 yielded less congestion as compared to scenario 2 for motorcycles. The critical density reduced by 58.3% and 37.5% for Kireka and Nakawa motorcycle approaches whilst it decreased by 43.2% and 25.0% on the URA and Ntinda minor motorcycle approaches. Important to note, the speed of motorcycles in scenario 3 increased slightly compared to the average speed in scenario 2. The vehicles on the main road experienced average speed values between 8.0 and 20.0km/h like in scenario 2. The average speed of Nakawa approach was the highest on the main road while the two minor approaches had higher average speed compared to major motorcycle approaches. Likewise, this scenario qualified for safety analysis.

An equally important result is that scenario 2 had slightly better maximum flow for both the main road and the dedicated motorcycle lanes as evidenced in Table 18 in comparison with other scenarios. Scenario 3 had better maximum flow results than both the base and scenario 1. It is also critical to note that in the study Passenger Car Units (PCUs) were not used.

Table 18: Capacity per scenario

Scenario	Maximum flow (veh/h)	Maximum flow (motorcycles/h)	Total flow (maximum) (veh/h)
Base scenario			20,000
Scenario 1: Straight crossings	8,800	0	8,800
Scenario 2: Deflected crossings	12,000	15,200	27,200
Scenario 3: Roundabout	11,000	14,800	25,800

5.1.5 Level of Service (LoS)

Level of Service (LoS) based on experienced delay in the intersection was evaluated for five random seeds and using 2-minute time intervals. This evaluation implied that a maximum frequency of 450 (60min/2 min=30x5seeds=150x3 directions per approach=450) was possible for the one-hour traffic per approach with three directions. Likewise, a startup period of 600s was considered for traffic to be in the system but was excluded from further analysis of delay as explained in earlier chapters. The delay thresholds per LoS are defined in section 3.8.2, Table 9.

Frequency distribution per LoS was examined per approach and the corresponding charts are shown in Figure 36 and Figure 37 for the main road and motorcycle approaches, respectively.

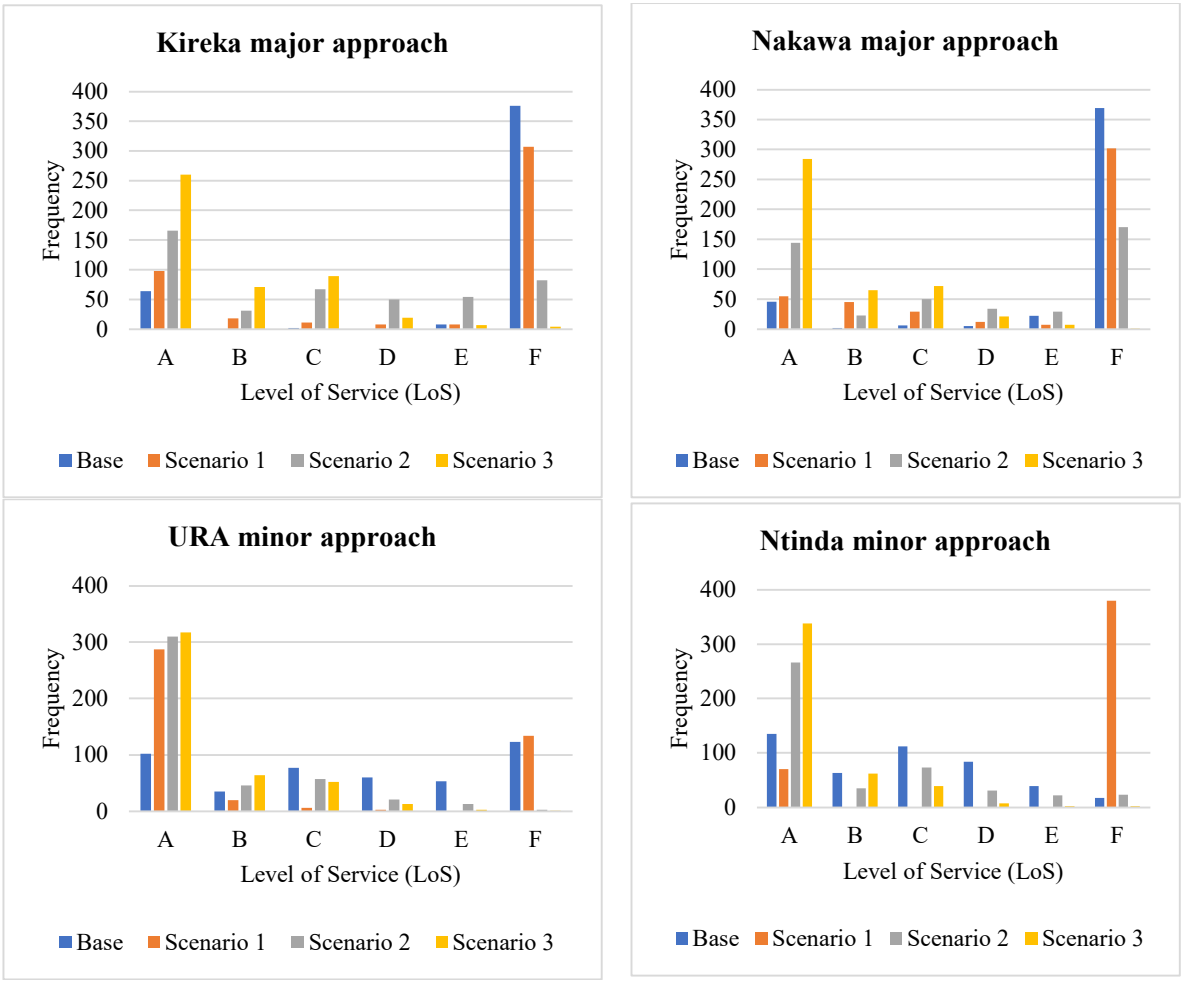

Figure 36: LoS per scenario on the main road approaches (scenario 1-Straight crossings; scenario 2-deflected crossings; scenario 3-roundabout)

It can be seen from the above figure that scenarios 2 and 3 yield better LoS with significantly more observations showing relatively low to medium delays (LoS A-C) whereas the baseline and scenario 1 yield predominantly medium to long delays (LoS D-F) on all approaches except the URA approach. Of note is that all approaches in scenario 3 operated at LoS A-C for more than 93% of the (off-peak) time. Therefore, users were delayed by less than 25s at the intersection.

Evidently, scenarios 2 and 3 provide much better-quality transport for all motorcycle approaches than scenario 1 and the base as illustrated in Figure 37. Scenario one always operated at LoS F with no single motorcycle detected by the data collection points. The traffic conditions in scenario 1 were dire compared to even the base case. While motorcyclists experienced relatively better conditions on the minor road approaches during the base case, they were delayed by over 50s on the major approaches (Kireka and Nakawa) for about 80% of the time. To be specific, motorcyclists were delayed by less than 25s to exit the intersection from the URA and Ntinda minor approaches for 48% and 69% of the time, respectively.

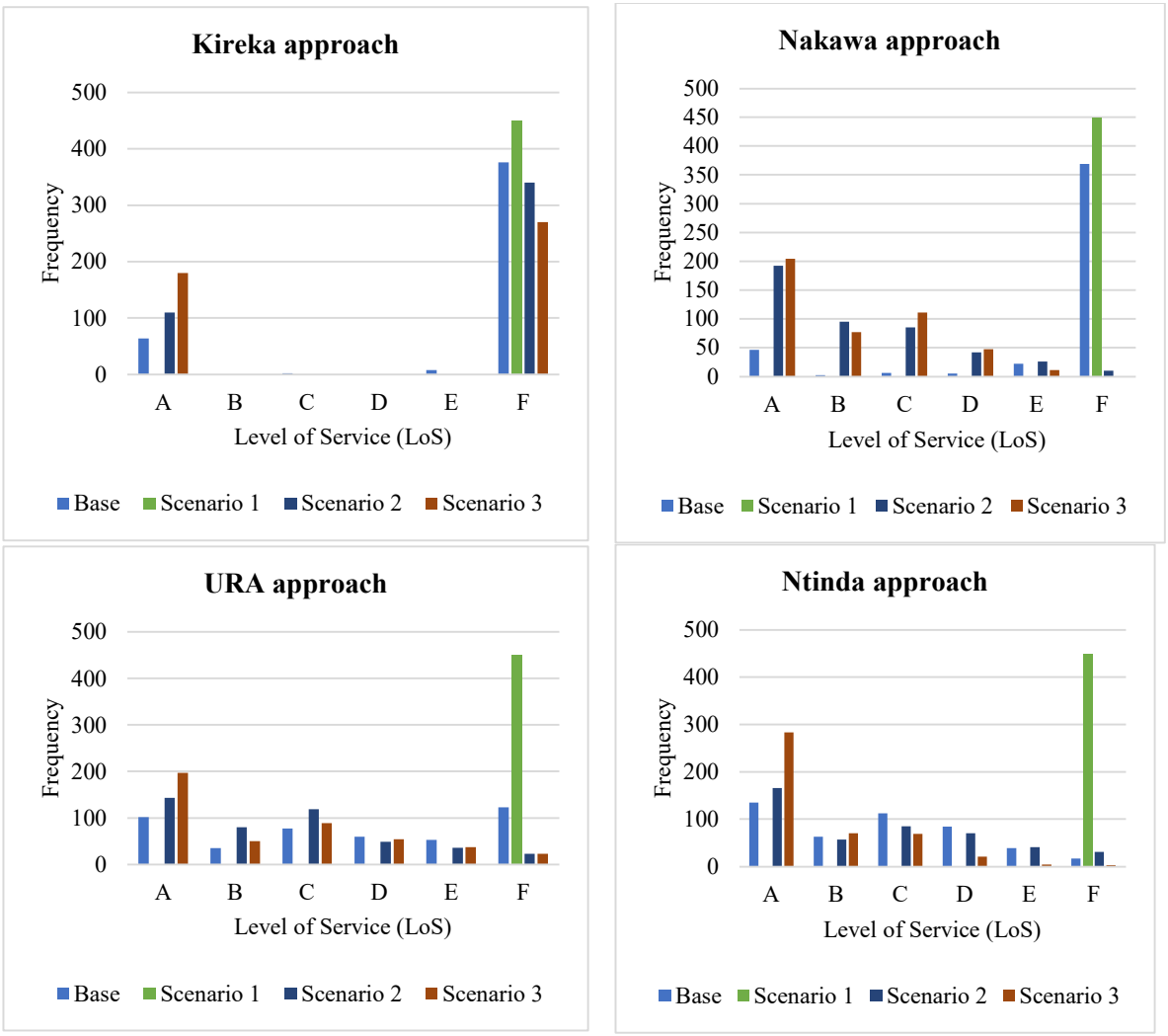

Figure 37: LoS per scenario on motorcycle approaches (scenario 1-Straight crossings; scenario 2-deflected crossings; scenario 3-roundabout)

During scenarios 2 and 3, motorcyclists on the Kireka approach were delayed by more than 50s to exit the intersection for 76% and 60% of the time, respectively, because of high demand. However, those motorcyclists on Kireka approach were delayed by less than 10s for 40% of the time in the third scenario and about 25% in the second scenario. On the other hand, motorcyclists who approached from Nakawa or the minor approaches (Ntinda and URA) in both scenario 1 and scenario 2 generally faced better operating conditions. For scenario 2, motorcyclists, who used the Nakawa approach were delayed by less than 25s for 83% of the time while those who used the URA and Ntinda minor approaches were delayed by the same for 76% and 68.4% of the time. Considering scenario 3, motorcyclists who used the Nakawa approach were delayed by less than 25s for 86% of the time whilst those who approached the intersection suing the URA and Ntinda minor approaches were delayed by the same for 74.7% and 93.7% of the time, respectively.

Undoubtedly, scenarios 2 and 3 offer much better traffic conditions in terms of delay or LoS for both users on the main road and dedicated motorcycle lane. Scenario 1 did not favor motorcyclists to the extent that they experience better traffic conditions in the base case. For this reason, scenario 1 was not further subjected to safety analysis as the case in traffic flow analysis.

In summary, the percentage increments of traffic flow parameters for scenarios 2 and 3 are presented in Table 19.

Table 19: Percentage increments of traffic flow parameters of scenarios 2 and 3 in comparison with the simulated base

Scenario	Approach	Flow per approach	Main road			Motorcycle lane		
			Critical density	Average speed	LoS A-C	Critical density	Average speed	LoS A-C
Scenario 2: Deflected crossings	Kireka major	25.0	-50.0	12.5	44.0	-40.0	14.5	9.8
	Nakawa major	25.0	-33.3	19.2	36.2	-33.3	6.2	70.7
	URA minor	56.7	-40.0	11.1	44.2	-26.6	22.7	28.4
	Ntinda minor	76.0	-40.0	33.3	14.2	-40.0	60.0	-0.4
Scenario3: roundabout	Kireka major	2.5	-60.0	15.6	78.7	-75.0	125.0	25.3
	Nakawa major	23.1	-58.3	10.8	81.6	-58.3	84.6	75.1
	URA minor	76.6	-60.0	83.3	48.7	-58.3	148.0	27.1
	Ntinda minor	72.0	-25.0	12.0	28.7	-55.0	95.6	24.9

The following are the main observations:

- Combined flow on the main roads and motorcycle lanes increased more in scenario 2 than in scenario 3.
- Congestion reduced with decrease of critical density on the main roads and motorcycle lanes.
- Average speed generally increased but higher margins were recorded for motorcycles in scenario 3. However, the speed was still below 30km/h in all cases.
- More main road traffic and motorcycles in scenario 3 experienced low to medium delays (less than 25s) than in scenario 2.

5.2 Safety

Safety impact of dedicated motorcycle lanes was analyzed using distribution of severe critical conflicts observed and simulated at the study intersection. The severe critical conflicts were further categorized according to the associated interaction of vehicle types as well as conflict type. In addition, conflict rates of the severe critical conflicts were determined in order to consider exposure. These conflict rates were also sub-divided following the interaction and conflict types.

5.2.1 Distributions of severe critical conflicts

Both TTC and PET were used to develop distributions of severe critical conflicts for the observed data and simulated data as discussed in section 3.8.3 and section 4.4.2. Observed severe critical conflicts were defined based only on PET unlike simulated ones with both PET and TTC as shown in Figure 38 and Figure 39.

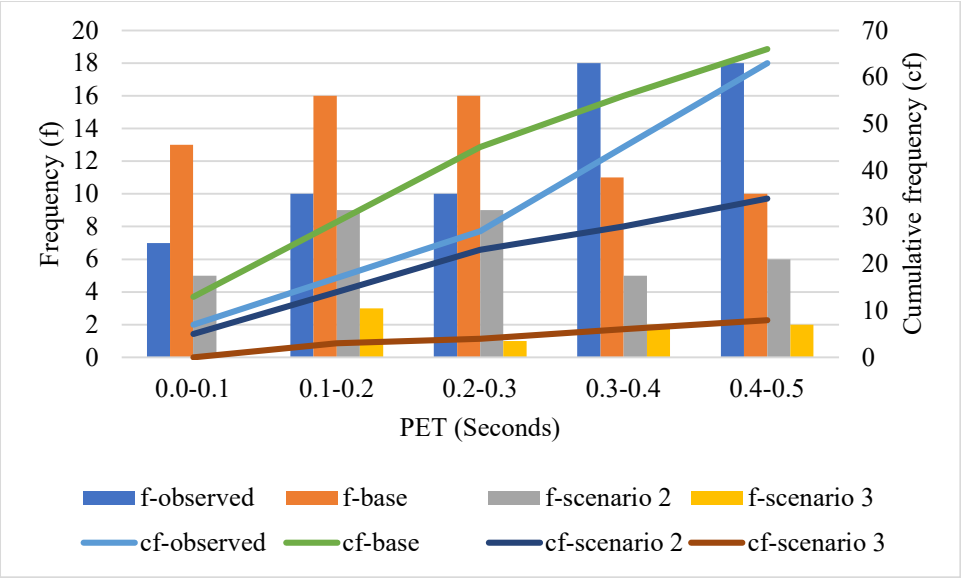

Figure 38: Distribution of observed and simulated severe critical conflicts based on PET[3]

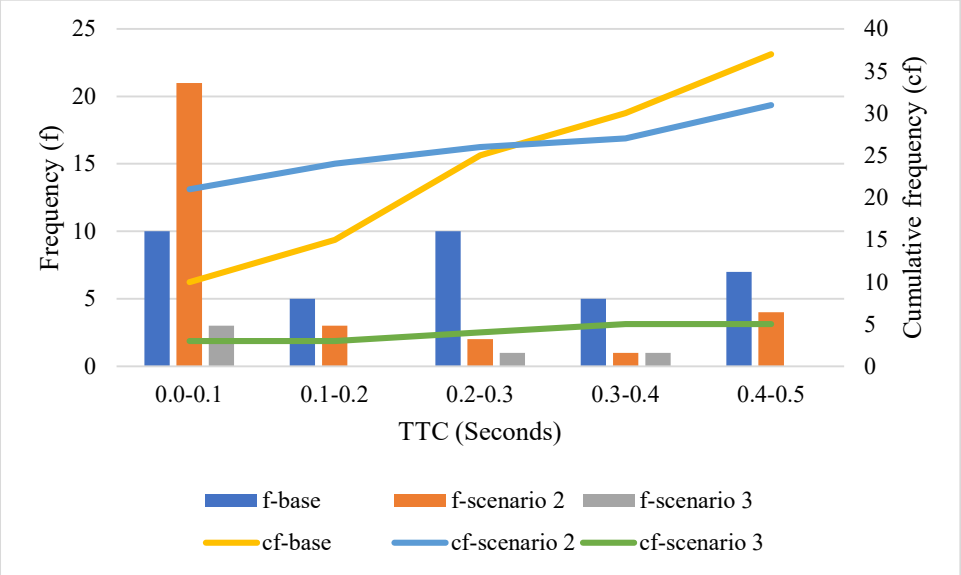

Figure 39: Distribution of simulated severe critical conflicts based on TTC[4]

The two figures above reveal that scenarios 2 and 3 reduce severe critical conflicts in comparison with the base scenario and observed PET. Application of a roundabout (scenario 3) reduced severe critical conflicts by 87.9% while dedicated motorcycle lanes with deflected crossings (scenario 2) reduced these conflicts by 48.5% compared to the base scenario. Notably, it was accepted that the base and observed PET values for severe critical conflicts were comparable based on a chi-square goodness-of-fit test as explained in section 4.4.2.

The number of severe critical conflicts was further sub-divided into three categories depending on interactions, that is Vehicle-to-Vehicle (V2V), Vehicle-to-Motorcycle (V2M) and Motorcycle-to-Motorcycle (M2M). The reductions of scenarios 2 and 3 in respect to the base is indicated in Table 20 for severe critical conflicts. The p-values were determined using the

[3] scenario 1: straight crossings; scenario 2: deflected crossing; scenario 3: roundabout

[4] scenario 1: straight crossings; scenario 2: deflected crossing; scenario 3: roundabout

chi-square goodness-of-fit test as described in section 4.4.2 using all the severe critical conflicts per scenario as a control.

Table 20: Reductions of severe critical conflicts per scenario and interaction category in comparison with the base simulated scenario

Interaction type	Frequency			Reduction (%)	
	Base	Scenario 2	Scenario 3	Scenario 2	Scenario 3
Control (all)	66	34	8	48.5	87.9
V2V	6	5	1	16.7	83.3
V2M	31	10	2	67.7	93.5
M2M	29	19	5	34.5	82.8

According to the above table, scenario 3 reduced severe critical conflicts based on interaction type by higher margins compared to scenario 2. V2M severe critical conflicts decreased more in both scenarios 2 and 3 followed by M2M conflicts.

The severe critical conflicts were further categorised based on conflict type as indicated in Table 21 and the associated reductions of scenarios 2 and 3 in respect to the base were calculated.

Table 21: Reductions of severe critical conflicts per scenario and conflict type in comparison with the base simulated scenario[5]

Conflict type	Frequency			Reduction (%)	
	Base	Scenario 2	Scenario 3	Scenario 2	Scenario 3
Control (all)	66	34	8	48.5	87.9
Crossing	45	20	1	55.6	97.8
Rear-end	18	10	2	44.4	88.9
Lane change	3	4	5	-33.3	-66.7

It is evident from Table 21 that severe critical conflicts for both crossing and rear-end conflict types reduced by a higher 93.4% (average) in scenario 3 than an average reduction of 50.0% in scenario 2. However, severe critical conflicts for lane change conflict type increased more in scenario 3 than in scenario 2.

5.2.2 Severe critical conflict rates

With the application of exposure which in this study was adopted as the total observed or simulated traffic per scenario, conflict rates per 1,000 vehicles were determined. These rates are continuous and hence paired samples t-tests were used to compare the difference between the average rates per scenario.

The severe critical conflict rates were determined based on interaction types (V2V, V2M, and M2M and conflict types (crossing, rear-end and lane change) per scenario. These rates are illustrated in Figure 40. The conflict rates for the observed and base cases represents vehicles inclusive of motorcycles since they shared the same road. However, in scenarios 2 and 3, motorcycles were separated from main road traffic and so V2V interactions were on the main road while M2M interactions were on the dedicated motorcycle lanes.

[5] scenario 1: straight crossings; scenario 2: deflected crossing; scenario 3: roundabout

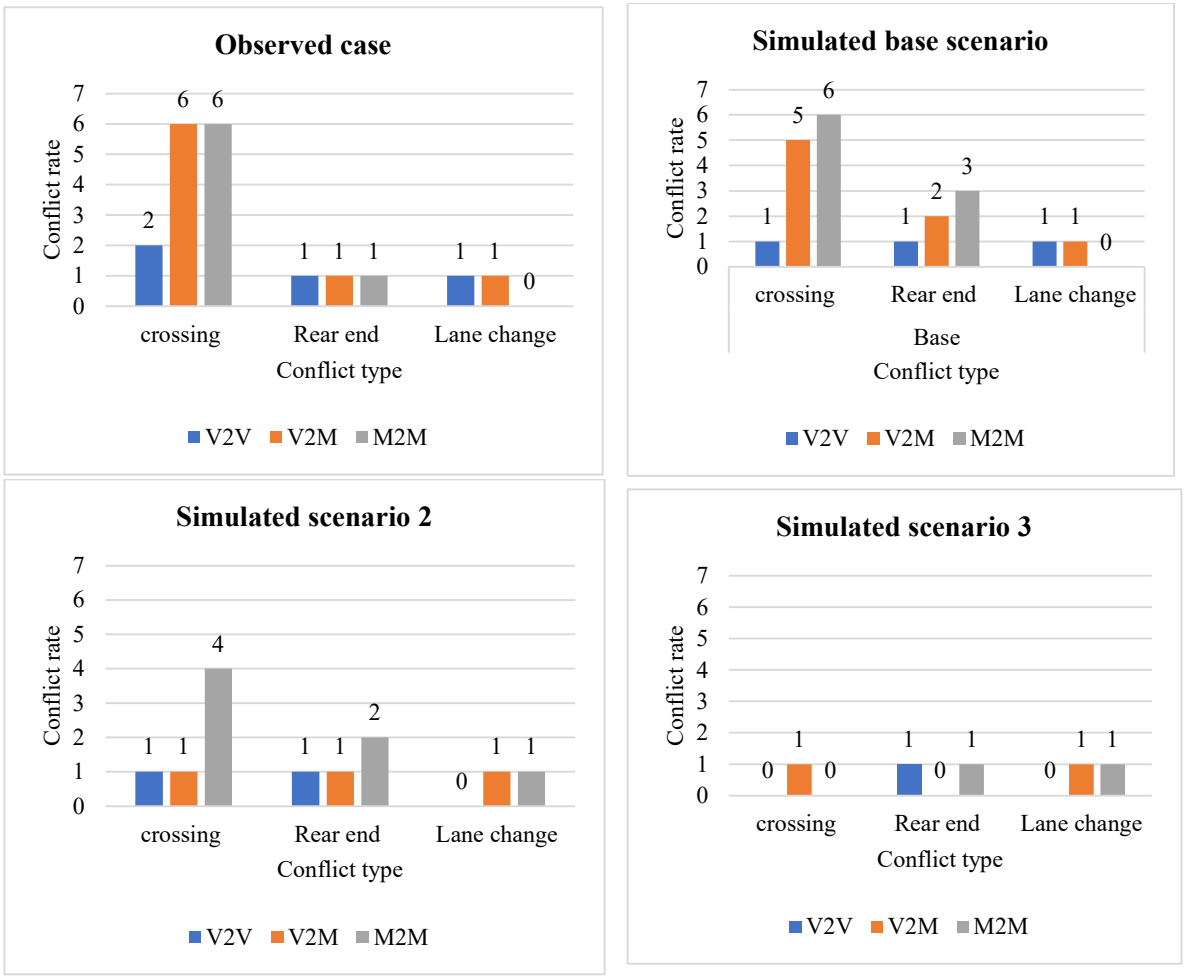

Figure 40: Severe critical conflict rate per 1000 total vehicles for the observed data and per simulated scenario[6]

The severe critical conflict rates for the observed case and simulated base case were comparable based on the above figure. Crossing severe critical conflicts were the highest, followed by rear-end and lastly lane change. The severe critical conflict rates were generally reduced considering scenarios 2 and 3 in comparison with the base. However, rear-end severe critical conflicts slightly increased in the base simulated case in comparison with the observed data. In addition, crossing rates were almost zero in scenario 3 with a roundabout but rear-end and lane change severe critical conflicts still occurred.

The difference between the average severe critical conflict rates was further confirmed using a paired samples t-test. With a p-value (0.1054) greater than 0.05, the null hypothesis that the mean difference between the observed and base simulated severe critical conflict rates was zero could not be rejected. Therefore, the observed and base simulated severe critical conflict rates had comparable mean value and were comparable. Additionally, the percentage reduction of severe critical conflict rates for scenarios 2 and 3 in comparison with the base simulated case were calculated per conflict and interaction type and are shown in Table 22.

[6]scenario 2: deflected crossings; scenario 3: roundabout

Table 22: Percentage reductions of severe critical conflict rates for scenario 2 and scenario 3 in comparison to the base simulated scenario

Conflict type	Interaction type	Scenario 2-Deflected crossings	Scenario 3-Roundabout
Crossing	V2V	0.0	100
	V2M	80.0	80.0
	M2M	33.3	100
Rear-end	V2V	0.0	0.0
	V2M	50.0	100
	M2M	33.3	66.7
Lane change	V2V	100	100
	V2M	0.0	0.0
	M2M	-100	-100

Generally, it is observed from the above table that the severe critical conflict rates were reduced more by scenario 3 than scenario 2 other than the rate for M2M and lane change types that increased in both scenarios. The overall reductions on these rates per simulated scenario in comparison with the base simulated case were thus calculated and are indicated in Table 23.

Table 23: Overall reduction of severe critical conflict rates per scenario in comparison to the base simulated scenario

Scenario	Total severe critical conflict rate	Reduction (%)
Base (control)	20	
Scenario 2-deflected crossings	12	40
Scenario 3- roundabout	5	75

Severe critical conflict rates reduced by a higher effect of 75% in scenario 3 compared to 40% in scenario 2. The difference between the scenarios was tested using paired samples t-test. While the p-value (0.0519) was slightly higher than 0.05 for scenario 2, it was lower for scenario 3 (p-value=0.0255). More evidence was thus required to reject the null hypothesis for scenario 2 but not scenario 3. The mean difference between the base simulated case and simulated scenario 2 was equal to zero but not for scenario 3. Therefore, scenario 3 outperforms scenario 2 considering the reduction of the severe critical conflict rates.

The analysis was further extended to determine the reductions of severe critical conflicts on either interaction or conflict types. First, the conflict rates were added up per scenario and interaction type as shown in Table 24. Using paired samples t-test, the p-value of each reduction was thus determined.

Table 24: Reductions of severe critical conflicts per scenario and interaction category in comparison with the base simulated case[7]

Interaction type	Total severe critical conflict rate			Reduction (%)	
	Base	Scenario 2	Scenario 3	Scenario 2	Scenario 3
V2V	3	2	1	33.3	66.7
V2M	8	3	2	62.5	75.0
M2M	9	7	2	22.2	77.8

The severe critical conflict rates per interaction type were reduced by generally higher effects in scenario 3 than scenario 2. On average, the rates reduced by 73.1% in scenario 3 compared

[7] scenario 2: deflected crossings; scenario 3: roundabout

to 39.4% in scenario 2. Statistical testing using paired samples t-test revealed that all the rates between scenarios were not significant at 95% confidence other than for V2V severe critical conflict rate for scenario 3. The obtained p-values for V2V, V2M and M2M average conflict rates of scenario 2 and the base were 0.2478, 0.1642, and 0.1558, respectively. In addition, p-values for V2V, V2M and M2M average rates of scenario 3 and the base were 0.0207, 0.1209, and 0.1819, respectively. The null hypotheses were not rejected for the former group and so the mean differences between the severe critical conflict rates for the simulated base case and the simulated scenarios 2 and 3 were equal to zero. Regarding V2V severe critical conflict rate for scenario 3, the null hypothesis was rejected and, therefore, there was sufficient evidence to accept that the mean of these rates for simulated base case was different from that of the corresponding rates for scenario 3.

Secondly, the conflict rates were summed up per scenario and conflict type as shown in Table 25. The p-value of the difference between a scenario and the base case was determined using paired samples t-test.

Table 25: Reductions of severe critical conflicts per scenario and conflict type in comparison with the base simulated case[8]

Conflict type	Total severe critical conflict rate			Reductions (%)	
	Base	Scenario 2	Scenario 3	Scenario 2	Scenario 3
Crossing	12	6	1	50.0	91.7
Rear-end	6	4	2	33.3	66.7
Lane change	2	2	2	0.0	0.0

Generally, severe critical conflict rates per conflict type reduced more in scenario 3 than in scenario 2. On average, these rates reduced by 52.8% for all conflict types in scenario 3 compared to 27.8% in scenario 2. Paired samples t-tests at 95% confidence resulted into p-vales greater than 0.05 for rates of crossing and lane change conflict types but not rear-end. The obtained p-values for crossing, rear-end and lane change average conflict rates of scenario 2 and the base were 0.1223, 0.0420 and 0.3852, respectively. In addition, p-values for crossing, rear-end and lane change average conflict rates of scenario 3 and the base were 0.0733, 0.0403, and 0.4021, respectively. The null hypotheses for rates of crossing and lane change conflict types were not rejected at 95% confidence and hence more evidence was required. On the other hand, the null hypotheses for rates of rear-end conflict types for both scenarios 2 and 3 were rejected at 95% confidence. Therefore, the means of rear-end rates for simulated base case and simulated scenarios 2 and 3 were different.

Notably, the rates of crossing severe critical conflicts for scenario 3 were reduced by 91.7%. With a reliability of 92.7%, the null hypothesis that the mean difference of severe critical conflict rates for the base simulated case and scenario 3 was zero could be rejected.

From this safety evaluation, scenario 3 with a roundabout contributes more to safety than scenario 2 with deflected crossings for motorcycles but both are worthy applying at unsignalized intersections depending on site conditions. In addition, severe critical conflict rates take into account of exposure and hence reflect the impact of a scenario better than using distributions. As a result, the former (use of conflict rates) was a foundation for further discussion about safety in this study.

[8] scenario 2: deflected crossings; scenario 3: roundabout

6|Discussion and Conclusion

In section 6.1, key findings per scenario in the study regarding traffic performance (traffic flow and safety) are discussed while concerns with the methodology are explained in section 6.2. The study limitations are described in section 6.3. In addition, conclusions are made in section 6.4.

6.1 Discussion of main findings

The study advocates for uni-directional motorcycle lanes that are separated from main traffic to improve both safety and traffic flow. Well designed and raised kerbs or preferably space barriers can be provided between the main traffic lane and the dedicated motorcycle lanes depending on site conditions as guided by the Malaysian (2018) guidelines for exclusive motorcycle lanes. This concept is known as homogeneity principle under sustainable safety and aims to separate traffic according to mass, direction, and speed (SWOV, 2008). In this case, all three are achieved with dedicated motorcycle lanes. Moreover, motorcycles were the fastest in the conflict area according to observed data and so their separation may greatly impact on both crash frequency and severity. In this study, traffic flow was macroscopically evaluated using fundamental diagrams (flow-density) as well as Level of Service (LoS) per approach. The safety impact of dedicated motorcycle lanes was also evaluated using distributions of severe critical conflicts and their conflict rates per conflict type and interaction category. Main findings regarding traffic flow and safety are further discussed in this section per scenario (scenario 1: straight crossings, scenario 2: deflected crossings and scenario 3: roundabout).

6.1.1 Scenario 1: Straight crossings

First and foremost, scenario 1 focused on provision of dedicated motorcycle lanes with straight crossings through the intersection. Motorcyclists were blocked on their dedicated lanes especially on the Kireka major approach and consequently all motorcycle approaches. For this reason, scenario 1 was not subjected to safety analysis. This blockage was due to high demand compared to what could be allowed to transverse the intersection at the main motorcycle bottleneck points. These points were narrow and constrained outflow of approaching motorcyclists. The reduced distance between these points provided less storage space for the motorcyclists waiting to cross the intersection. The conditions were worsened by the fact that the straight crossings were through many conflict points on the intersection. Thus, waiting motorcyclists in the storage space had to wait for longer periods to be able to find some sufficient gap time. One may think that giving priority to such motorcyclists can solve the problem, but it would instead worsen the situation for the main road traffic. Henceforth, the alternative is to redesign the dedicated motorcycle lanes and increase storage space for waiting motorcyclists which may be unrealistic since much wider lanes are needed.

Furthermore, motorcycles blocked only one main approach per random seed in the microsimulation but in actual sense, these (motorcycles) may block all the approaches. Secondly, as motorcyclists' urge to cross increases then they may be compelled to find their way through the intersection. This action would entirely block all the main traffic creating a gridlock and increased delays for all road users. The risk to even use the main road would increase and this would not achieve the objective of separating the motorcyclists from traffic in terms of mass, speed and direction as proposed in the sustainable safety.

Another option for scenario 1 was to increase capacity of the dedicated motorcycle lanes especially at the bottleneck. This option necessitates more space and is deemed expensive for local authorities. For example, increasing the width of the motorcycle lanes, demands more financial resources and land. This provision may as well constrain space for other road users such as sidewalks for pedestrians. Suitable designs of road infrastructure may be needed for wider motorcycle lanes not to be misused by other vehicles. For example, well designed narrow sections can be intermittently provided along the motorcycle lane if safety precautions (traffic signs and road marking) are considered to reduce misuse by other vehicles.

6.1.2 Scenario 2: Deflected crossings

With separation of motorcycles from vehicles at the unsignalized intersection by using deflected crossings, total severe critical conflict rate reduced by 40% from 20 to 12 severe critical conflicts per 1000 vehicles. Specifically, the severe critical conflict rate of vehicle-to-motorcycle (V2M) interaction type reduced by 62.5% from 8 to 3 severe critical conflicts per 1000 vehicles while the rate for crossing conflict type decreased by 50% from 12 to 6 severe critical conflicts per 1000 vehicles. The large mass difference between vehicles and motorcycles increases the interest in the performance of a scenario towards reducing conflicts associated to V2M interaction type. On the other hand, crossing, rear-end and lane change conflicts are expected at unsignalized intersections according to literature.

Scenario 2 offsets the drawbacks of scenario 1. Provision of deflected crossing points allows motorcycles to cross at the shortest distance possible. Motorcyclists spend less time in the conflict area (are exposed less to conflicts) and hence this increases their outflow and safety. Additionally, motorcycles cross fewer conflict areas than in scenario 1 and hence decision making is quicker and simpler compared to the situation in scenario 1.

Importantly, motorcycles in scenario 2 had sufficient storage space as they waited to cross and hence this minimized blockage of not only their lanes but also the main road. The storage space was adequate to balance both inflow and outflow without spillage which facilitated smooth traffic conditions during the simulation. The same situation is expected in real traffic conditions. The approach also availed some storage space for main traffic especially where the vehicles have to safely yield for the motorcycles. Such yielding traffic would result into more blockage in scenario 1 on the main road which is not the case in scenario 2. Therefore, more traffic can exit the intersection in scenario 2 than in scenario 1. This justifies the increase in maximum flow for both motorcycle lanes and main road. The increase was more substantial on the minor roads since vehicles were delayed for much less time. Subsequently, waiting vehicles are not delayed for long to the extent that they may decide to use available unsafe alternatives such as the main road.

While the average speed was in the same range for both scenario 2 and the base, the critical density generally reduced. This reduction can be attributed to the general decrease in the traffic volume on the main road by creating separate space for the motorcycles. Notably, motorcycles were more than 50% of the traffic volume in the base case. Substantial reduction of congestion on the main road was achieved. For instance, 50% reduction of the critical density on the Kireka main approach guarantees better travel quality to vehicular users. All this is attributed to the creation of separate and dedicated motorcycle lanes at the unsignalized intersection. In addition, exposure to conflicts is reduced since fewer vehicles or motorcycles are using either the main road or the dedicated motorcycle lanes.

In addition to the above stated benefits for scenario 2, motorcycles on the major approach such as Kireka can cross only the Ntinda minor approach. The reverse is true for those motorcycles approaching on the minor approaches. The high demand of motorcycles on the Kireka approach can find adequate gap times on the minor approach and hence exit the intersection with minimal interference of traffic. On the other hand, the low demand on the minor approaches can also cross the busy major approaches in the available time gaps. Therefore, traffic effectively and efficiently transverses the intersection in scenario 2. Concerning safety, increased gaps times for either major or minor traffic avail enough time for drivers to react to demanding situations that may result into conflicts. Secondly, there is general reduction of exposure to conflicts for main road traffic as well as motorcycles.

In relation to average speed, generally higher speeds were realized on the dedicated motorcycle lanes than the main road. This discrepancy is in line with distribution of conflicting speeds per vehicle type in which motorcycles were the fastest at the intersection. The high speed definitely implied that these motorcyclists are susceptible to conflicts at the intersection. However, their speeds were generally lower than the threshold of 30km/h for safe speeds in mixed traffic according to the safe systems approach (WHO & UN, 2021). At the same time, vehicles on the Ntinda main road adopted higher speeds in scenario 2 but lower than 30km/h. This variation can be attributed to the fact that the road is dual carriage and hence the tendency by motorists to increase speed as suggested by Goldenbeld et al. (2017).

6.1.3 Scenario 3: Roundabout

In this scenario, dedicated motorcycle lanes were added together with a roundabout separated for motorcycles and main traffic. This separation of motorcycles from vehicles resulted in a reduction of total severe critical conflict rate from 20 to 5 conflicts per 1000 vehicles (75% reduction). In particular, the severe critical conflict rate of vehicle-to-motorcycle (V2M) interaction type lowered by 75.0% from 8 to 2 severe critical conflicts per 1000 vehicles while the rate for crossing conflict type declined by 91.7% from 12 to 1 severe critical conflicts per 1000 vehicles. About traffic flow, the highest flow on all approaches increased. For example, the highest flow of the Nakawa approach increased by 23.1%. Traffic congestion was reduced by 60% on either of the major approaches. These results are further explained in this section.

In this study, the width of the dedicated motorcycle lanes in all scenarios was the same to make robust deductions about the traffic conditions. However, capacity can be increased by using wider lanes without compromising safety since such lanes may facilitate overtaking of motorcycles. Additionally, wider motorcycle lanes can be used by other vehicles such as cars and so they (motorcycle lanes) must be well designed to deter cars from accessing them. As a result of narrow dedicated motorcycle lanes, congestion was observed in both scenario 2 and 3 on the Kireka motorcycle approach. However, less congestion was experienced in scenario 3 than the base and scenario 2. This finding can be attributed to improved visibility and reduced number of conflict areas for the motorists to negotiate. Soteropoulos and Stadlbauer (2017) point out that motorists in a roundabout do not have to look at all directions since vehicles come from one direction. The same researchers also note that roundabouts reduce the number of conflict points and so these points reduced for both main road traffic and motorcycles on their lanes. The same reasoning explains the reduced congestion on the dedicated motorcycle lanes. In addition, the motorcyclists at the roundabout were faster than in the previous scenarios but less than 30km/h. Their speed was higher on the minor approaches, and this can be due to the small volume of motorists entering the roundabout from that approach and hence not

substantially reducing speed as the motorcyclists approached the intersection. The slight increase in speed for scenario 3 can also be associated with the tangential design of the entrances to the study intersection. Reducing the radius of the entrances would compel drivers to adopt lower speeds in order to safely navigate through the intersection.

Increase of lane width for motorcycle lanes especially near bottlenecks and for major approaches is essential. This is aimed at increasing throughput and thus better Level of Service (LoS) can be experienced by the motorcyclists and their passengers. This issue is evident from the LoS computations for the major approaches (Kireka and Nakawa) where the delay was more than 50s for over 60% of the time. In the current study, the lane width was not increased to be consistent in design and understand the traffic flow impact of both scenarios 2 and 3. Better quality service of motorcycle dedicated lanes is likely to increase the acceptability and usability of the new facilities. If compromised, there are chances of the motorcyclists using the main road and hence the separation objective would not be achieved, and other traffic should also accept the lane is for motorcycles only.

In this scenario, the number of conflict areas is reduced for the main traffic and hence more outflow is expected. This justifies the less delay experienced by both motorcyclists and other motorists on the main road with better LoS. However, scenario 2 outperformed scenario 3 in terms of traffic flow. This can be attributed to the fact that the study focused on off-peak flow and hence distance travelled in the conflict area is significant. In a roundabout, motorists are channeled through longer circular routes and consequently spend more time. In contrast, scenario 2 had more direct crossing for the main road traffic and hence more outflow during the design period (off-peak). The capacity of the roundabout is expected to be higher than that of a 4-leg intersection during peak hours (Rahmat et al., 2021).

Roundabouts reduce conflicts areas for Vehicle-to-Vehicle (V2V), Vehicle-to-Motorcycle (V2M) and Motorcycle-to-Motorcycle (M2M) interactions and hence the rate of occurrence (frequency) of conflicts is generally reduced. Smaller conflict areas are dispersed over the intersection which reduces the mental workload required for a motorist to enter or exit. In this way, 3-leg intersections are created per entrance or exit which separates motorists in both time and space. Exiting motorists tend to be on the left while those proceeding to the next exit remain on the right. Conversely, this separation is not always adhered to especially in mixed traffic of developing countries hence leading to slight increments of both lane change and rear-end conflicts as established in the study. This is not the case for scenario 2 that included a 4-leg intersection for main traffic. Additionally, the approaches to the roundabout are radial which creates islands in scenario 3. These islands can be used by pedestrians to safely cross the narrower road sections by acting as refugee areas.

Pertaining motorcycle storage space at the intersection, scenario 3 had less space compared to scenario 2 and this justifies why the latter yielded better traffic flow results with slightly higher total flow (maximum). More smooth traffic conditions were observed in scenario 2 thus more traffic was able to exit the intersection. The curve in scenario 2 is outward of the intersection while it is inward for scenario 3 which provides more visibility in the latter case. Motorcyclists can decide to safely cross the main traffic entrances or exits with less speed variations than in scenario 2. Outstandingly, some motorcyclists do not come to a halt in scenario 3 thus increasing their output. This benefit is however offset by the less storage hence slightly less traffic can exit the intersection in comparison with scenario 2. At the same time, the reduced

visibility in scenario 2 increases drivers' reaction time towards potential conflicts hence the lower reduction on severe critical conflicts.

In both scenario 2 and scenario 3, M2M interactions are minimized when motorcycles approach the intersection and must reduce speed. This behavior is even evident from observed data with a higher speed distribution for approaching motorcycles than those in the conflict area. In this study, low average speeds were obtained not only for the base case but also for all scenarios. This was in accordance with the conflicting speed distributions that were adopted from observed data. The low-speed ranging from 8-25km/h implies that minor crashes are expected at the intersection. This narrative is also sustained by safe system approach as championed by the global action plan for road safety for the decade 2021–2030. The approach advocates for desired speed of less than 30km/h in urban areas (WHO & UN, 2021) with a view of accommodating human errors and hence improving road safety. However, some drivers approach at relatively higher speed than 50km/h as observed in the field. Higher speeds were observed on the minor approaches (Ntinda and URA) as well as the Nakawa approach. This anomaly can be attributed to the less traffic on the minor approaches and a slope of 4.5% on the Nakawa approach towards the intersection. In addition, the Ntinda approach was dual carriage, and this may facilitate drivers to adopt higher speeds.

While scenario 2 has wider approaches to be crossed by motorcyclists, scenario 3 has narrower sections which can easily be traversed. Such crossing points form the only interaction areas between motorcyclists and main traffic (V2M). Not only is the distance in the conflict area reduced in scenario 3 but also visibility for both the motorcyclists and main road traffic as they come from one direction (Soteropoulos & Stadlbauer, 2017). Visibility is further enhanced by increasing the width of the motorcycle splitter island to accommodate at least one vehicle. A waiting vehicle in this space can ably observe any approaching motorcycle on the left and avail right of way with no conflict. Secondly, conflict between the waiting vehicle and any other proceeding vehicle (V2V) in the main roundabout minimized hence more safer traffic conditions.

As seen from the respective illustrations for both scenario 2 and scenario 3 (see section 5.1.3, Figure 30 and section 5.1.4, Figure 33), pedestrians can cross the road at the same time with the motorcyclists and on their own allocated space. Therefore, these two options also increase safety for pedestrians. Nonetheless, proper road marking and appropriate traffic signs can further be put in place to demarcate the space for pedestrians and then motorcyclists. The impact of road marking and traffic signs on safety was not in the study scope and hence further research can be undertaken.

If the motorcycle crossing points are not blocked during peak time, then the motorcycles can exit the intersection. However, if these crossing points are blocked by the main road traffic, the motorcycles may even be compelled to use the main road which compromises safety. Thus, control measures of vehicles during peak time such as traffic police can ensure that these points are never blocked by stopping vehicles further away from the intersection. It is also likely that the enhanced intersection capacity with implementation of dedicated motorcycle lanes (scenarios 2 and 3) may not be exceeded during peak time at some locations.

Generally, high flows are obtained for both observed and simulated traffic. According to Aoyama et al. (2020), a maximum flow of 2,000veh/h/lane is expected at signalized intersections. This flow corresponds with a time headway of 1.8s and can be obtained for homogenous traffic following the Highway Capacity Manual (HCM, 2000) provisions. At

unsignalized intersections, maximum flow is less than 2000veh/h/lane (for signalized intersection) due to less organization. However, high flows between 3,000 to 9,000veh/h were obtained in this study. It is important to note that these flows are per approach. Secondly, vehicles form more than two lanes as they enter the intersection during off-peak time and per approach as observed from the video images and site visit. This behavior was simulated by increasing the number of approach lanes to two and allowing vehicles to place anywhere on the lanes. The intersection is not marked at all and so lanes are formed by the traffic according to demand.

In addition, motorcycles percolate between the formed lanes since they travel at higher speeds as established from the conflicting speeds. Therefore, about five operational lanes were formed especially on major approaches of Kireka and Nakawa as observed in the video images. The lanes can even be more than five if motorcycles use the entire lane width. This behavior results into rare scenarios where 6-12 vehicles (including motorcycles) are counted in 5-second intervals in both observed and simulated data which accounts for the high flows on the fundamental diagrams. The low traffic volume on the minor roads at the study intersection as well as high flow for the through directions on the major roads also yield high outflow at the Kireka and Nakawa approaches. Less conflicts are created due to limited variation of speed in the conflict area for the through traffic.

Notably, previous studies in developing countries have also highlighted the high traffic flow at unsignalized intersections with mixed traffic. For example Joewono et al. (2011) obtained maximum flow of above 3,500pcu/h for an unsignalized intersection in Malaysia. Moreover, the researchers adopted the least maximum flow of all the directions as the maximum flow. In addition, the study pointed out that mixed traffic with no gap acceptance behavior was experienced at the intersection. Drivers were more aggressive at the intersections and did not stop but rather negotiated through the intersection at relatively higher speeds. All these factors explain the high flow results observed and simulated at the study intersection.

With regard to the three road safety countermeasure dimensions of exposure, risk and consequence as highlighted by Rumar (1999), the implementation of dedicated motorcycle lanes mainly reduces exposure and thus the decrease of risk for the vulnerable motorcyclists explained above.

6.2 Discussion of methodology

This section focusses on mainly microsimulation modelling as well as the application of surrogate safety measures in the study. Microsimulation was carried out using VISSIM to generate traffic flow data and vehicle trajectories. These trajectories were then processed in the Surrogate Safety Assessment Model (SSAM) for conflicts in which both Post Encroachment Time (PET) and Time to Collision (TTC) were used. The extent to which these methods were effective is described in this section.

6.2.1 Microsimulation modelling

From literature review, microsimulation models could simulate mixed traffic in developing countries that is non-lane based by making some key changes in the platforms. VISSIM was used in this study to develop a microsimulation model, but the same considerations can be utilized with other platforms if they are permitted or incorporated by their developers.

The first consideration is to import 2D/3D vehicle models into the microsimulation models to develop realistic models. Therefore, these 2D/3D models can either be imported from already established online sources such as 3D warehouse or created using some applications. For instance, SketchUp.

Conflict areas avail right of way and so they must be set properly to allow smooth movement of vehicles at the intersection without blockage. Generally, conflict areas can be set to give right of way to minor approaches because if not given enough gaps, the entire intersection is blocked. That is all the approaches are blocked and the intersection is rendered unfunctional. It would be much better if the conflict areas can be changed by coding (COM interface) during a simulation run in order to represent the negotiating nature of traffic at such intersections.

Regarding movement of vehicles, more narrower lanes can be used instead of one lane. For example, two lanes of 2m and 1.5m can be used for a 3.5m lane. Vehicles then place anywhere on the lane and can be overtaken by the motorcycles. The option to place anywhere on the lane and not strictly in the middle of a lane or left or right is activated. In addition, motorcycles are allowed to overtake both on the left and right of a slow-moving vehicle as observed in the video images.

This study shows that calibrating parameters for lateral behavior is essential while modelling non-lane based and mixed traffic in developing countries. Both the lateral distance at standstill and at 50km/h influence how the vehicles interact and can use the available space in the intersection. Traffic flow is highly influenced by these parameters as seen from sensitivity analysis.

For any microsimulation model, actual speed, deceleration, and acceleration distributions are highly significant. First, different speed distributions under free low conditions on the approaches and then in the conflict area are applied. These distributions are developed from field data in order to depict the reality. Deceleration and acceleration (desired, maximum and minimum) affect vehicle performance and so are limited to specific vehicle types. These distributions are important for the behavior of vehicles within the conflict areas since vehicles decelerate as they approach and thereafter accelerate as they are exiting. This behavior greatly affects the traffic flow limits of the intersection. Vehicular flow is reduced in microsimulations if deceleration or acceleration takes more time than in real traffic.

Some drawbacks were experienced during the use of microsimulation in this study. First, the number of simulated critical conflicts (PET threshold of 1.5s) was lower than the observed critical conflicts to the extent that the distributions were statistically different. The microsimulation was better at replicating severe critical conflicts than at replicating the total number of critical conflicts Therefore, severe critical conflicts (PET threshold of 0.5s) were used in this study. The video images of the actual intersection showed that vehicles approached each conflict area and negotiated through the intersection which had several conflict areas. Moreover, the motorcycles were impatient at the intersection and did not follow strict lanes which was not the case in the microsimulation. For instance, three waiting motorcycles would in reality cross by finding any available space and thus conflicting with other vehicles. It was not possible to simulate such conditions since microsimulation models donot have the functionality to reflect behavior in developing countries. This point is sustained by the review of Mahmud et al. (2019) focusing on microsimulation for traffic in developing countries as well as research by Caliendo and Guida (2012). These two studies emphasised that microsimulation was developed for traffic effiency rather than safety evalution. Therefore,

microsimulation platforms such as VISSIM can be improved so that vehicles accept small time gaps.

Another key weakness of microsimulation was that the number of rear-end severe critical conflicts was higher in the base scenario compared to the observed data. It was observed that trailing vehicles drove right through stopped or slow moving vehicles that partially completed lane changes. This observation was also made during validation of Surrogate Safety Assessment Model (SSAM) by the U.S. Department of Transportation (2008) using VISSIM and was more pronounced for simulations that permitted free lane changing. This study allowed free lane changing in order to simulate non-lane based and mixed traffic in developing countries.

6.2.2 Surrogate safety measures and conflicts

To understand the impact of dedicated motorcycle lanes onto road safety, surrogate safety measures were applied in this study. Even when they are still not conclusive, the causes of traffic conflicts are similar to those for crashes (Bulla-Cruz et al., 2020). According to Johnsson et al. (2018), surrogate safety indicators assume that traffic conflicts are related to safety. The researchers further pointed out that it is possible to determine the frequency of crashes based on the known frequency of less severe but more frequent conflicts. Therefore, the distributions of severe critical conflicts and severe critical conflict rates computed in this study are indicative of the safety (crash and/or injury rates) at the intersection.

Determining the right PET threshold for non-lane based and mixed traffic at unsignalized intersections in urban areas of developing countries is still a challenge. A PET threshold of 1.0s for critical conflicts was recommended by Paul and Ghosh (2020) for heterogenous traffic but on unsignalized intersections along intercity highways. In this study, a PET threshold of 1.5s resulted into different distributions of observed and simulated base scenario and so critical conflicts were not comparable. Thus, severe critical conflicts were studied in the study by applying a lower threshold of 0.5s.

Using PET, distributions and rates of severe critical conflicts were determined. More accuracy was obtained after considering the exposure of total simulated traffic per scenario. Exposure data reduces the noise in the observed data especially where high traffic results into more conflicts. Therefore, realistic traffic situations are analyzed with the use of conflict rates.

From the above discussion of the applied methods, the use of microsimulation research design was best suited for this study. The non-existent dedicated motorcycle lanes in Kampala could best be tested by modelling on a computer and trying several alternatives at the highly risky unsignalized intersections. Traffic flow was ably simulated but not all safety concerns at the study intersection. Thus, microsimulation modelling can further be improved to incorporate the dynamics in non-lane based and mixed traffic in urban areas of developing countries.

6.3 Study limitations

The following study limitations were faced during execution and must be considered while interpreting and applying the study results.

- The study used data collected using the already installed cameras by the Uganda Police which have a limited field of view and thus the collected data was prone to obstruction and counting errors for some directions.

- VISSIM has inherent weaknesses in modelling mixed traffic condition of developing countries. For example, the use of conflict areas with a particular direction having right of way is not consistent with heterogenous traffic where vehicles negotiate through the intersection without any form of priority or strict lanes. These conflict areas were fixed throughout the simulation time. In addition, sharing of opposite lanes (typical single carriage road) cannot be replicated in VISSIM. Other situations that were not modelled include: over loading of motorcycles, motorcycles carrying not only passengers but also luggage of wider dimensions than the motorcycle, effect of roadside businesses, effect of unmarked road as well as potholes or uneven road surface on traffic, effect of traffic police at intersections who control traffic movements, access of motorcycles to sidewalks at any time and position, and unfixed pedestrian crossing points.
- Pedestrian interactions with vehicles were not considered since the Surrogate Safety Assessment Model (SSAM) is not validated for pedestrian conflicts as indicated on the Federal Highway Administration website (FHWA, 2022). Therefore, VISSIM does not include pedestrian trajectories for SSAM analysis to obtain conflicts.
- Driver behavior at the cross intersection was assumed to remain the same for the improved design with a roundabout.
- The study used the same optimum values for mixed traffic for both the main road and motorcycle dedicated lanes but with minimum modifications.
- Only off-peak traffic was considered in the study but not peak traffic conditions.
- The effect of a nearby police station (about 100m on the right-hand side of the Ntinda approach) on traffic was not taken into account during the study.

6.4 Conclusion(s)

As mentioned in section 1.2, the main research question of this study was:

What are the effects of introducing dedicated motorcycle lanes on traffic efficiency and safety in non–lane based and mixed traffic at unsignalized intersections in urban areas of developing countries?

The sub-questions pointed out below were examined in line to the main objective:

i. To what extent is microsimulation suitable for traffic flow and safety evaluation of unsignalized intersections in urban areas of developing countries?
ii. How do motorcycle dedicated lanes affect the traffic flow at unsignalized intersections?
iii. What is the impact of applying motorcycle dedicated lanes on traffic conflicts and interactions at unsignalized intersections in urban areas of developing countries using both PET and TTC?

The high motorcycle demand which is over 50% of traffic justifies the need to plan, organize and control their usage in these urban areas. Introduction of dedicated motorcycle lanes as stated in the main research question is necessary especially at unsignalized intersections that form bottlenecks for traffic and are associated with high motorcycle crash risk. This microsimulation study confirms that these motorcycle lanes can increase traffic flow and improve safety at unsignalized intersections during off-peak time.

Regarding the first sub-question, microsimulation models can replicate the driver behavior of mixed traffic that is non-lane based and in urban areas of developing countries but for traffic flow analysis than safety evaluation. This conclusion is premised not only on the findings of this research but also literature. Due to the inadequacies of microsimulation models in replicating behavior for evaluation of traffic conflicts, the Post Encroachment Time (PET) threshold was lowered from 1.5s for critical conflicts to 0.5s for severe critical conflicts. The study, thus focused on severe critical conflicts since not enough evidence was available to statistically confirm that the distributions of observed critical conflicts and base simulated critical conflicts were similar. Other important modifications for microsimulation models include use of narrower lanes, importation of locally available vehicles, development of speed, acceleration, and deceleration distributions specific to a vehicle type and preferably per approach, proper setting of conflict areas to minimize blockage and calibration of driver behavior parameters. All these measures are aimed at replicating the field conditions.

In response to the second sub-question, motorcycle dedicated lanes increase the capacity of unsignalized intersections if they are well designed. For instance, motorcycle dedicated lanes with straight crossings at the intersection create blockage which reduces capacity and so should be avoided. Contrarily, the use of deflected crossings for motorcycles and then roundabout separated for main traffic and motorcycles increased the highest flow of the intersection by 31% and 20%, respectively. More space is created for motorcycles to enter and exit the intersections with minimal interference of the main road traffic. Subsequently, the main road traffic is also better organized and utilizes the space in the intersection both effectively and efficiently.

Furthermore, the implementation of motorcycle dedicated lanes reduces the critical density that is the number of vehicles per distance (km). Deflected motorcycle crossings and roundabout options reduced critical density by 38.6% and 63.7%, respectively. This reduction is significant as the vehicles including motorcycles are less congested. In all cases, the average speed was within the range of 8-25km/h both on the main road as well as on the motorcycle dedicated lanes. Important to note, the average speed of motorcycles increased slightly with consideration of the roundabout option, but the values were still below the recommended 30km/h speed limit in urban areas by the safe systems approach.

With respect to delay, motorcycle dedicated lanes improve the operational conditions by reducing the time lost by each vehicle. Majority of the motorists are expected to experience low to medium delays (Level of Service-LoS A to C). Implying that these motorists would be delayed at unsignalized intersections for less than 25s. While in the current situation, traffic is delayed by more than 50s for 82% of the off-peak time according to the simulations, the delay of main traffic reduced to less than 25s for 50% of the time and 76% of the time for the motorcycles with implementation of motorcycle dedicated lanes with deflected crossings at unsignalized intersections. Likewise, the implementation of roundabouts avails even better traffic conditions for both motorcycles and main road traffic. To be specific, main road traffic and motorcyclists would experience delay of less than 25s for 93% and 85% of the off-peak time, respectively, with implementation of roundabouts for motorcycle dedicated lanes at unsignalized intersections. Arithmetic averages were considered for LoS per approach but excluded the Kireka approach for motorcycles. Motorcycles approaching the intersection from Kireka experienced some congestion and were thus delayed by more than 50s for 80% of the time. This is critical and clearly shows the importance of increasing capacity on major

approaches in order not to compel the motorcyclists back onto the main road in times of congestion.

Concerning the third sub-question, this study focused on severe critical conflicts with PET and TTC threshold less than 0.5s since the distribution of simulated base scenario was similar to that of observed data. In contrast, the distributions for critical conflicts with a PET and TTC thresholds of 1.5s were different. Generally, traffic severe critical conflicts and their interactions are reduced by implementing motorcycle dedicated lanes at unsignalized intersections if they are well designed. For example, more benefits are expected by using either deflected crossings or roundabouts than straight crossings. The number of severe critical conflicts reduced by 87.9% with application of roundabout for the main road traffic and motorcycles which is higher than a decrease of 48.5% after the application of dedicated motorcycle lanes with deflected crossings. At the same time, deflected crossings for motorcycles reduced severe critical conflict rate by 40.0% whilst it decreased by 75.0% with intersection improvement to a roundabout for main road traffic and motorcycles. With respect to interactions, Vehicle-to-Vehicle (V2V), Vehicle-to-Motorcycle (V2M) and Motorcycle-to-Motorcycle (M2M) categories were considered. It was established that severe critical conflicts interactions generally reduced with a roundabout and V2M conflicts reduced more due to separation of traffic. In addition, severe critical conflicts were classified according to conflict types of crossing, rear-end and lane change. On average, the associated severe critical conflicts to these types also decreased more with a roundabout than use of motorcycle lanes with deflected crossing. Therefore, dedicated motorcycle lanes with a roundabout are safer in off-peak time than those lanes with deflected crossings and the current situation. These reductions of both severe critical conflicts and their rates imply that introduction of motorcycle lanes can yield a positive road safety effect.

Consequently, dedicated motorcycle lanes with deflected crossings can be implemented at the study intersection or other existing 4-leg and 3-leg unsignalized intersections since minimal modifications would be required. In addition, the approach requires less space as compared to either roundabouts or the option to increase capacity of straight crossings. The study confirms that motorcycle lanes with deflected crossings are more traffic efficient in off-peak time. Scenario 3 with a roundabout separated for motorcycles and main road traffic can be considered for improvement of the study intersection or for new projects in Kampala and other cities in developing countries.

7|Recommendations

The following scientific and practical recommendations are made in this study. Practical recommendations concerning the implementation of dedicated motorcycle lanes can as well be applied by other cities in developing countries.

7.1 Scientific recommendations

The scientific recommendations include the following:

- Consider calibrating the behavior of motorcyclists specifically using motorcycle dedicated lanes at unsignalized intersections.
- Perform a study to calibrate the traffic conditions in developing countries using both traffic flow and safety indicators.
- Further study the impact of speed calming measures either on the motorcycle dedicated lanes or on the main road or both as a solution to increased risk of high speeds by motorists towards the intersections.
- Further study the impact of road marking and traffic signs on road safety with implementation of motorcycle dedicated lanes.
- Initiate a study on the impact of dedicated motorcycle lanes on road safety and traffic flow during peak hours at unsignalized intersections.
- Investigate the conflicts between motorcyclists and pedestrians especially at unsignalized intersections in urban areas.
- Carry out a study to ascertain the acceleration and deceleration distributions (desired, maximum, minimum) of different vehicle types used in developing countries.
- Perform a study to calibrate driver behavior at roundabouts for motorcyclists and vehicles in general.
- Implement a study to establish the Post Encroachment Time (PET) threshold for conflicts at unsignalized intersections in urban areas of developing countries.
- Investigate the effect of dedicated motorcycle lanes on both traffic and safety after implementation of a pilot study (use before and after analysis).

7.2 Practical recommendations

The practical recommendations include the following:

- Develop procedures to introduce and implement motorcycle dedicated lanes on existing and new roads in Kampala with unsignalized intersections.
- Consider revising the Ugandan guidelines to include the provision of uni-directional motorcycle dedicated lanes on urban roads with unsignalized intersections.
- Carry out a pilot study on at least one unsignalized intersection to further understand the dynamics of motorcycle dedicated lanes and the target users. For instance, appreciate the acceptability and usability of these lanes in Kampala.
- Consider implementation of dedicated motorcycle lanes with deflected crossings on existing intersections while roundabouts can be opted for new projects.

- Advocate for increased education and road safety campaigns for motorcyclists and traffic in general.
- Incorporate complexities associated with traffic in developing countries in microsimulation such as dynamic conflict areas and others mentioned in section 6.3 for VISSIM.

References

Adewumi, A. O., & Arasomwan, A. M. (2015). Improved Particle Swarm Optimizer with Dynamically Adjusted Search Space and Velocity Limits for Global Optimization. In *International Journal on Artificial Intelligence Tools* (Vol. 24, Issue 5). https://doi.org/10.1142/S0218213015500177

Aoyama, E., Yoshioka, K., Shimokawa, S., & Morita, H. (2020). Estimating saturation flow rates at signalized intersections in Japan. *Asian Transport Studies*, *6*(August), 100015. https://doi.org/10.1016/j.eastsj.2020.100015

Baertsch, L. (2020). *Quantifying the economic benefits of public transportation in Kampala*. *August*.

Bajaj. (2022). *Specifications*. https://globalbajaj.com

Balikuddembe, J. K., Ardalan, A., Stephen, M. K., Raza, O., & Davoud, K. Z. (2020). Risk factors associated with road traffic injuries at the prone-areas in Kampala city: a retrospective cross-sectional study. *Journal of Injury and Violence Research*, *13*(1), 13–22. https://doi.org/10.5249/jivr.v13i1.1347

Bandi, M. M., & George, V. (2020). Calibration of Vehicle and Driver Characteristics in VISSIM and ANN- based Sensitivity Analysis. *International Journal of Microsimulation*, *13*(2), 79–101. https://doi.org/10.34196/ijm.00219

Baran, M., Erman, E., Moses, R., Sando, T., Boot, W., Abdelrazig, Y., & Olusegun, J. (2019). ScienceDirect Assessment of traffic performance measures and safety based on driver age and experience : A microsimulation based analysis for an unsignalized T-intersection. *Journal of Traffic and Transportation Engineering (English Edition)*, *6*(5), 455–469. https://doi.org/10.1016/j.jtte.2018.05.004

Barrera, J., Alvarez-Bajo, O., Flores, J., & Coello, C. A. C. (2016). Limiting the velocity in the particle swarm optimization algorithm. *Computacion y Sistemas*, *20*(4), 635–645. https://doi.org/10.13053/CyS-20-4-2505

Bhattacharyya, K., Maitra, B., & Boltze, M. (2020). *Calibration of Micro-Simulation Model Parameters for Heterogeneous Traffic using Mode-Specific Performance Measure*. *2674*(1), 135–147. https://doi.org/10.1177/0361198119900130

Bicycle Dutch. (2015). *From on street cycle lane to bi-directionally cycleway*. http://www.bicycledutch.wordpress.com

Bicycle Dutch. (2020). *Cycle lanes in the Netherlands*. http://www.bicycledutch.wordpress.com

Bulla-Cruz, L. A., Laureshyn, A., & Lyons, L. (2020). Event-based road safety assessment: A novel approach towards risk microsimulation in roundabouts. *Measurement: Journal of the International Measurement Confederation*, *165*. https://doi.org/10.1016/j.measurement.2020.108192

Caliendo, C., & Guida, M. (2012). Microsimulation approach for predicting crashes at unsignalized intersections using traffic conflicts. *Journal of Transportation Engineering*,

138(12), 1453–1467. https://doi.org/10.1061/(ASCE)TE.1943-5436.0000473

Campolongo, F., Cariboni, J., & Saltelli, A. (2007). An effective screening design for sensitivity analysis of large models. *Environmental Modelling and Software*, *22*(10), 1509–1518. https://doi.org/10.1016/j.envsoft.2006.10.004

Chaipanha, W., Tanwanichkul, L., & Pitaksringkarn, J. (2019). Impact of motorcycles and shoulder width on two-lane highway capacity in Thailand using traffic micro-Simulation model. *International Journal of GEOMATE*, *17*(64), 166–173. https://doi.org/10.21660/2019.64.14383

Chen, G. (2010). Road traffic safety in African Countries - status, trend, contributing factors, countermeasures and challenges. *International Journal of Injury Control and Safety Promotion*, *17*(4), 247–255. https://doi.org/10.1080/17457300.2010.490920

Chen, Zhang, Y., & Borken-Kleefeld, J. (2019). When is Enough? Minimum Sample Sizes for On-Road Measurements of Car Emissions. *Environmental Science and Technology*, *53*(22), 13284–13292. https://doi.org/10.1021/acs.est.9b04123

Clerc, M., & Kennedy, J. (2002). The particle swarm-explosion, stability, and convergence in a multidimensional complex space. *IEEE Transactions on Evolutionary Computation*, *6*(1), 58–73. https://doi.org/10.1109/4235.985692

Correa, J. C. (2017). Exploring the synergy between motorists and motorcyclists in urban mobilization. *First Complex Systems Digital Campus World E-Conference*, 291–295. https://doi.org/10.1007/978-3-319-45901-1_32

CROW. (2019). *Design Guide for Bicycle Traffic*.

Dabiri, S., & Abbas, M. (2016). Arterial traffic signal optimization using Particle Swarm Optimization in an Integrated VISSIM-MATLAB simulation Environment. *IEEE Conference on Intelligent Transportation Systems, Proceedings, ITSC*, 766–771. https://doi.org/10.1109/ITSC.2016.7795641

Dadashzadeh, N., Ergun, M., Kesten, S., & Žura, M. (2019). An automatic calibration procedure of driving behaviour parameters in the presence of high bus volume. *Promet - Traffic & Transportation*, *31*(5), 491–502. https://doi.org/10.7307/ptt.v31i5.3100

Damani, J., & Vedagiri, P. (2021). Safety of motorised two wheelers in mixed traffic conditions: Literature review of risk factors. *Journal of Traffic and Transportation Engineering (English Edition)*, *8*(1), 35–56. https://doi.org/10.1016/j.jtte.2020.12.003

De Silva, V., Tharindra, H., Vissoci, J. R. N., Andrade, L., Mallawaarachchi, B. C., Østbye, T., & Staton, C. A. (2018). Road traffic crashes and built environment analysis of crash hotspots based on local police data in Galle, Sri Lanka. In *International Journal of Injury Control and Safety Promotion* (Vol. 25, Issue 3, pp. 311–318). https://doi.org/10.1080/17457300.2018.1431932

Eberhart, R, & Shi, Y. (2000). Comparing inertia weights and constriction factors in particle swarm optimization. *Proceedings of the 2000 Congress on Evolutionary Computation, CEC 2000*, 84–88. https://doi.org/10.1109/CEC.2000.870279

Eberhart, Russell, & Kennedy, J. (1995). A new optimizer using particle swarm theory. *In: Proceedings of the IEEE Symposium on Micro Machine and Human Science, Nagoys, Japan*, 39–43. https://ieeexplore.ieee.org/abstract/document/494215.

El-Basyouny, K., & Sayed, T. (2013). Safety performance functions using traffic conflicts. *Safety Science*, *51*(1), 160–164. https://doi.org/10.1016/j.ssci.2012.04.015

FHWA. (2022). *Surrogate Safety Assessment Model Overview*. http://highways.dot.gov/research/safety

Francis, F., Moshiro, C., Hans Yngve, B., & Hasselberg, M. (2021). Investigation of road infrastructure and traffic density attributes at high-risk locations for motorcycle-related injuries using multiple correspondence and cluster analysis in urban Tanzania. *International Journal of Injury Control and Safety Promotion*, *0*(0), 1–11. https://doi.org/10.1080/17457300.2021.1930060

Friedrich, M., Pestel, E., Schiller, C., & Simon, R. (2019). Scalable GEH: A Quality Measure for Comparing Observed and Modeled Single Values in a Travel Demand Model Validation. *Transportation Research Record*, *2673*(4), 722–732. https://doi.org/10.1177/0361198119838849

Ge, Q., & Menendez, M. (2014). An Efficient Sensitivity Analysis Approach for Computationally Expensive Microscopic Traffic Simulation Models. *International Journal of Transportation*, *2*(2), 49–64. https://doi.org/10.14257/ijt.2014.2.2.04

Gerald, B. (2018). A Brief Review of Independent, Dependent and One Sample t-test. *International Journal of Applied Mathematics and Theoretical Physics*, *4*(2), 50. https://doi.org/10.11648/j.ijamtp.20180402.13

Gettman, D., & Head, L. (2003). Surrogate Safety Measures from Traffic Simulation Models. *Transportation Research Record*, *1840*, 104–115. https://doi.org/10.3141/1840-12

Gettman, D., Pu, L., Sayed, T., & Shelby, S. (2008). *Surrogate safety assessment model and validation: Final report*.

Ghazwan, A. H., & Lindskog, P. (2005). Road Safety in South east Asia, Factors Affecting Motorcycle Safety. *ICTCT Extra Workshop, Campo Grande*.

Gichaga, F. J. (2017). The impact of road improvements on road safety and related characteristics. *IATSS Research*, *40*(2), 72–75. https://doi.org/10.1016/j.iatssr.2016.05.002

Glendon, A. I. (2007). Driving violations observed: An Australian study. *Ergonomics*, *50*(8), 1159–1182. https://doi.org/10.1080/00140130701318624

Goldenbeld, C., Schermers, G., & Loenis, B. (2017). *Increase number of lanes, European Road Safety Decision Support System, developed by the H2020 Project SafetyCube*. www.roadsafety-dss.eu

Gopalakrishnan, S. (2012). A Public Health Perspective of Road Traffic Accidents. *Journal of Family Medicine and Primary Care*, *1*, 144–150.

Goyani, J., Paul, A. B., Gore, N., Arkatkar, S., & Joshi, G. (2021). Investigation of Crossing Conflicts by Vehicle Type at Unsignalized T- Intersections under Varying Roadway and Traffic Conditions in India Investigation of Crossing Conflicts by Vehicle Type at Unsignalized T-Intersections under Varying Roadway and Traffi. *Journal of Transportation Engineering Part A Systems*, *147*(2), 1–18. https://doi.org/10.1061/JTEPBS.0000479

Goyani, J., Pawar, N., Gore, N., & Arkatkar, S. (2019). Investigation of Traffic Conflicts at

Unsignalized Intersection for Reckoning Crash Probability Under Mixed Traffic Conditions. *Journal of the Eastern Asia Society for Transportation Studies*, *13*, 2091–2110.

Guerrero-Ibañez, J., Contreras-Castillo, J., & Zeadally, S. (2021). Deep learning support for intelligent transportation systems. *Transactions on Emerging Telecommunications Technologies*, *32*(3), 1–22. https://doi.org/10.1002/ett.4169

Haddon, J. W. (1973). Energy Damage and the ten counter-measure strategies. *Human Factors*, *15*(5), 355–366.

Hasain, N. M., & Ahmed, M. A. (2021). Safety Enhancement of Unsignalized Intersection Using Microsimulation and Surrogate Safety Measures. *IOP Conference Series: Earth and Environmental Science*, *796*. https://doi.org/10.1088/1755-1315/796/1/012016

Inter-American Development Bank. (2019). *A Surrogate video-based safety methodology for diagnosis and evaluation of low-cost pedestrian-safety countermeasures*.

Joewono, P., Mehdi, H. P., & Seyed, M. R. G. (2011). Capacity of unisignalised intersections under mixed traffic conditions. *Social and Behavioral Sciences*, *16*, 676–685.

Johnsson, C., Laureshyn, A., & De Ceunynck, T. (2018). In search of surrogate safety indicators for vulnerable road users: a review of surrogate safety indicators. *Transport Reviews*, *38*(6), 765–785.

KCCA. (2019). *Statistical Abstract For Kampala City*. https://www.kcca.go.ug/media/docs/Statistical-Abstract-2019.pdf

Kerajaan Malaysia. (2018). *Geometric Guideline for Exclusive Motorcycle Lane*.

Khavas, R. G., Hellinga, B., & Masouleh, A. Z. (2017). Identifying parameters for microsimulation modeling of traffic in inclement weather. *Journal of the Transportation Research Board*, *2613*(1), 52–60. https://doi.org/10.3141/2613-07

Killi, D. V., & Vedagiri, P. (2014). Proactive Evaluation of Traffic Safety at An Unsignalized Intersection Using Micro- Simulation. *Journal of Traffic and Logistics Engineering*, *2*(2), 140–145. https://doi.org/10.12720/jtle.2.2.140-145

Kiwango, G., Francis, F., Hasselberg, M., Chillo, O., & Moshiro, C. (2020). Perception of unsafe driving behaviour and reported driving behaviour among commercial motorcyclists in Dar es Salaam, Tanzania. *Transportation Research Part F: Traffic Psychology and Behaviour*, *74*(2020), 30–39. https://doi.org/10.1016/j.trf.2020.08.011

Kumar, R., Durai, B. K., Parida, P., Saleh, W., & Gupta, K. (2012). Driving Cycle for Motorcycle Using Micro-Simulation Model. *Journal of Environmental Protection*, *03*(09), 1268–1273. https://doi.org/10.4236/jep.2012.329144

Kwikiriza, B. C. (2016). Causes and effects of traffic congestion in kampala city. *Research Gate*, *December*.

Laureshyn, A., & Varhelyi, A. (2018). *The Swedish Traffic Conflict Technique - Observer's manual*.

Lee, T. C., Polak, J. W., & Bell, M. G. H. (2009). New approach to modeling mixed traffic containing motorcycles in urban areas. *Journal of the Transportation Research Board*, *22*(2140), 195–205. https://doi.org/10.3141/2140-22

Lenorzer, A., Casas, J., Dinesh, R., Zubair, M., Sharma, N., Dixit, V., Torday, A., & Brackstone, M. (2015). Modelling and simulation of mixed traffic. *Australasian Transport Research Forum*, 1–12.

Mahmud, Ferreira, L., Hoque, S., & Tavassoli, A. (2019). Micro-simulation modelling for traf fi c safety : A review and potential application to heterogeneous traffi c environment. *International Association of Traffic and Safety Sciences*, *43*, 27–36.

Mahmud, Ferreira, L., & Tavassoli, A. (2016). Traditional Approaches to Traffic Safety Evaluation (TSE): Application Challenges and Future Directions. *Bridging the East and West: Theories and Practices of Transportation in the Asia Pacific - Selected Papers from the Proceedings of the 11th Asia Pacific Transportation Development Conference and the 29th ICTPA Annual Conference*, 242–262. https://doi.org/10.1061/9780784479810.028

Majeed, P. G., & Kumar, S. (2014). Genetic Algorithms in Intrusion Detection Systems: A Survey. *International Journal of Innovation and Applied Studies*, *5*(3), 233–240. http://www.issr-journals.org/ijias/

Matcha, B. N., Namasivayam, S. N., Hosseini Fouladi, M., Ng, K. C., Sivanesan, S., & Eh Noum, S. Y. (2020). Simulation Strategies for Mixed Traffic Conditions: A Review of Car-Following Models and Simulation Frameworks. *Journal of Engineering*, *2020*. https://doi.org/10.1155/2020/8231930

Morris, M. D. (1991). Factorial sampling plans for preliminary computational experiments. *Technometrics*, *33*(2), 161–174. https://doi.org/10.1080/00401706.1991.10484804

MOWT. (2010). *Road Design Manual: Geometric Design*. *1*.

Mwanje, D. M. (2017). *Causes and costs of traffic jams in Kampala*. *12*.

Mwine, M. (2022a). *Base microsimulation of Spear Motors Junction in Kampala, Uganda*. [Video].YouTube. https://youtu.be/TQ74Ir2ouDg

Mwine, M. (2022b). *Microsimulation of Spear Motors Junction in Kampala, Uganda with deflected motorcycle crossings*. [Video].YouTube. https://youtu.be/eyxBWZKiSb8

Mwine, M. (2022c). *Microsimulation of Spear Motors Junction in Kampala with a roundabout and separate motorcycles lanes*. [Video].YouTube. https://youtu.be/1oN1q33kL6g

Mwine, M. (2022d). *Microsimulation of Spear Motors Junction in Kampala with straight dedicated motorcycle crossings*. [Video].YouTube. https://youtu.be/xsDcUF4puLs

National Planning Authority. (2020). Third National Development Plan (NDPIII) 2020/21-2024/25. *National Planning Authority*. http://envalert.org/wp-con20/06/NDP-3-Finale.pdf

Ndagire, M., Kiwanuka, S., Paichadze, N., & Kobusingye, O. (2019). Road safety compliance among motorcyclists in Kawempe Division, Kampala, Uganda: a cross-sectional study. *International Journal of Injury Control and Safety Promotion*, *26*(3), 315–321. https://doi.org/10.1080/17457300.2019.1607395

Nguyen, H. H. (2013). A Comprehensive Review of Motorcycle Safety Situation in Asian Countries. *Journal of Society for Transportation and Traffic Studies*, *4*(3).

Oporia, F., Kisakye, A. N., Nuwematsiko, R., Bachani, A. M., Isunju, J. B., Halage, A. A., Swaibu, Z., Atuyambe, L. M., & Kobusingye, O. (2018). An analysis of trends and

distribution of the burden of road traffic injuries in Uganda, 2011 to 2015: A retrospective study. *Pan African Medical Journal*, *31*, 1–8. https://doi.org/10.11604/pamj.2018.31.1.15223

PAHO, & WHO. (2014). *Motorcycle use in the Americas: Measures to Improve the Safety of Motorcycle Riders*.

Pakgohar, A., Tabrizi, R. S., Khalili, M., & Esmaeili, A. (2011). The role of human factor in incidence and severity of road crashes based on the CART and LR regression: A data mining approach. *Procedia Computer Science*, *3*, 764–769. https://doi.org/10.1016/j.procs.2010.12.126

Paul, M., Charan, V., Soni, V., & Ghosh, I. (2017). *Calibration Methodology of Microsimulation Model for Unsignalized Intersection under Heterogeneous Traffic Conditions*. https://doi.org/10.1061/9780784482025.063

Paul, M., & Ghosh, I. (2020). Post encroachment time threshold identification for right-turn related crashes at unsignalized intersections on intercity highways under mixed traffic. *International Journal of Injury Control and Safety Promotion*, *27*(2), 121–135. https://doi.org/10.1080/17457300.2019.1669666

Paul, M., Pakhariya, T., & Ghosh, I. (2018). *Traffic Calming and Management Based Safety Evaluation at Unsignalized Intersection Using Microsimulation*.

Pembuain, A., Priyanto, S., & Suparma, L. (2019). *The Effect of Road Infrastructure on Traffic Accidents*. *186*, 147–153. https://doi.org/10.2991/apte-18.2019.27

PTV. (2021a). *COM manual*.

PTV. (2021b). *PTV VISSIM 2021 User manual*.

Radin Umar, R. S. (2006). Motorcycle safety programmes in Malaysia: how effective are they? *International Journal of Injury Control and Safety Promotion*, *13*(2), 71–79. https://doi.org/10.1080/17457300500249632

Rahmat, K., Sugiarto, S., & Saleh, S. M. (2021). Impact of dedicated mini roundabout on the capacity and level of services of the unsignalized intersection. *IOP Conference Series: Materials Science and Engineering*, *1087*(1), 012002. https://doi.org/10.1088/1757-899x/1087/1/012002

Rumar, K. (1999). Transport Safety Visions, Targets and Strategies: Beyond 2000. *European Transport Safety Council ETSC, Brussels*.

Sacchi, E., Sayed, T., & Deleur, P. (2013). A comparison of collision-based and conflict-based safety evaluations: The case of right-turn smart channels. *Accident Analysis and Prevention*, *59*, 260–266. https://doi.org/10.1016/j.aap.2013.06.002

Saini, H. K., Chouhan, S. S., & Kathuria, A. (2022). Exclusive motorcycle lanes: A systematic review. *IATSS Research*, *xxxx*. https://doi.org/10.1016/j.iatssr.2022.05.004

Saliby, E., & Pacheco, F. (2002). An empirical evaluation of sampling methods in risk analysis simulation: Quasi-Monte Carlo, descriptive sampling, and Latin Hypercube Sampling. *Winter Simulation Conference Proceedings*, *2*(Saliby 1990), 1606–1610. https://doi.org/10.1109/wsc.2002.1166440

Schepers, P. (2013). *A safer road environment for cyclists*.

Schepers, P., Twisk, D., Fishman, E., Fyhri, A., & Jensen, A. (2017). The Dutch road to a high level of cycling safety. *Safety Science*, *92*, 264–273. https://doi.org/10.1016/j.ssci.2015.06.005

Segui-Gomez, M., Addo-Ashong, T., Raffo, V. I., & Venter, P. (2021). *ROAD SAFETY DATA IN AFRICA: A proposed minimum set of road safety indicators for data collection, analysis, and reporting*. www.ssatp.org

Seo, T., Kawasaki, Y., Kusakabe, T., & Asakura, Y. (2019). Fundamental diagram estimation by using trajectories of probe vehicles. *Transportation Research Part B: Methodological*, *122*, 40–56. https://doi.org/10.1016/j.trb.2019.02.005

Shi, Y., & Eberhart, R. (1998). A Modified particle swarm optimizer. *Proceedings of the IEEE Conference on Evolutionary Computation, ICEC*, 69–73. https://doi.org/10.1109/icec.1998.699146

Siddharth, S. M. P., & Ramadurai, G. (2013). Calibration of VISSIM for Indian Heterogeneous Traffic Conditions. *Procedia - Social and Behavioral Sciences*, *104*, 380–389. https://doi.org/10.1016/j.sbspro.2013.11.131

Silva, P. B., Andrade, M., & Ferreira, S. (2020). Machine learning applied to road safety modeling: A systematic literature review. *Journal of Traffic and Transportation Engineering (English Edition)*, *7*(6), 775–790. https://doi.org/10.1016/j.jtte.2020.07.004

Singh, S., Rajesh, V., Adhikari, P., & Santhakumar, S. M. (2020). Micro-simulation study on the effect of motorised two-wheelers on traffic speed characteristics. *Traffic Engineering*. https://doi.org/10.1080/00050326.1959.10440426

Siya, A., Ssentongo, B., Abila, D. B., Kato, A. M., Onyuth, H., Mutekanga, D., Ongom, I., Aryampika, E., & Lukwa, A. T. (2019). Perceived factors associated with boda-boda (motorcycle) accidents in Kampala, Uganda. *Traffic Injury Prevention*, *20*(sup2), S133–S136. https://doi.org/10.1080/15389588.2019.1658084

Soteropoulos, A., & Stadlbauer, S. (2017). *Convert junction to roundabout, European Raod Safety Decision Support System, developed by the H2020 project SafetyCube*. http://www.roadsafety-dss.eu/

Sowjanya, & Kumar, P. G. (2018). Accident Analysis using Microscopic Simulation and Surrogate Safety Assessment Model. *International Journal of Research and Innovation in Applied Science*, *3*(10), 26–31. www.rsisinternational.org

Srinivasula, S. R., Chepuri, A., Arkatkar, S. S., & Joshi, G. (2020). Developing proximal safety indicators for assessment of un-signalized intersection–a case study in Surat city. *The International Journal of Transportation Research*, *12*(5), 303–315. https://doi.org/10.1080/19427867.2019.1589162

SWOV. (2008). Advancing sustainable safety. In *Safety Science* (Vol. 46, Issue 2). https://doi.org/10.1016/j.ssci.2007.06.013

SWOV. (2018). *Sustainable Safety 3rd edition – The advanced vision for 2018-2030*.

Sykes, P. (2007). Transport planning with microsimulation. *Journal of Maps*, *3*(1), 122–134. https://doi.org/10.1080/jom.2007.9710833

Tarko, A. P. (2018). Surrogate measures of safety. *Transport and Sustainability*, *11*, 383–405. https://doi.org/10.1108/S2044-994120180000011019

Tettamanti, T., Csikós, A., Varga, I., & Eleőd, A. (2015). Iterative Calibration of VISSIM Simulator Based on Genetic Algorithm. *Acta Technica Jaurinensis*, *8*(2), 145–152. https://doi.org/10.14513/actatechjaur.v8.n2.365

Tran, D. Q., Trinh, H. T., & Nguyen, H. Q. (2013). Application of VISSIM microsimulation model for the motorcycle traffic in Ho Chi Minh City. *10th EASTS Conference 2013 EAST at Taiwan*.

Transoft Solutions. (2020). *Transoft Solutions acquires Canadian based Brisk Synergies to leverage machine learning and vision analytics for safer cities*.

Transoft Solutions. (2022). *Glossary*. http//:results.eu.trafxsafe.com

Transport for London. (2016). *Urban Motorcycle Design Handbook*.

Tripodi, A., Mazzia, E., Reina Barranco, F., Caporali, E., Schermers, G., & Craen, S. de. (2020). *Motorcycle Safety in Africa*. FRED Engineering / SWOV.

U.S. Department of Transportation. (2008). Surrogate Safety Assessment Model and Validation: Final Report. In *Publication No. FHWA-HRT-08-051*.

UBOS. (2020). *Statistical Abstract*.

Uganda Police. (2016). *Annual Crime Report*.

Uganda Police. (2017). *Annual Crime Report*.

Uganda Police. (2018). *Annual Crime Report*.

Uganda Police. (2019). *Annual Crime Report*.

Uganda Police. (2020). *Annual Crime Report*.

United Nations. (2018). *Road Safety Performance Review Uganda*.

Vaca, S. D., Feng, A. Y., Ku, S., Jin, M. C., Kakusa, B. W., Ho, A. L., Zhang, M., Fuller, A., Haglund, M. M., & Grant, G. (2020). Boda bodas and road traffic injuries in uganda: An overview of traffic safety trends from 2009 to 2017. *International Journal of Environmental Research and Public Health*, *17*(6). https://doi.org/10.3390/ijerph17062110

Van der Griend, R. ., & Siemonsma, W. J. . (2011). *Introducing Sustainable Urban Transport: A case of Kampala, Uganda*.

Vasconcelos, L., Neto, L., Seco, Á. M., & Silva, A. B. (2014). Validation of the Surrogate Safety Assessment Model for Assessment of Intersection Safety. *Transportation Research Record: Journal of the Transportation Research Board*, *2432*(1), 1–9. https://doi.org/10.3141/2432-01

Vedagiri, P., & Killi, D. V. (2015). Traffic safety evaluation of uncontrolled intersections using surrogate safety measures under mixed traffic conditions. *Journal of the Transportation Research Board*, *2512*, 81–89. https://doi.org/10.3141/2512-10

Vermeiren, K., Verachtert, E., Kasaija, P., Loopmans, M., Poesen, J., & Van Rompaey, A. (2015). Who could benefit from a bus rapid transit system in cities from developing countries? A case study from Kampala, Uganda. *Journal of Transport Geography*, *47*, 13–22. https://doi.org/10.1016/j.jtrangeo.2015.07.006

Vuong, X. C., Mou, R. F., & Vu, T. T. (2019). Safety impact of timing optimization at mixed-traffic intersections based on simulated conflicts: A case study of Hanoi, Vietnam. *4th International Conference on Intelligent Transportation Engineering, ICITE 2019*, 247–251. https://doi.org/10.1109/ICITE.2019.8880215

Wang, C., Quddus, M. A., & Ison, S. G. (2013). The effect of traffic and road characteristics on road safety: A review and future research direction. *Safety Science*, *57*, 264–275. https://doi.org/10.1016/j.ssci.2013.02.012

Wegman, F., Aarts, L., & Bax, C. (2008). Advancing sustainable safety. National road safety outlook for The Netherlands for 2005-2020. *Safety Science*, *46*(2), 323–343. https://doi.org/10.1016/j.ssci.2007.06.013

WHO. (2018). *Global Status Report on Road Safety*.

WHO. (2022). *Road Safety Factsheet*. http://afro.who.int/health-topics

WHO, & UN. (2021). *Global Plan: Decade of Action for Road Safety 2021-2030*.

Worldometers. (2022). *Uganda Population*. https://www.worldometers.info/world-population/uganda-population

Zeng, X., Wang, D., & Wu, J. (2015). Evaluating the Three Methods of Goodness of Fit Test for Frequency Analysis. *Journal of Risk Analysis and Crisis Response*, *5*(3), 178. https://doi.org/10.2991/jrarc.2015.5.3.5

Zheng, L., Ismail, K., & Meng, X. (2014). Traffic conflict techniques for road safety analysis: Open questions and some insights. *Canadian Journal of Civil Engineering*, *41*(7), 633–641. https://doi.org/10.1139/cjce-2013-0558

Appendices

Appendix A: Base model development

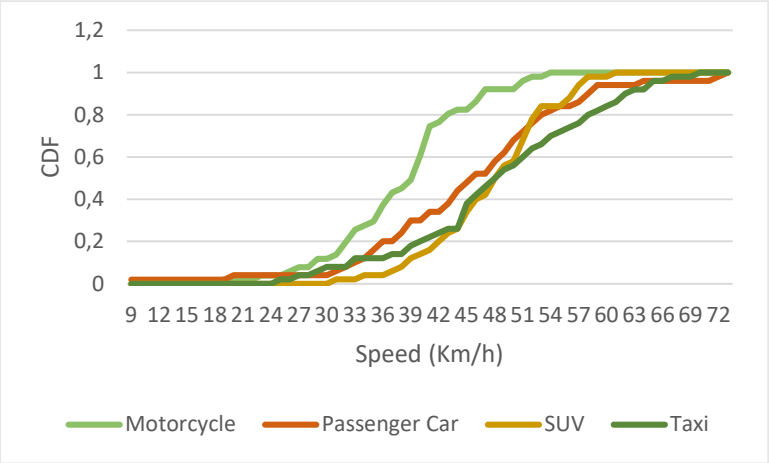

Figure A.1: Spot speed distribution for Kireka approach (50-100m)

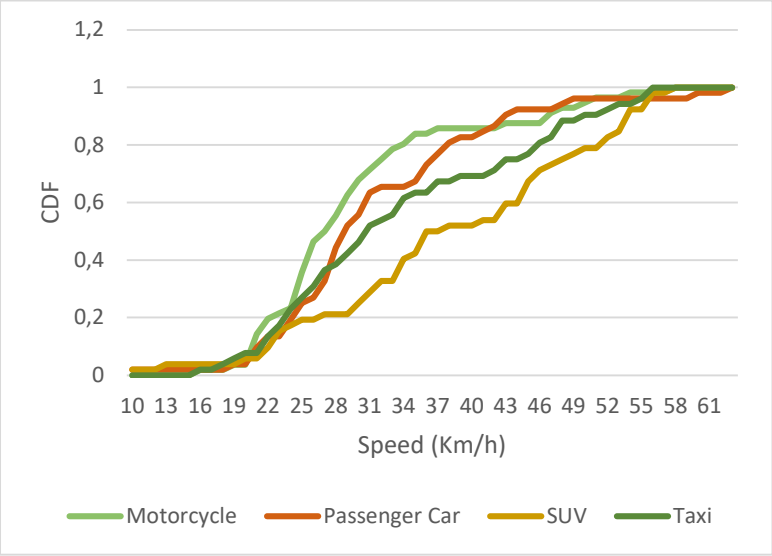

Figure A.2: Spot speed distribution for Nakawa approach (50-100m)

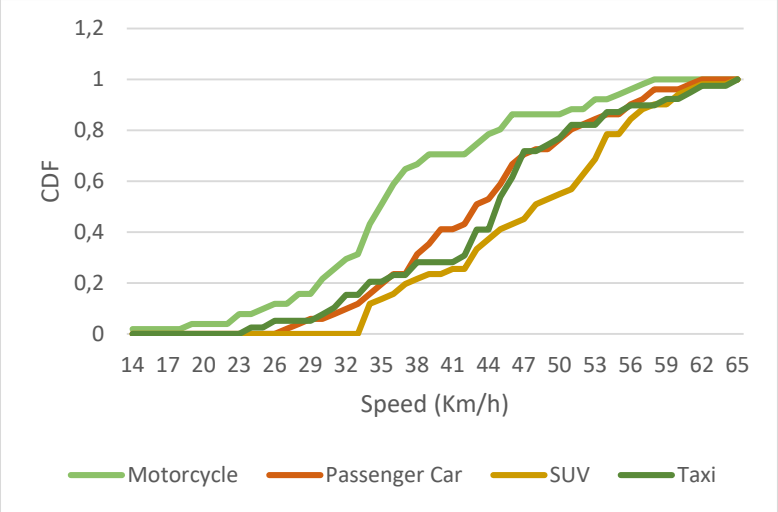

Figure A.3: Spot speed distribution for URA approach (50-100m)

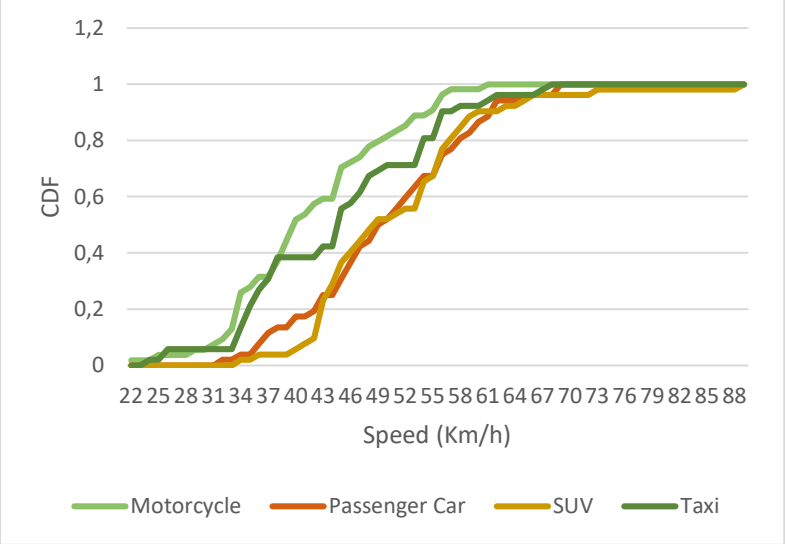

Figure A.4: Spot speed distribution for Ntinda approach (50-100m)

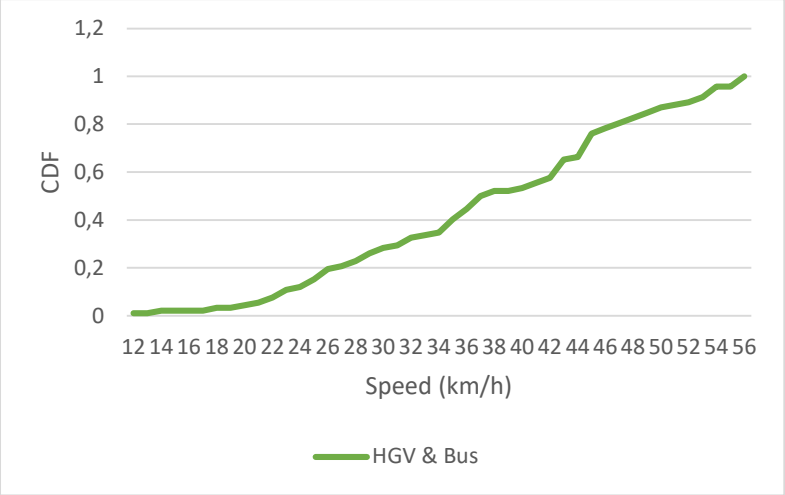

Figure A.5: Spot speed distribution for HGV and bus for all approaches (50-100m)

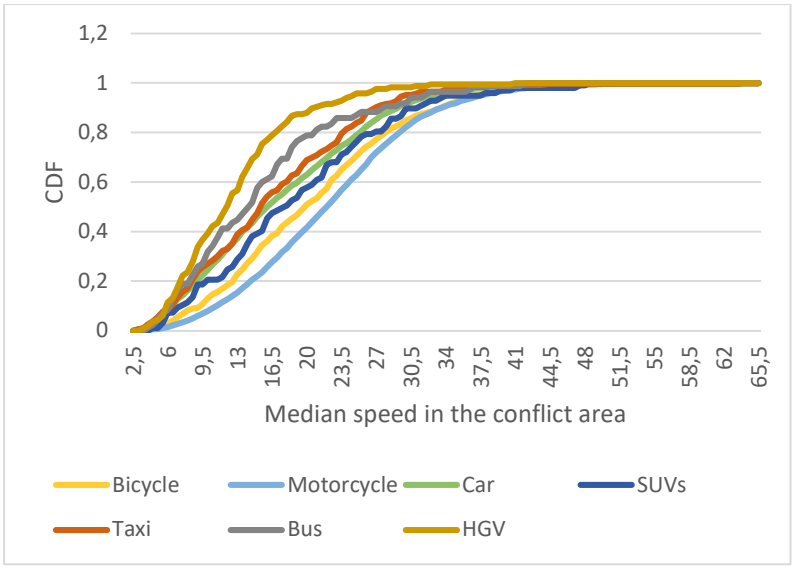

Figure A-6: Distribution of speed per vehicle type in the conflict area

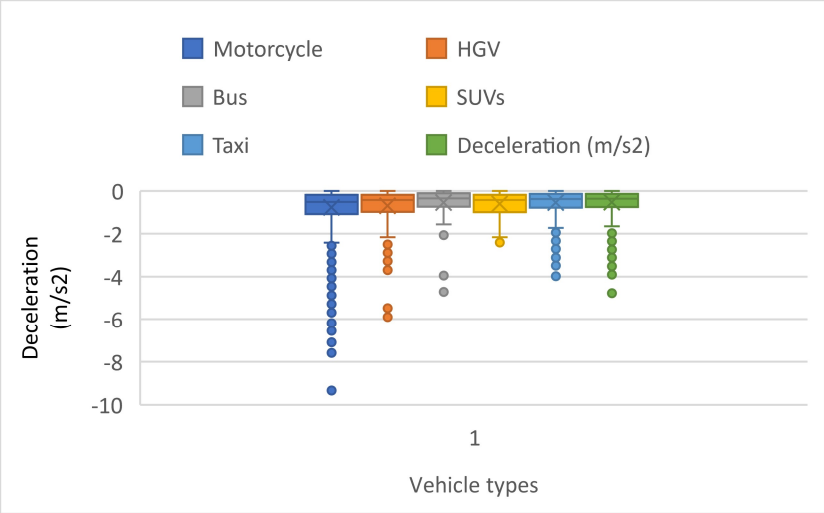

Figure A-7: Box plots of maximum deceleration of vehicle types in the conflict area

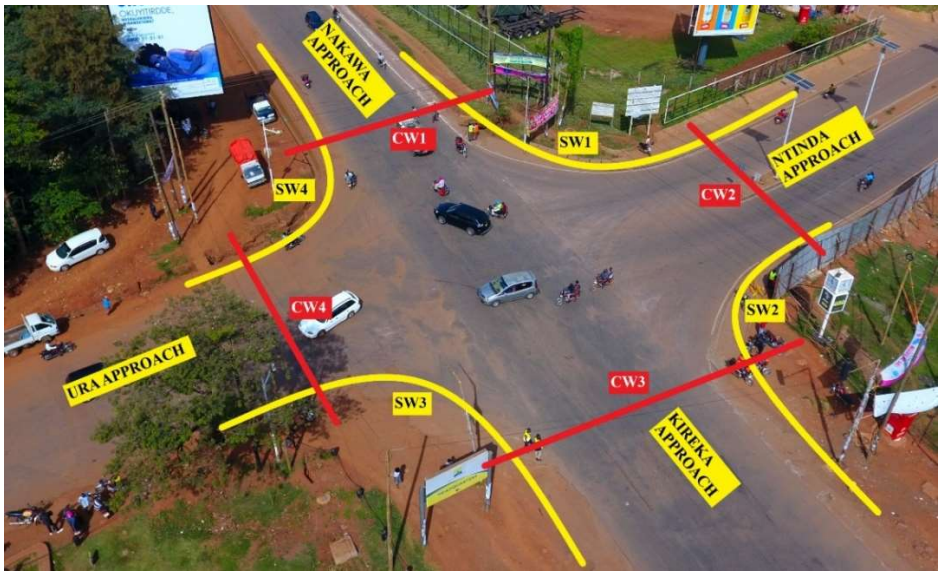

Figure A-8: Pedestrian movements at the study intersection

Table A.8: General modifications in VISSIM

S/N	VISSIM object	Modification(s)
1.	2D/3D models	Vehicle identified in the field were imported to VISSIM such as taxi, probox among others
2.	Vehicle types	Vehicle types were formulated in respect to site observations such as taxi, SUVs among others. Different 2D models were incorporated per vehicle type. Capacity was also set. For example, the capacity of a motorcycle was adjusted to 3 persons.
3.	Vehicle classes	Eight vehicle classes were considered, and these include car, HGV, Bus, Pedestrian, motorcycle, Bicycle, SUVs and taxis or matatus.
4.	Speed distributions	The distributions were adjusted for both the approaches and conflict area per vehicle class.
5.	Acceleration/ deceleration functions	These functions were adjusted based on acceleration and deceleration from trajectory data per vehicle class.
6.	Driving and link behavior types	Three behavior types were used. First, urban motorized driver behavior for the normal carriageway. Sidewalks had their own that permitted access by pedestrians and some cyclists and motorcyclists. In addition, motorcycle lanes were also accorded their own type with adjusted values.
7.	Vehicle composition	6 compositions were made that is 4 for the approaches, one for the sidewalks and last one for motorcycle lanes. Relative flows per vehicle type were allocated.
8.	Conflict areas	Priority was accorded mainly for the major roads but at some conflict points vehicles from minor roads were given priority. This was to replicate the field observations where vehicles generally negotiate through the conflict area without observing priority.
9.	Priority rules	These rules were used for pedestrian and motorcycle crossing points in respect to all potential conflicts. Pedestrians and motorcyclists were allowed to cross at a time gap of 3.0s and 2.0s, respectively, as observed in the video images.
10.	Reduced speed areas	Connectors in the conflict area were incorporated with reduced speed areas to about 10m per approach. Speed distributions of the conflicting vehicles were applied.
11.	Vehicle inputs	Road user data from field data per hour was used together with specific vehicle compositions. Time intervals of 2 minutes were used to control the inflow of the vehicles in VISSIM based on Poison distribution (PTV, 2021b).
12.	Vehicle routes	Static vehicle routes for all possible directions as observed in the video images were considered. Every approaching road user had three options of right turn, through and left turn.
13.	Overtake right (default)	Was turned on for all vehicles
15.	Overtake left	Was allowed for motorcycles, cyclists and taxis based on field observations
16.	Links	2m wide lanes were used in order to simulate non-lane based traffic for approaches with a single lane.

Table A.9: Evaluation modifications in VISSIM

S/N	VISSIM object	Modification(s)
1.	Nodes	One node for the conflict area to measure delay and Level of Service (LoS)
2.	Data collection points	Placed near the conflict area per approach
3.	Vehicle travel time measurements	A pair of detectors was placed per movement/direction with the starting point slightly before the conflict area and the end point placed slightly after the conflict point.
4.	Queue Counters	Default settings were maintained that is to begin measuring queue when speed is less than 5km/h and stop when it is 10km/h
5.	Sections	One section was defined for the conflict area including pedestrian crossing points to extract specific SSAM results. For scenarios, the section was expanded to include the motorcycle crossing points.
6.	Configuration	Turned on collecting data for the above methods Direct output was also turned on for the same methods Intervals corresponding to the measure (either 120s for most outputs or 5s for traffic flow)
7.	Data collection measurements	Defined using data collection points per approach including one on a motorcycle lane.

Table A.10: Traffic data for base model development per road user type and direction

Direction	Pedestrian	Motorcycle	Passenger Car	SUVs	Taxi	Bus	HGV	Total
Nakawa Left	0	12	62	2	6	0	3	85
Nakawa Through	0	562	291	44	181	31	44	1153
Nakawa Right	0	114	64	4	10	4	16	212
URA Left	0	6	1	1	0	0	0	8
URA Through	0	58	57	7	3	0	12	138
URA Right	0	63	34	2	1	1	11	113
Kireka Left	0	87	29	2	1	0	4	123
Kireka Through	0	1206	459	31	154	17	61	1928
Kireka Right	0	16	8	0	0	0	2	25
Ntinda Left	0	285	39	2	9	1	5	341
Ntinda Through	0	92	34	2	2	0	8	138
Ntinda Right	0	8	20	0	0	0	0	28
URA Crosswalk	17	0	0	0	0	0	0	17
URA-Kireka Sidewalk	69	30	0	0	0	0	0	99
Kireka Crosswalk	77	0	0	0	0	0	0	77
Ntinda Crosswalk	38	0	0	0	0	0	0	38
Ntinda-Kireka Sidewalk	42	32	0	0	0	0	0	74
Nakawa Crosswalk	77	0	0	0	0	0	0	77
Nakawa-Ntinda Sidewalk	42	32	0	0	0	0	0	74
Nakawa-URA Sidewalk	69	30	0	0	0	0	0	99
Total	431	2634	1098	97	367	54	166	4847

Appendix B: Sensitivity Analysis

Table B-1: Detailed description of key VISSIM parameters used in this study (PTV, 2021a)

Behavior	ID	Model Parameters	Description
Following	1	W74ax	Average standstill distance-defines the average desired distance between two cars. It has a variation between-1.0 m and 1.0m which is normally distributed at around 0.0m with a standard deviation of 0.3m.
	2	W74bxAdd	Additive part of safety distance-value for the determination of the desired safety distance d. Enables the adaption of the time needs.
	3	W74bxMult	Multiplicative part of the safety distance-value for the determination of the desired safety distance d. Enables the adaption of the time needs. Greater value=greater distribution (standard deviation) of safety distance.
	4	LookAheadDistMin	Look ahead distance(min)-the minimum distance that a vehicle can see forward in order to react to other vehicles either in front or to the side of it (within the same link). Vehicles take into account the look-ahead distance in addition to the entered number of preceding vehicles. The minimum look-ahead distance is relevant if the lateral behavior of vehicles have to be considered: If the minimum look-ahead distance is zero, only the number of observed vehicles is taken into account.
	5	LookBackDistMin	The minimum look back distance defines the minimum distance that a vehicle can see backwards in order to react to other vehicles behind (within the same link). The minimum look-back distance is important when modelling lateral vehicle behavior: If several vehicles can overtake within a lane, this value needs to be greater than zero, e.g. in urban areas it could be 20-30m, with correspondingly larger values in other places.
Lane change	6	MaxDEcelOwn	Maximum deceleration (own)-maximum deceleration for changing lanes based on the specified routes for the own/leading overtaking vehicle.
	7	MaxDEcelTRail	Maximum deceleration (trailing vehicle)-Maximum deceleration for changing lanes based on the specified routes for the following vehicle.
	8	DiffusTm	Diffusion time: The maximum amount of time a vehicle can wait at the emergency stop distance for a necessary change of lanes. When this time is reached the vehicle is taken out of the network, at the same time a warning is written to the *.err file.
	9	MinHMinFrontRearCleardwy	Minimum clearance (front/rear) -Minimum distance to the leading and to the trailing vehicle on the new lane to allow a lane change
	10	SafDistFactLnChg	Safety distance reduction factor: Is taken into account for each lane change. It concerns the following parameters: (1) The safety distance of the trailing vehicle on the new lane for determining whether a lane change will be carried out; (2) The safety distance of the lane changer itself; (3) The distance to the preceding, slower lane changer. During the lane change Vissim reduces the safety distance to the value that results from the following multiplication: Original safety distance • safety distance reduction factor.
Lateral	11	LatDistStandDef	Lateral distance at standstill-Default value for the distance at standing at 0 km/h (unit according to network settings [m] or [ft]). Minimum distance between vehicles when overtaking within the lane and keeping the distance to

			vehicles in the adjacent lanes. The minimum distance is linearly interpolated for other speeds than at 0 km/h and 50 km/h.
	12	LatDistDrivDef	Default value for the distance at 50 km/h (unit according to network settings [m] or [ft]). Minimum distance between vehicles when overtaking within the lane and keeping the distance to vehicles in the adjacent lanes. The minimum distance is linearly interpolated for other speeds than at 0 km/h and 50 km/h.
	13	LatDistStand for motorcycles	Distance standing at 0 km/h (unit according to network settings [m] or [ft]). Minimum distance between vehicles when overtaking within the lane and keeping the distance to vehicles in the adjacent lanes. The minimum distance is linearly interpolated for other speeds than at 0 km/h and 50 km/h. Behavior that differs from standard overtaking behavior for certain vehicle classes.
	14	LatDistDriv for taxis	Distance driving at 50 km/h (unit according to network settings [m] or [ft]). Minimum distance between vehicles when overtaking within the lane and keeping the distance to vehicles in the adjacent lanes. The minimum distance is linearly interpolated for other speeds than at 0 km/h and 50 km/h. Behavior that differs from standard overtaking behavior for certain vehicle classes.
	15	LatDistDriv for motorcycles	

Table B-2: Absolute mean and ranking after sensitivity analysis in descending order (random seed=42)[1]

Absolute mean			**Ranking**		
ONT	**QN**	**QU**	**ONT**	**QN**	**QU**
2229.4	2212.3	2526.9	13	13	13
758.2	1102.6	1565.5	12	12	12
519.1	932.8	1471.0	15	15	14
293.9	541.7	1346.9	11	14	11
251.2	285.1	765.8	14	11	15
217.4	212.7	651.8	10	2	10
118.2	188.1	396.3	3	3	1
103.2	179.0	349.0	1	1	2
64.6	164.5	85.6	2	10	3
2.8	3.6	9.3	5	4	5
2.6	1.1	6.5	4	5	4
0	0	0	6	6	6
0	0	0	7	7	7
0	0	0	8	8	8
0	0	0	9	9	9

[1] ONT=Occupation time for Ntinda through, QN=Queue length for Ntinda approach, QU=Queue length for URA approach

Table B-3: Absolute mean and ranking after sensitivity analysis in descending order (random seed=45)[2]

Absolute mean			Ranking		
ONT	QN	QU	ONT	QN	QU
1203.5	2292.2	2672.3	13	13	13
531.9	1052.3	1347.5	12	12	15
457.2	1014.0	1063.4	11	11	12
354.1	690.2	958.0	15	15	11
162.0	451.2	903.4	1	14	14
148.2	381.6	749.6	10	10	10
106.0	191.4	406.6	14	3	2
87.7	185.3	281.1	3	1	1
74.9	138.0	267.7	2	2	3
3.2	7.6	9.7	4	5	5
1.8	0.1	5.1	5	4	4
0	0	0	6	6	6
0	0	0	7	7	7
0	0	0	8	8	8
0	0	0	9	9	9

Table B-4: Absolute mean and ranking after sensitivity analysis in descending order (random seed=47)[3]

Absolute mean						Ranking					
ONR	ONT	OUR	OUT	QN	QU	ONR	ONT	OUR	OUT	QN	QU
2871.2	628.6	806.3	1891.1	2446.7	3731.9	13	14	13	13	13	13
1148.2	625.2	536.2	642.6	1329.5	1657.0	15	3	11	14	11	15
633.6	497.7	297.4	438.6	880.1	1291.1	11	13	3	11	15	11
579.2	491.9	260.7	349.6	736.3	956.2	12	15	12	15	12	14
513.5	357.0	245.1	315.8	581.9	869.2	14	11	15	3	14	12
195.6	319.0	225.1	315.4	317.0	384.9	2	12	14	10	2	10
169.1	306.0	134.5	292.1	305.6	185.0	10	10	10	12	1	3
126.2	92.5	78.7	130.1	263.8	169.4	3	1	2	2	10	2
99.6	64.2	66.4	125.4	120.4	156.8	1	2	1	1	3	1
7.8	4.2	3.7	6.6	12.1	14.3	4	4	4	4	5	4
3.4	2.3	3.2	4.3	8.4	10.3	5	5	5	5	4	5
0	0	0	0	0	0	6	6	6	6	6	6
0	0	0	0	0	0	7	7	7	7	7	7
0	0	0	0	0	0	8	8	8	8	8	8
0	0	0	0	0	0	9	9	9	9	9	9

[2] ONT=Occupation time for Ntinda through, QN=Queue length for Ntinda approach, QU=Queue length for URA approach

[3] ONR=Occupation time for Ntinda right turn, ONT=Occupation time for Ntinda through, OUR=Occupation time for URA right turn, OUT= Occupation time for URA through, QN=Queue length for Ntinda approach, QU=Queue length for URA approach

Table B-5: Absolute mean and ranking after sensitivity analysis in descending order (random seed=49)[4]

Absolute mean				Ranking			
ONR	ONT	QN	QU	ONR	ONT	QN	QU
2303.7	2448.5	2687.9	2066.6	13	13	13	13
900.9	936.0	965.7	1529.4	11	11	11	11
728.5	911.3	649.9	1095.0	12	15	14	15
614.5	823.4	571.4	846.4	15	14	12	12
571.1	651.8	400.6	794.5	14	12	10	14
253.3	486.8	384.5	398.4	10	10	15	10
203.4	247.8	311.3	363.7	2	2	1	1
178.8	196.9	218.2	319.6	1	1	2	2
78.4	124.6	77.2	197.4	3	3	3	3
11.2	11.0	7.6	13.1	4	4	4	4
7.7	2.6	0.1	8.4	5	5	5	5
0	0	0	0	6	6	6	6
0	0	0	0	7	7	7	7
0	0	0	0	8	8	8	8
0	0	0	0	9	9	9	9

[4] ONR=Occupation time for Ntinda right turn, ONT=Occupation time for Ntinda through, QN=Queue length for Ntinda approach, QU=Queue length for URA approach

Appendix C: Calibration and validation

Table C-1: Maximum occupation time and maximum queue length for calibration (field data)[5]

Date	**06/02/2022**							
Time Interval (minutes)	**Maximum vehicle travel time (s)**						**Maximum queue length (m)**	
	All vehicles				**Motorcycles**			
	Ntinda-R	**Ntinda-T**	**URA-R**	**URA-T**	**Ntinda-R**	**URA-R**	**Ntinda**	**URA**
0-2	25	10	31	17	12	12	0	0
2-4	15	13	9	33	17	6	10	4
4-6	22	27	31	37	12	7	4	10
6-8	17	15	10	8		6	0	0
8-10	8	10	9	42	8	6	0	0
10-12	17	59	22	31	7	6	8	4
12-14	14	20	25	24	4	4	8	0
14-16	16	16	18	12	4	6	16	12
16-18	4	21	58	15	4	6	0	16
18-20	17	34	13	14	4	7	25	0
20-22	7	33	22	14	7	11	12	0
22-24	16	6	32	11	4	9	10	5
24-26	31	21	29	76	4	4	20	10
26-28	14	16	16	38	4	6	0	0
28-30	15	17	17	45	4	6	4	6
30-32	16	6	10	14	4	14	4	0
32-34	12	13	25	34	4	6	0	8
34-36	16	4	12	23	4	6	0	15
36-38	14	4	25	10	4	6	4	16
38-40	16	8	25	32	4	6	0	4
40-42	14	5	89	14	4	12	0	8
42-44	16	16	25	19	4	6	0	10
44-46	16	9	25	12	4	8	20	0
46-48	16	10	11	19	4	8	28	15
48-50	11	16	25	23	4	5	25	0
50-52	16	16	45	24	4	6	0	4
52-54	16	10	32	24	4	7	12	0
54-56	13	20	14	20	4	6	4	0
56-58	16	7	24	24	4	6	0	0
58-60	16	3	25	6	4	6	4	4

[5] R-Right turn, T-Through

Table C-2: Detailed calibration results

Behavior	ID	Parameter description	Random seeds				
			42	**45**	**47**	**49**	**51**
Following	1	Average standstill distance	2.00	1.78	1.66	1.94	2.18
	2	Additive part of safety distance	1.17	0.63	0.98	0.56	1.25
	3	Multiplicative part of the safety distance	1.87	2.32	1.79	0.62	1.62
	4	Look ahead distance-min	22.79	20.49	16.27	23.39	17.12
	5	Look back distance-min	18.88	15.65	9.61	3.33	15.36
Lane change	10	Safety distance reduction factor (lane change)	0.51	0.65	0.47	0.40	0.72
Lateral	11	Default Lateral distance at standstill	0.23	0.27	0.28	0.17	0.31
	12	Default Lateral distance at 50km/h	0.73	0.80	0.79	0.56	0.77
	13	Lateral distance at standstill for motorcycles	0.11	0.12	0.05	0.08	0.14
	14	Lateral distance at 50km/h for taxis	0.62	0.57	0.55	0.59	0.40
	15	Lateral distance at 50km/h for motorcycles	0.48	0.41	0.52	0.56	0.36
Objective function			**6.28**	**6.89**	**5.60**	**6.26**	**6.53**

Table C-3: Simulated data for t-test during calibration[6]

Time Interval (minutes)	Maximum vehicle travel time (s)						Maximum queue length (m)	
	All vehicles				Motorcycles			
	Ntinda-R	Ntinda-T	URA-R	URA-T	Ntinda-R	URA-R	Ntinda	URA
0-2	33.32	16.98	19.54	9.93	0.00	16.29	8.54	10.96
2-4	18.69	10.90	35.01	15.39	0.00	12.40	0.00	10.64
4-6	22.02	10.54	12.06	23.70	16.99	12.06	10.82	0.00
6-8	0.00	20.91	19.12	17.63	0.00	9.12	10.27	6.58
8-10	12.67	12.07	22.67	21.93	12.67	8.22	0.00	7.35
10-12	15.49	20.42	18.81	11.61	9.78	8.81	4.80	11.96
12-14	14.84	11.32	18.78	13.14	0.00	18.73	0.00	6.21
14-16	25.31	18.99	19.90	17.41	10.83	7.64	0.00	0.00
16-18	13.81	12.58	19.55	19.88	5.01	10.71	11.70	8.56
18-20	26.86	17.24	31.59	15.36	8.94	11.59	8.07	0.00
20-22	13.08	9.57	24.07	13.03	13.08	7.81	12.57	5.01
22-24	23.52	25.71	13.52	15.60	12.34	9.69	11.21	7.13
24-26	16.98	14.20	27.15	13.90	0.00	0.00	0.00	0.00
26-28	22.40	12.40	17.01	16.51	122.71	12.18	8.15	10.07
28-30	41.94	16.84	21.87	17.27	5.94	21.87	0.00	11.25
30-32	11.28	11.25	15.70	29.06	12.16	9.64	0.00	0.00
32-34	16.64	17.48	15.90	16.99	16.64	15.90	0.00	7.40
34-36	22.87	21.16	21.24	21.16	0.00	0.00	0.00	8.01
36-38	34.05	18.29	29.83	17.99	6.05	12.62	11.28	10.64
38-40	12.13	22.60	55.56	40.29	7.87	5.56	9.92	16.19
40-42	0.00	18.53	41.90	23.68	0.00	6.42	10.10	6.27
42-44	0.00	11.27	28.78	17.00	0.00	7.06	0.00	12.77
44-46	19.32	14.91	14.29	15.89	19.32	13.00	12.41	10.55
46-48	18.52	23.23	14.87	28.11	11.29	0.00	6.18	0.00
48-50	27.52	17.20	29.01	46.68	7.88	9.01	0.00	9.02
50-52	27.57	12.55	31.90	36.78	15.64	0.00	8.29	7.57
52-54	24.36	15.29	26.78	19.15	24.36	16.78	2.93	0.00
54-56	18.24	7.92	23.57	20.46	7.83	0.00	3.81	6.85
56-58	4.93	13.86	18.27	12.27	0.00	7.25	2.87	8.15
58-60	20.36	8.27	15.68	18.16	20.60	0.00	7.67	14.32

[6] R-Right turn, T-Through

Table C-4: Maximum occupation time and maximum queue length for validation (field data)[7]

Date	**26/02/2022**							
Time Interval (minutes)	**Maximum vehicle travel time (s)**						**Maximum queue length (m)**	
	All vehicles				**Motorcycles**			
	Ntinda-R	**Ntinda-T**	**URA-R**	**URA-T**	**Ntinda-R**	**URA-R**	**Ntinda**	**URA**
0-2	5	20	25	59	5	7	4	5
2-4	7	27	37	17	7	15	4	0
4-6	12	17	28	22	8	18	35	11
6-8	21	11	9	10	2	9	21	4
8-10	8	7	12	11	5	5	8	6
10-12	13	7	14	16	9	14	2	4
12-14	8	10	11	9	8	7	5	15
14-16	7	15	17	6	4	17	12	0
16-18	17	10	6	13	17	6	8	20
18-20	7	10	34	20	5	24	10	24
20-22	12	32	38	25	6	5	5	7
22-24	13	22	22	8	9	20	7	0
24-26	4	11	5	12	4	5	0	0
26-28	8	16	23	23	5	23	8	0
28-30	8	19	10	13	7	5	0	12
30-32	14	26	29	38	4	11	4	0
32-34	20	24	19	17	5	19	5	0
34-36	16	38	19	37	6	19	18	12
36-38	7	17	23	25	7	9	0	0
38-40	21	14	16	23	21	13	0	0
40-42	12	13	14	13	4	4	0	0
42-44	6		60	39	5	6	8	35
44-46	9	18	31	16	4	20	5	7
46-48	9	36	10	19	14	19	0	0
48-50	7	7	29	29	7	10	4	0
50-52	7	55	10	52	7	21	0	6
52-54	9	21	38	36	4	10	13	9
54-56	7	11	11	22	7	38	0	0
56-58	8	42	17	38	3	5	15	12
58-60	12	19	27	26	5	8	4	11

[7] R-Right turn, T-Through

Table C-5: Traffic data for validation per road user category and direction

Direction	Pedestrian	Motorcycle	Passenger Car	SUVs	Taxi	Bus	HGV	Total
Nakawa Left	0	16	11	2	1	0	4	34
Nakawa Through	0	915	223	30	140	8	89	1405
Nakawa Right	0	140	38	6	9	1	10	204
URA Left	0	20	5	2	0	1	3	31
URA Through	0	135	65	8	4	0	19	231
URA Right	0	83	39	1	2	1	6	132
Kireka Left	0	158	48	2	4	0	3	215
Kireka Through	0	1587	398	22	137	18	87	2249
Kireka Right	0	10	9	1	0	1	8	30
Ntinda Left	0	56	45	0	0	0	8	109
Ntinda Through	0	97	45	2	2	1	7	154
Ntinda Right	0	44	14	0	0	0	4	63
URA Crosswalk	22	0	0	0	0	0	0	22
URA-Kireka Sidewalk	195	235	0	0	0	0	0	431
Kireka Crosswalk	72	0	0	0	0	0	0	72
Ntinda Crosswalk	72	0	0	0	0	0	0	72
Ntinda-Kireka Sidewalk	72	50	0	0	0	0	0	122
Nakawa Crosswalk	72	0	0	0	0	0	0	72
Nakawa-Ntinda Sidewalk	72	50	0	0	0	0	0	122
Nakawa-URA Sidewalk	195	235	0	0	0	0	0	431
Total	772	3833	941	76	299	31	248	6200

Table C-6: Observed and simulated traffic counts for Kireka approach on 26/02/2022 from 10.30 to 11.30

Time interval	**observed**	**Simulated random seed**				
		42	**45**	**47**	**49**	**51**
10.30-10.35	213	192	198	195	223	227
10.35-10.40	198	184	182	179	179	184
10.40-10.45	195	178	184	185	212	178
10.45-10.50	221	234	208	201	204	234
10.50-10.55	225	244	231	211	211	208
10.55-11.00	214	201	194	199	191	198
11.00-11.05	196	158	186	152	188	178
11.05-11.10	204	172	215	212	186	194
11.10-11.15	218	238	201	235	201	205
11.15-11.20	197	179	182	187	198	216
11.20-11.25	217	188	209	205	203	198
11.25-11.30	195	172	176	178	161	185
Total	**2,493**	**2,340**	**2,366**	**2,339**	**2,357**	**2,405**

Table C-7: Simulated data for t-test during microscopic validation (seed=42)

Time Interval (minutes)	Maximum vehicle travel time (s)						Maximum queue length (m)	
	All vehicles				Motorcycles			
	Ntinda-R	Ntinda-T	URA-R	URA-T	Ntinda-R	URA-R	Ntinda	URA
0-2	15.11	20.71	15.19	16.88	15.11	5.39	0.00	8.69
2-4	0.00	21.95	25.21	17.54	0.00	0.00	0.00	11.23
4-6	17.35	24.14	15.94	15.47	0.00	17.58	2.02	11.08
6-8	0.00	13.68	13.47	17.74	11.90	0.00	8.57	0.00
8-10	12.91	17.87	19.19	14.92	0.00	9.39	0.00	10.87
10-12	14.48	24.51	8.20	17.18	14.48	0.00	0.00	3.50
12-14	19.59	22.40	14.17	17.76	5.24	4.10	8.11	5.31
14-16	26.15	13.20	14.02	27.15	23.82	5.02	7.53	9.60
16-18	18.66	16.54	32.25	18.83	6.87	5.81	0.00	0.00
18-20	19.12	26.42	32.47	14.17	0.00	13.59	10.04	0.00
20-22	12.14	16.31	17.41	18.31	5.14	17.41	0.00	13.39
22-24	20.16	15.03	33.97	32.11	0.00	0.00	0.00	11.74
24-26	11.79	21.64	10.25	19.33	11.79	10.74	0.00	5.33
26-28	8.04	25.01	11.89	16.07	10.18	16.82	0.00	8.24
28-30	0.00	0.00	38.16	10.81	0.00	28.71	14.66	6.01
30-32	12.62	22.40	17.26	24.57	16.61	7.24	0.00	10.42
32-34	22.67	18.50	13.25	13.52	8.44	7.72	9.91	0.00
34-36	21.61	13.59	26.86	18.50	18.69	5.38	0.00	5.21
36-38	0.00	26.81	20.05	17.14	0.00	6.80	0.00	8.99
38-40	15.85	14.77	22.68	14.05	6.34	16.21	8.12	8.47
40-42	13.19	17.32	25.74	17.55	7.19	15.10	0.00	10.40
42-44	15.91	21.36	17.82	13.38	4.54	7.36	11.56	7.68
44-46	19.10	16.74	21.14	23.58	12.49	10.34	18.36	9.89
46-48	0.00	20.85	6.62	33.99	19.98	6.62	6.53	7.05
48-50	16.92	18.62	9.71	19.20	0.00	13.48	9.48	7.27
50-52	14.36	26.84	18.82	18.47	0.00	20.44	17.05	10.41
52-54	12.97	18.44	23.73	14.64	4.08	5.26	8.61	11.06
54-56	15.28	22.19	13.95	25.90	4.41	12.30	0.00	0.00
56-58	13.82	28.04	20.09	24.71	0.00	18.61	0.00	8.10
58-60	5.25	13.78	11.51	15.36	4.86	8.27	12.41	7.49

Table C-8: Simulated data for t-test during microscopic validation (seed=45)

Time Interval (minutes)	Maximum vehicle travel time (s)						Maximum queue length (m)	
	All vehicles				Motorcycles			
	Ntinda-R	Ntinda-T	URA-R	URA-T	Ntinda-R	URA-R	Ntinda	URA
0-2	14.35	26.18	12.94	23.92	0.00	14.90	0.00	0.00
2-4	21.37	14.74	15.85	16.09	24.30	17.60	0.00	6.43
4-6	0.00	15.60	15.33	17.39	0.00	11.99	0.00	5.10
6-8	17.90	15.71	12.91	25.83	17.90	14.37	14.71	7.27
8-10	20.77	21.65	14.13	16.53	20.77	15.63	0.00	9.80
10-12	0.00	19.89	18.96	19.40	0.00	12.20	8.08	4.95
12-14	18.99	11.39	20.66	17.27	18.32	27.97	0.00	8.07
14-16	12.93	20.38	25.99	14.49	12.93	11.66	0.00	0.00
16-18	18.32	12.89	17.80	16.24	12.28	24.29	0.00	10.95
18-20	0.00	27.64	16.75	12.69	0.00	18.48	9.91	24.42
20-22	17.19	17.98	10.34	21.04	17.19	10.69	10.51	12.90
22-24	0.00	13.70	13.22	16.72	0.00	16.65	0.00	10.64
24-26	37.41	14.81	10.77	28.15	17.41	11.74	0.00	0.00
26-28	15.43	14.97	18.55	13.17	15.43	19.52	0.00	4.71
28-30	0.00	20.45	17.99	20.58	0.00	25.36	11.06	0.00
30-32	17.60	20.27	13.90	12.96	23.38	11.72	14.35	8.05
32-34	15.50	20.61	17.31	20.61	22.86	19.07	0.00	9.77
34-36	14.27	16.07	17.78	23.58	0.00	21.59	10.18	8.44
36-38	19.79	15.07	13.62	22.85	19.79	13.02	10.90	10.02
38-40	25.21	19.89	25.41	21.40	15.21	16.70	0.00	10.25
40-42	18.89	18.64	17.96	15.58	12.96	17.32	0.00	5.58
42-44	0.00	25.57	21.06	15.36	0.00	18.10	0.00	5.62
44-46	21.53	18.11	10.49	22.67	16.69	10.10	8.11	10.45
46-48	31.97	25.06	15.21	18.53	13.97	16.30	10.44	0.00
48-50	22.29	21.16	25.68	16.76	15.21	18.98	10.11	14.95
50-52	24.61	30.47	18.54	19.97	0.00	20.46	8.74	8.89
52-54	0.00	19.13	94.84	17.40	0.00	119.69	0.00	5.04
54-56	0.00	15.65	19.30	24.44	0.00	35.91	0.00	15.55
56-58	16.08	14.60	17.07	17.94	11.63	16.14	0.00	7.77
58-60	0.00	15.24	19.40	12.36	0.00	11.26	13.84	0.00

Table C-9: Simulated data for t-test during microscopic validation (seed=47)

Time Interval (minutes)	Maximum vehicle travel time (s)						Maximum queue length (m)	
	All vehicles				Motorcycles			
	Ntinda-R	Ntinda-T	URA-R	URA-T	Ntinda-R	URA-R	Ntinda	URA
0-2	8.85	11.90	11.50	12.15	0.00	9.41	0.00	10.50
2-4	8.86	16.77	39.77	25.52	8.86	5.21	10.33	4.44
4-6	12.31	23.05	14.12	12.72	12.31	8.04	8.53	0.00
6-8	14.90	14.72	29.42	16.85	6.34	9.75	10.37	0.00
8-10	0.00	22.58	26.69	11.87	0.00	7.08	17.62	11.12
10-12	19.63	11.83	23.96	14.59	5.07	7.54	0.00	7.57
12-14	13.29	18.69	38.93	13.09	5.91	16.65	14.44	7.39
14-16	17.65	20.12	29.14	16.09	0.00	0.00	11.22	5.70
16-18	16.37	16.21	30.84	15.27	7.94	5.81	0.00	4.27
18-20	16.24	17.85	15.75	15.40	26.24	4.13	0.00	0.00
20-22	11.63	21.58	26.65	16.43	22.91	8.64	2.36	4.99
22-24	18.93	22.81	0.00	16.39	0.00	0.00	11.06	10.25
24-26	12.82	16.79	16.72	25.58	6.12	13.57	10.81	8.13
26-28	14.82	24.32	16.54	24.72	7.82	19.80	9.95	8.90
28-30	17.72	17.26	21.45	15.68	7.84	10.97	10.73	9.66
30-32	14.49	23.85	22.06	23.34	0.00	0.00	8.13	9.36
32-34	16.01	13.28	8.88	14.56	6.01	12.03	11.56	11.28
34-36	11.54	19.52	16.60	8.49	11.54	12.52	0.00	10.55
36-38	16.08	23.60	22.75	18.79	6.08	0.00	17.98	11.47
38-40	10.48	17.66	12.71	17.02	7.88	6.69	14.22	4.11
40-42	17.32	15.60	12.80	19.19	22.01	12.18	20.61	7.95
42-44	15.77	24.51	14.98	22.28	0.00	14.79	11.70	9.30
44-46	9.87	19.28	15.31	17.85	9.87	13.90	8.21	11.59
46-48	14.33	25.56	13.66	15.69	5.33	5.88	10.52	0.00
48-50	0.00	16.77	17.21	43.10	0.00	7.21	14.04	10.45
50-52	0.00	15.02	13.33	26.43	7.59	11.74	10.28	8.93
52-54	10.19	33.35	15.67	33.69	0.00	6.83	0.00	6.00
54-56	15.03	30.32	18.61	36.78	5.03	7.65	8.18	6.46
56-58	12.66	23.46	19.40	12.57	6.82	6.96	0.00	5.55
58-60	15.99	15.24	10.95	20.34	13.88	6.37	0.00	6.47

Table C-10: Simulated data for t-test during microscopic validation (seed=49)

Time Interval (minutes)	Maximum vehicle travel time (s)						Maximum queue length (m)	
	All vehicles				Motorcycles			
	Ntinda-R	Ntinda-T	URA-R	URA-T	Ntinda-R	URA-R	Ntinda	URA
0-2	8.37	21.36	48.66	16.54	8.37	8.66	7.63	7.52
2-4	0.00	21.40	19.95	16.03	0.00	5.61	11.34	8.54
4-6	9.31	17.07	7.67	20.48	37.03	6.61	0.00	8.66
6-8	0.00	25.71	16.17	20.01	0.00	13.83	0.00	6.52
8-10	12.24	18.70	33.35	22.35	32.24	0.00	10.34	6.75
10-12	14.42	17.86	27.01	22.46	0.00	5.39	14.94	17.91
12-14	11.10	18.45	18.56	33.41	12.02	5.48	0.00	0.00
14-16	9.96	21.95	10.53	23.78	39.96	10.53	0.00	7.98
16-18	25.15	23.33	21.70	18.58	32.68	18.55	0.00	12.35
18-20	18.03	24.66	57.26	17.65	0.00	7.26	6.80	0.00
20-22	9.80	18.68	25.28	22.48	5.54	8.17	5.89	0.00
22-24	0.00	14.75	19.67	15.82	0.00	19.67	0.00	9.64
24-26	25.55	18.34	12.48	15.19	0.00	15.34	0.00	17.96
26-28	12.20	24.77	21.25	11.93	54.37	5.18	7.36	4.69
28-30	19.00	18.19	14.02	14.72	0.00	8.16	16.83	6.52
30-32	16.03	21.70	11.31	31.74	62.89	7.35	0.00	8.59
32-34	15.45	10.72	16.56	16.63	21.10	6.56	0.00	8.62
34-36	15.82	27.13	21.18	14.90	65.82	0.00	0.00	0.00
36-38	0.00	12.99	28.31	31.29	0.00	0.00	0.00	17.64
38-40	14.72	15.80	16.79	16.28	17.08	11.73	10.45	11.40
40-42	10.08	14.48	13.55	22.74	24.96	15.24	13.13	6.32
42-44	13.81	17.34	10.82	14.19	28.26	7.34	8.47	11.38
44-46	15.69	19.76	10.50	18.08	40.69	10.50	0.00	10.78
46-48	18.68	19.91	24.28	17.96	0.00	19.18	7.71	0.00
48-50	22.81	19.94	26.72	15.90	22.81	26.72	7.87	7.12
50-52	21.14	24.84	15.36	12.16	21.14	0.00	17.16	0.00
52-54	0.00	17.82	15.54	17.74	32.76	15.54	6.25	4.74
54-56	26.66	22.18	16.98	14.90	13.24	5.64	0.00	5.42
56-58	18.24	13.31	27.79	16.50	10.14	7.41	10.92	6.52
58-60	16.33	16.09	31.34	13.42	10.88	9.14	0.00	7.70

Table C-11: Simulated data for t-test during microscopic validation (seed=51)

Time Interval (minutes)	Maximum vehicle travel time (s)						Maximum queue length (m)	
	All vehicles				Motorcycles			
	Ntinda-R	Ntinda-T	URA-R	URA-T	Ntinda-R	URA-R	Ntinda	URA
0-2	18.82	25.89	9.93	33.00	25.07	9.00	8.11	7.19
2-4	15.28	23.61	14.37	20.36	63.20	14.37	11.09	0.00
4-6	0.00	23.07	12.01	19.83	35.74	9.79	0.00	9.92
6-8	13.98	14.58	15.18	15.76	15.01	30.75	0.00	9.70
8-10	9.27	17.08	16.33	20.84	0.00	19.92	0.00	10.86
10-12	10.50	15.77	27.52	11.32	10.50	0.00	0.00	11.26
12-14	16.71	18.91	18.93	17.29	22.74	23.38	0.00	14.38
14-16	0.00	24.04	16.79	12.88	0.00	18.79	10.98	15.45
16-18	0.00	20.62	10.72	14.79	0.00	11.43	0.00	10.53
18-20	5.88	12.67	33.30	16.65	5.88	10.74	0.00	0.00
20-22	14.43	19.99	19.34	23.55	24.43	19.25	0.00	11.05
22-24	10.44	17.54	31.00	13.49	0.00	23.32	0.00	12.11
24-26	8.29	17.55	28.17	15.52	26.92	0.00	7.87	15.70
26-28	16.84	23.50	27.30	35.51	0.00	0.00	6.08	0.00
28-30	17.74	18.98	17.52	15.08	35.97	0.00	0.00	0.00
30-32	18.49	14.73	13.03	17.99	48.77	16.51	0.00	0.00
32-34	21.37	14.70	29.47	19.44	11.28	9.47	10.36	9.83
34-36	13.16	16.28	21.31	32.27	54.26	21.31	0.00	8.94
36-38	23.59	16.90	12.65	11.31	0.00	9.46	0.00	7.07
38-40	14.73	12.13	17.59	12.39	23.12	16.18	0.00	12.68
40-42	18.92	15.91	17.96	16.37	51.37	17.10	14.59	3.93
42-44	9.44	33.06	26.57	20.30	15.83	6.57	0.00	0.00
44-46	18.26	23.10	20.90	13.59	28.26	13.19	11.57	0.00
46-48	12.63	17.36	10.20	16.77	32.63	6.71	5.48	8.53
48-50	18.14	10.00	11.54	16.60	0.00	11.50	0.00	11.50
50-52	14.45	9.56	11.41	19.09	47.79	9.45	0.00	6.33
52-54	11.17	31.02	14.41	11.47	0.00	14.22	0.00	9.60
54-56	20.83	29.24	12.52	17.90	20.83	12.52	10.12	5.41
56-58	19.19	14.20	12.38	19.93	16.55	13.45	10.92	11.18
58-60	0.00	15.64	29.88	19.34	0.00	11.10	2.66	3.13

Table C-12: p-values for microscopic validation for all seeds

Random seed	Maximum vehicle travel time (s)						Maximum queue length (m)	
	All vehicles				Motorcycles			
	Ntinda-R	Ntinda-T	URA-R	URA-T	Ntinda-R	URA-R	Ntinda	URA
42	0.09351	0.83343	0.36384	0.11315	0.85473	0.09887	0.33250	0.73530
45	0.09488	0.65410	0.60699	0.08569	0.06183	0.05623	0.22568	0.64444
47	0.07355	0.98471	0.41159	0.18415	0.72569	0.00775	0.37852	0.80726
49	0.08642	0.82021	0.96998	0.10530	0.00117	0.05079	0.43084	0.69607
51	0.084208	0.70688	0.284043	0.075198	0.000508	0.83349	0.063748	0.629417

Table C-13: Observed and simulated traffic counts for Nakawa approach on 26/02/2022 from 10.30 to 11.30

Time interval	observed	Simulated random seed				
		42	45	47	49	51
10.30-10.35	137	123	143	130	129	128
10.35-10.40	140	155	124	125	122	148
10.40-10.45	151	167	162	162	129	139
10.45-10.50	147	134	137	132	131	163
10.50-10.55	141	126	125	153	144	154
10.55-11.00	125	111	138	107	134	137
11.00-11.05	130	118	139	143	115	121
11.05-11.10	152	136	147	109	150	162
11.10-11.15	131	141	121	127	127	121
11.15-11.20	128	115	115	130	129	117
11.20-11.25	156	172	164	134	129	146
11.25-11.30	105	117	118	122	116	91
Total	**1,643**	**1,615**	**1,633**	**1,574**	**1,555**	**1,627**

Table C-14: Observed and simulated traffic counts for URA approach on 26/02/2022 from 10.30 to 11.30

Time interval	observed	Simulated random seed				
		42	45	47	49	51
10.30-10.35	38	32	44	31	34	44
10.35-10.40	18	15	24	22	15	20
10.40-10.45	24	18	31	30	31	28
10.45-10.50	38	44	30	33	32	35
10.50-10.55	29	37	34	36	25	34
10.55-11.00	27	35	33	35	32	43
11.00-11.05	42	37	48	51	38	36
11.05-11.10	33	43	28	25	35	27
11.10-11.15	21	15	15	18	28	26
11.15-11.20	35	41	27	43	41	29
11.20-11.25	48	41	43	39	43	35
11.25-11.30	41	33	35	29	39	36
Total	**394**	**391**	**392**	**392**	**393**	**393**

Table C-15: Observed and simulated traffic counts for Ntinda approach on 26/02/2022 from 10.30 to 11.30

Time interval	observed	Simulated random seed				
		42	**45**	**47**	**49**	**51**
10.30-10.35	35	34	27	32	33	34
10.35-10.40	21	22	33	24	22	19
10.40-10.45	24	26	14	23	23	22
10.45-10.50	30	35	24	28	29	32
10.50-10.55	32	26	24	31	30	27
10.55-11.00	34	38	35	29	31	36
11.00-11.05	35	35	26	37	34	31
11.05-11.10	29	25	32	33	26	31
11.10-11.15	24	25	31	23	24	18
11.15-11.20	22	19	25	19	23	25
11.20-11.25	21	20	18	20	20	25
11.25-11.30	18	17	18	23	22	23
Total	**325**	**322**	**307**	**322**	**317**	**323**

Appendix D: Results

Table D-1: Number of observed and simulated (base scenario) critical conflicts (PET)

PET(s)	Observed	Base	Total
0.00-0.25	20	29	**49**
0.25-0.50	43	37	**80**
0.50-0.75	122	10	**132**
0.75-1.00	159	25	**184**
1.00-1.25	138	15	**153**
1.25-1.50	199	14	**213**
Total	**681**	**130**	**811**

Table D-2: Expected number of observed and simulated (base scenario) critical conflicts (PET)

PET(s)	Observed	Base	Total
0.00-0.25	41.15	7.85	**49**
0.25-0.50	67.18	12.82	**80**
0.50-0.75	110.84	21.16	**132**
0.75-1.00	154.51	29.49	**184**
1.00-1.25	128.47	24.53	**153**
1.25-1.50	178.86	34.14	**213**
Total	**681**	**130**	**811**

Table D-3: Number of observed and simulated (per scenario) severe critical conflicts (PET and TTC)

PET & TTC(s)	PET				TTC		
	Observed	Base	Scenario 2	Scenario 3	Base	Scenario 2	Scenario 3
0.0-0.1	7	13	5	0	10	21	3
0.1-0.2	10	16	9	3	5	3	0
0.2-0.3	10	16	9	1	10	2	1
0.3-0.4	18	11	5	2	5	1	1
0.4-0.5	18	10	6	2	7	4	0
Total	**63**	**66**	**34**	**8**	**37**	**31**	**5**

Table D-4: Expected number of observed and simulated (base scenario) severe critical conflicts (PET)

PET(s)	Observed	Base	Total
0.0-0.1	9.77	10.23	**20**
0.1-0.2	12.70	13.30	**26**
0.2-0.3	12.70	13.30	**26**
0.3-0.4	14.16	14.84	**29**
0.4-0.5	13.67	14.33	**28**
Total	**63**	**66**	**129**

Table D-5: Number of severe critical conflicts per scenario for all conflict and interaction types[8]

Scenario/case	Conflict type	V2V	V2M	M2M	Total
Observed	crossing	7	25	25	**57**
	Rear end	2	1	1	**4**
	Lane change	1	1	0	**2**
Base	crossing	2	22	21	**45**
	Rear end	3	7	8	**18**
	Lane change	1	2	0	**3**
Scenario 2	crossing	3	4	13	**20**
	Rear end	2	3	5	**10**
	Lane change	0	3	1	**4**
Scenario 3	crossing	0	1	0	**1**
	Rear end	1	0	1	**2**
	Lane change	0	1	4	**5**
Total		**22**	**70**	**79**	**171**

Table D-6: Total vehicles used in safety analysis (exposure data)

Scenario/case	Motorcycles and all through and right turn vehicles
Observed	4,466
Base	3,718
Scenario 2	4,127
Scenario 3	4,356

[8] V2V- Vehicle-to-vehicle, V2M- Vehicle-to-motorcycle, M2M- Motorcycle-to-motorcycle

Appendix E: Ethical approval

Date 25-Mar-2022
Contact person Dr. Cath Cotton, Policy Advisor Academic Integrity
E-mail c.m.cotton@tudelft.nl

Human Research Ethics Committee
TU Delft
(http://hrec.tudelft.nl/)

Visiting address
Jaffalaan 5 (building 31)
2628 BX Delft

Postal address
P.O. Box 5015 2600 GA Delft
The Netherlands

Ethics Approval Application: Micro-Simulation Study of Motorcycle Facilities and their Road Safety Impact at Unsignalized Intersections in Kampala, Uganda
Applicant: Farah, Haneen

Dear Haneen Farah,

It is a pleasure to inform you that your application mentioned above has been approved.

Please note that this approval is subject to your ensuring that the following conditions are fulfilled:

1) the data management and transfer with both SWOV and the Ugandan police are approved as GDPR compliant (whether in the EU or Uganda) by the Privacy Team;
2) the travel to Uganda meets faculty approval requirements.

Good luck with your research!

Sincerely,

Dr. Ir. U. Pesch
Chair HREC
Faculty of Technology, Policy and Management